Sulaimani Dental Journal

A Scientific journal published by the College of Dentistry- University of Sulaimani
April 2026
Volume 13, Issue 1

ISSN: 2309-4656 (Print)
ISSN: 2521-3857 (Online)

College of Dentistry

Google scholar DOAJ Crossref DORA

Sulaimani

Dental Journal

An Open Access Journal Published by the College of Dentistry, University of Sulaimani

Publication Office: College of Dentistry, University of Sulaimani, Sulaymaniyah, Iraq Tel: +(964) 533270913 - +(964) 7702106211 / P.O. Box: 1124-30 Sulaymaniyah - Iraq
E-mail: sdj@univsul.edu.iq

ISSN: 2309-4656

Volume 13

Issue 1

April 2026

Scope of the journal

The Sulaimani Dental Journal encourages submissions from all authors worldwide. Manuscripts are assessed by two experts solely and anonymously based on their contribution of original data, ideas, and presentation. All manuscripts must comply with the Instructions, which are available in more detail on our website, http://sdj.univsul.edu.iq.

The following types of manuscripts will be considered for publication: original articles, systematic reviews, review articles, case reports/case series, editorials, brief communications, and letters to the editor.

Manuscripts are accepted for consideration with the understanding that data, text, figures, photographs, and tables have not appeared in any other publication except as an abstract submitted and published in conjunction with a presentation by the author(s) at scientific meetings and that material has been submitted only to this journal.

Investigations on human subjects should conform to the guidelines noted in the World Health Organization Chronicle 1976; 30: 360-362. Research submitted to the journal should be approved by an ethical committee according to the World Medical Association Declaration of Helsinki 1964 and its last revision. Experimental animal studies need to be carried out according to the principles of laboratory animal research.

The editor and invited referees will critically review all articles within 2 months.

Editorial Board

Table of Contents

Volume 13, Issue 1: April 2026

Original Article

A Novel Approach to Gutta-Percha Disinfection: Evaluating Hypochlorous Acid Against Standard Endodontic Disinfectants

Didar S. Hama Gharib[*1], *Safeen O. Mahmood*[1]

Abstract

Objective: It is advisable to decontaminate gutta-percha cones before their insertion into the root canal system. The prevalence of contamination remains a contentious issue. This study aimed to assess and compare the effectiveness of several chemical agents for disinfecting gutta-percha cones (GP).

Methods: One hundred and ninety size F3 GP cones were used. The cones were contaminated with Enterococcus faecalis and Candida albicans following immersion. Three chemical agents were used: 2% chlorhexidine gluconate (CHX), 5.25% sodium hypochlorite (NaOCl), and 200ppm hypochlorous acid (HOCL). GP cones were immersed in the chemical agents for periods of 1 and 5 minutes. Following disinfection, the cones were incubated in thioglycolate broth, and the turbidity of the medium was used to indicate bacterial growth.

Results: CHX and NaOCl showed time-dependent regrowth of both microbes after short (1-minute) exposures; only a 5-minute NaOCl exposure achieved sustained bacterial elimination. In contrast, 200 ppm HOCl demonstrated immediate and complete eradication of both pathogens with all exposure times, showing no regrowth over 14 days.

Conclusions: HOCl proved superior to CHX and NaOCl, exhibiting rapid, stable, and prolonged antimicrobial efficacy without significant reduction over time.

Keywords: *Candida albicans, Enterococcus faecalis, Gutta-percha cone, Sodium hypochlorite, Chlorhexidine, Hypochlorous acid.*

Submitted: October 13, 2025, Accepted: December 17, 2025, Published: April 1, 2026.

Cite this article as: Hama Garib DS, Mahmood SO. A Novel Approach to Gutta-Percha Disinfection: Evaluating Hypochlorous Acid Against Standard Endodontic Disinfectants. Sulaimani Dent J. 2026;13(1):1-8.

DOI: https://doi.org/10.17656/sdj.10216

1. *Operative Dentistry and Endodontics Department, College of Dentistry, University of Sulaimani, Sulaimani, Iraq.*
2. *Basic Medical Sciences Department, College of Medicine, University of Sulaimani, Sulaimani, Iraq.*

** Corresponding author*: *didar.hamagharib@univsul.edu.iq.*

Published by the College of Dentistry, University of Sulaimani

Introduction

In dentistry, root canal therapy has long been utilized to protect and save teeth[1]. The essential goals of endodontic treatment are to eliminate microbial infection from the root canal system and prevent reinfection through effective cleaning, shaping, and obturation[2]. Despite advances in disinfection protocols, persistent infections remain a significant challenge, often attributed to resilient microorganisms such as Enterococcus faecalis and Candida albicans[3]. E. faecalis, a Gram-positive facultative anaerobe, is frequently isolated from failed root canal procedures due to its ability to form biofilms, survive in nutrient-deprived environments, and resist common antimicrobial agents[4]. In the same vein, C. albicans, an opportunistic fungal pathogen, has been more frequently associated with refractory endodontic infections, particularly in cases of compromised immune responses or inadequate disinfection[5]. The prevalence of these microorganisms in root canals can lead to periapical inflammation, delayed healing, and, ultimately, endodontic failure[6].

The most common core obturation material is gutta-percha (GP) cones because they are biocompatible and thermoplastic[7]. Despite being produced under aseptic conditions and sold in sealed packages, their sterilization is questionable and can be easily contaminated when they are handled, stored, or used in a clinical setting[8]. Effective disinfection before obturation is important for long-term treatment effectiveness because contaminated gutta-percha cones can bring bacteria back into the root canal system[9]. Multiple compounds, such as sodium hypochlorite (NaOCl), chlorhexidine gluconate (CHX), hydrogen peroxide, and alcohol solutions, have been utilized for the disinfection of gutta-percha[10]. 5% NaOCl is recognized for its strong antibacterial and tissue-dissolving capabilities [11], while 2% CHX is appreciated for its ability to adhere to surfaces and address a variety of bacteria and fungi[12]. However, each of these agents has its own set of challenges: NaOCl has the potential to cause cytotoxicity and compromise the structural integrity of gutta-percha[13]. Conversely, CHX is ineffective against certain bacterial strains and may produce precipitates when it interacts with NaOCl residues[14].

Considering these limitations, there is increasing interest in alternative disinfectants that provide superior antibacterial effectiveness while minimizing negative effects. Hypochlorous acid (HOCl), a naturally occurring compound produced by neutrophils during immunological reactions, has surfaced as a viable candidate[15]. HOCl is biocompatible and non-toxic to host tissues, and it exhibits rapid bactericidal and fungicidal efficacy at minimal concentrations (e.g., 200 ppm)[16]. It is effective against a wide range of infections, including antibiotic-resistant forms, by inflicting oxidative damage on microbial cell walls, proteins, and DNA[17]. Recent studies have demonstrated the potential of HOCl in the fields of wound care[18] and surface disinfection[19]. However, its efficacy in disinfecting gutta-percha cones, particularly compared with conventional agents, has been scarcely examined.

This research aims to assess and compare the antimicrobial effectiveness of 2% CHX, 5.25% NaOCl, and 200 ppm HOCl in disinfecting gutta-percha cones contaminated with E. faecalis and C. albicans. This study seeks to determine an appropriate disinfection technique by evaluating the relative death rates and residual antimicrobial effects, ensuring microbiological eradication without affecting material characteristics or biocompatibility. The findings may provide insight into how clinical endodontic techniques could be improved, leading to better treatment outcomes and reduced failure rates due to microbial persistence.

Materials and Methods

Sample preparation

A total of 190 ISO size (F3) GP cones (Dentsply Sirona, Ballaigues, Switzerland) were used in this study. All cones were handled aseptically throughout the experimental procedures using sterile gloves and instruments. Prior to contamination, the cones were exposed to ultraviolet (UV) light for 30 minutes to minimize pre-existing microbial contamination. The Ethical Committee at the College of Dentistry, University of Sulaimani, approved the research project with Code No. (COD-EC-24-0062) on December 16, 2024.

Microbial strains and inoculation

Two standard microbial strains, E. faecalis (ATCC 29212) and C. albicans (ATCC 10231), were used to simulate typical endodontic pathogens. The strains were individually cultured in Brain Heart Infusion (BHI) broth at 37°C for 24 hours to reach an approximate concentration of 10^8 CFU/mL. Each GP cone was submerged in a microbial suspension containing either E. faecalis or C. albicans for 30 minutes under sterile conditions to ensure uniform contamination.

Disinfection protocol

Next to contamination, 180 GP cones were randomly divided into three experimental groups (n=60/group) based on the disinfectant used:

Group A: 5.25% NaOCl, (CHLORAXID 5.25%, CERKAMED, Poland) / n=60 (30 for E. faecalis + 30 for C. albicans).

Group B: 2% CHX, (GLUCO-CHEX 2%, CERKAMED, Poland) / n=60 (30 for E. faecalis + 30 for C. albicans).

Group C: 200 HOCl, (SulOX, Sulox for antimicrobial disinfectants production, Iraq) / n=60 (30 for E. faecalis + 30 for C. albicans).

Then each group was further subdivided into two subgroups according to the duration of disinfection:

Subgroup 1: 1-minute immersion

Subgroup 2: 5-minute immersion

Following disinfection, each cone was rinsed in sterile distilled water for 10 seconds to remove residual disinfectant and prevent carryover into the culture medium.

Post-disinfection incubation and evaluation

The GP cones were aseptically transferred into sterile glass vials containing 5 mL of sterile thioglycolate broth (Condalab, Madrid, Spain) and incubated at 37°C under aerobic conditions. For each subgroup, samples were evaluated for microbial growth at three different time intervals: 24 hours, 7 days, and 14 days. At each interval, the turbidity of the broth was visually assessed as an indicator of microbial growth. In addition, 100 µL aliquots were taken from each vial and streaked onto blood agar plates to confirm microbial presence and identify persistent contamination.

Control groups

Positive control: A total of five Contaminated GP cones without disinfection were directly placed into thioglycolate broth.

Negative control: A total of five Sterile, uncontaminated GP cones were directly placed into thioglycolate broth to confirm asepsis during handling.

Outcome assessment

In each incubation period, the presence or absence of turbidity in the broth was the major outcome measure, indicating viable microbial growth. Agar culture confirmation was used as a secondary outcome to validate turbidity results. All procedures were performed in triplicate for each group to ensure reproducibility.

Statistical analysis

The data were expressed as absolute values and percentages [n (%)]. Statistical comparisons were conducted using SPSS software (Version 26.0, IBM Corp., Armonk, NY, USA). To evaluate differences in paired binary outcomes across incubation intervals, the non-corrected McNemar test was applied. This test was used to detect statistically significant changes in microbial growth status following exposure to chemical disinfectants at different time points (1, 7, and 14 days). Separate p-values were calculated to compare antimicrobial performance across time intervals: Pa (1-day vs. 7-day), Pb (1-day vs. 14-day), and Pc (7-day vs. 14-day). Statistical significance was indicated by a P-value < 0.05.

Results

The bactericidal efficacy of 2% CHX, 5.25% NaOCl, and 200 ppm HOCl against E. faecalis was evaluated across three incubation intervals as shown in Table 1 and Figure 1. One-minute exposure to CHX resulted in persistent bacterial survival across all time points (1 day: 40.0%; 7 days: 46.7%; 14 days: 60.0%), with no statistically significant differences among time points (p = 0.804, 0.439, and 0.814, respectively). By contrast, exposure to CHX for 5 min resulted in a marked growth inhibition at 1 day (6.7%), whereas incomplete regrowth was detected at 7 and 14 days (20.0% and 26.7%, respectively), with significant differences between the results of the assays after incubation for 24 h versus those obtained after longer incubation (p = 0.013 or p = 0.031).

The initial efficacy at one minute exposure was higher with NaOCl (5.25%) in comparison to the other tested solutions (0.0% growth at 1 day), however, bacterial regrowth occurred after 7 days (20.0%) and 14 days of storage time (40.0%), being statistically different from 1 day to 7-day contact time intervals, p = 0.008). Five-minute exposure to NaOCl resulted in sustained absence throughout all incubation periods (0.0% growth) and was not significantly different among any [p = 1.000]. HOCl (200 ppm) completely suppressed bacterial growth at all exposure times and time points tested (0.0% growth), and temporal trends in any comparison were not significant (p = 1.000). A total of 90 infected GP cones with C. albicans were treated by disinfection techniques (2% CHX, 5.25% NaOCl, and 200 ppm HOCl). After 1-min exposure, CHX and NaOCl resulted in a complete inhibition at day 1 (0%) but gradually regrew by day 7 (CHX: 33.3%, NaOCl: 33.3%) and by day 14 (CHX: 46.7%; NaOCl: 40%), with significant differences being found between the incubation periods of day 1 and both day 7 (CHX, p =.041; NaOCl, p =.041) and day 14 (CHX, p =.023; NaOCl, P =.049). After 5-minute exposure to 2% CHX and 5% NaOCl, sustained inhibition was observed at all time points, with mild

regrowth of NaOCl at day 14 (13.3%), which was statistically significant compared with that at the 1- and 7-day incubation periods (P = .002). In contrast, HOCl (200 ppm) maintained 100% antifungal efficacy at all exposure times, regardless of incubation duration; no regrowth was observed, and no significant differences among comparisons were observed (p = 1.000). These results highlight HOCl's stability as a fast and sustained antifungal agent, surpassing CHX and NaOCl in immediate and residual disinfection efficiency, as shown in Table 2 and Figure 2.

Table 1: Comparative effectiveness of the three chemical disinfectants on E. faecalis growth across incubation periods.

Groups	Exposure time	Microbial growth	Incubation time			p-value		
			Day 1	Day 7	Day 14	P a	P b	P c
2%CHX, n=30	1 Minute, n=15	Growth	6 (40.0%)	7 (46.7%)	9 (60.0%)	0.804	0.439	0. 814
		No growth	9 (60.0%)	8 (53.3%)	6 (40.0%)			
	5 Minutes, n=15	Growth	1 (6.7%)	3 (20.0%)	4 (26.7%)	0.013*	0.031*	0.077
		No growth	14 (93.3%)	12 (80.0%)	11 (73.3%)			
5%NaOCl, n=30	1 Minute, n=15	Growth	0 (0.0%)	3 (20.0%)	6 (40.0%)	0.008	0.078	0.238
		No growth	15 (100.0%)	12 (80.0%)	9 (60.0%)			
	5 Minutes, n=15	Growth	0 (0.0%)	0 (0.0%)	0 (0.0%)	1.000	1.000	1.000
		No growth	15 (100.0%)	15 (100.0%)	15 (100.0%)			
200 ppm HOCl, n=30	1 Minute, n=15	Growth	0 (0.0%)	0 (0.0%)	0 (0.0%)	1.000	1.000	1.000
		No growth	15 (100.0%)	15 (100.0%)	15 (100.0%)			
	5 Minutes, n=15	Growth	0 (0.0%)	0 (0.0%)	0 (0.0%)	1.000	1.000	1.000
		No growth	15 (100.0%)	15 (100.0%)	15 (100.0%)			

n; number of the samples, %; percentage, *; statistically significance, p-value; Significant level, Pa; P-value for (1-day vs. 7-day

Table 2: Comparative effectiveness of chemical disinfectants on C. albicans growth across incubation periods.

Groups	Exposure time	Microbial growth	Incubation time			p-value		
			Day 1	Day 7	Day 14	P a	P b	P c
2%CHX, n=30	1 minute, n=15	Growth	0 (0.0%)	5 (33.3%)	7 (46.7%)	0.041 *	0.023 *	0.629
		No growth	15 (100.0%)	10 (66.7%)	8 (53.3%)			
	5 Minutes, n=15	Growth	0 (0.0%)	0 (0.0%)	0 (0.0%)	1.000	1.000	1.000
		No growth	15 (100.0%)	15 (100.0%)	15 (100.0%)			
5%NaOCl, n=30	1 minute, n=15	Growth	0 (0.0%)	5 (33.3%)	6 (40.0%)	0.041 *	0.049 *	0.454
		No growth	15 (100.0%)	10 (66.7%)	9 (60.0%)			
	5 Minutes, n=15	Growth	0 (0.0%)	0 (0.0%)	2 (13.3%)	1.000	0.002 *	0.002 *
		No growth	15 (100.0%)	15 (100.0%)	13 (86.7%)			
200 ppm HOCl, n=30	1 minute, n=15	Growth	0 (0.0%)	0 (0.0%)	0 (0.0%)	1.000	1.000	1.000
		No growth	15 (100.0%)	15 (100.0%)	15 (100.0%)			
	5 Minutes, n=15	Growth	0 (0.0%)	0 (0.0%)	0 (0.0%)	1.000	1.000	1.000
		No growth	15 (100.0%)	15 (100.0%)	15 (100.0%)			

n; number of the samples, %; percentage, *; statistically significance, P-value; Significant level, Pa; P-value for (1-day vs. 7-day incubation), Pb; P-value for (1-day vs. 14-day), and Pc; P-value for (7-day vs. 14-day).

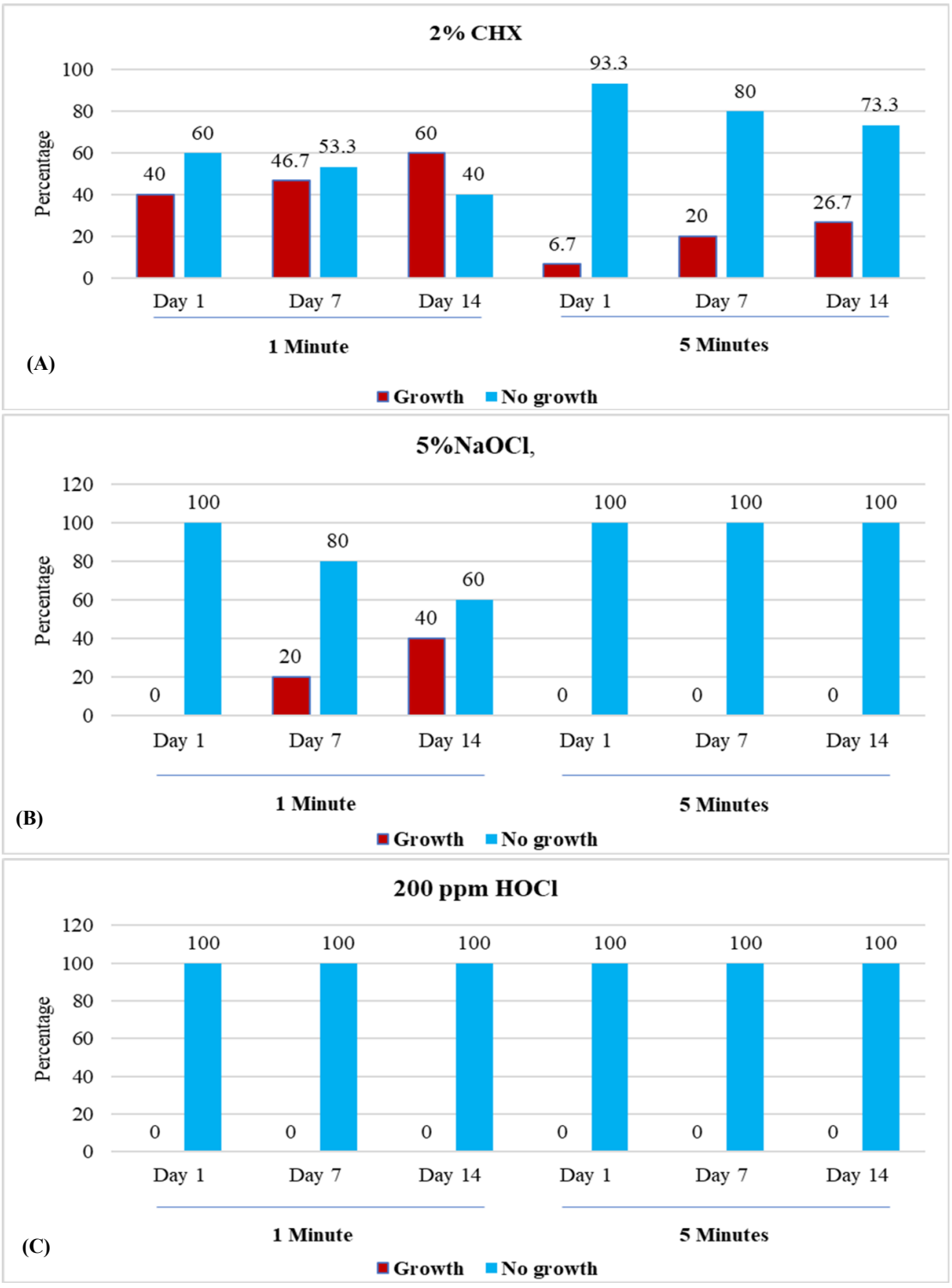

Figure 1: Comparative efficacy of 2% CHX (A), 5.25% NaOCl (B), and 200ppm HOCL (C) on Enterococcus faecalis growth across different incubation periods.

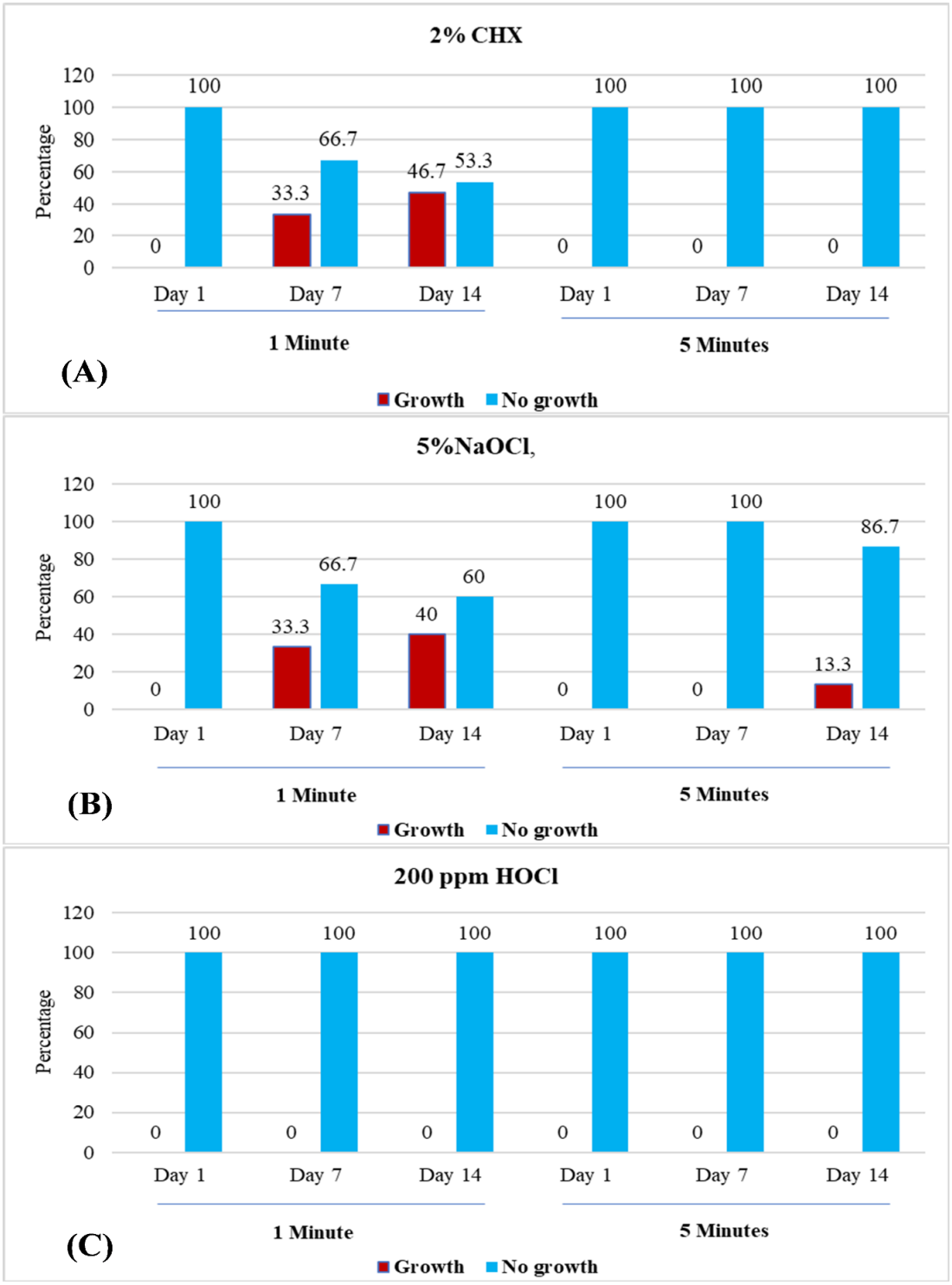

Figure 2: Comparative efficacy of 2% CHX (A), 5.25% NaOCl (B), and 200ppm HOCL (C) on *Candida albicans* growth across different incubation periods.

Discussion

This study assessed the antibacterial effectiveness of 2% CHX, 5.25% NaOCl, and 200 ppm HOCl in disinfecting GP cones contaminated with E. faecalis and C. albicans, over two exposure durations (1 and 5 minutes) and three incubation periods (1, 7, and 14 days). The results reveal substantial disparities in the short- and long-term antimicrobial actions of these agents, with 200 ppm HOCl exhibiting higher sustainability and enhanced antimicrobial activity compared to 2% CHX and 5.25% NaOCl.

Antibacterial Efficacy Against Enterococcus faecalis
A 1-minute exposure to 2% CHX resulted in persistent bacterial viability (40–60%) throughout all incubation periods, exhibiting no significant decline over time. Despite a 5-minute treatment, 2% CHX exhibited partial regrowth (20–26.7%) by days 7 and 14, demonstrating its low residual efficacy against E. faecalis. These results are consistent with a study showing that CHX is less effective against biofilm-embedded E. faecalis[4].

Strong initial bactericidal activity was shown by NaOCl (5.25%) (0% growth at 1 day after 1-minute exposure), but regrowth occurred at 7 and 14 days (20–40%), indicating that short-term exposure might not ensure long-term disinfection. Nonetheless, a 5-minute exposure to NaOCl resulted in complete and long-lasting elimination, underscoring the importance of prolonged exposure for dependable disinfection. These results are supported by studies demonstrating that NaOCl's efficacy decreases in the presence of organic debris[20,21].

HOCl (200 ppm) was outstanding, sustaining 100% inhibition at all exposure times and incubation intervals, with no regrowth. This consistency shows that HOCl is more stable and works as an antimicrobial for longer than CHX and NaOCl. This finding aligns with a study that reveals that neutral charges of HOCl molecules lead to deeper penetration into biofilms, which enhances its bactericidal effects[15].

Antifungal Efficacy Against Candida albicans
Both CHX and NaOCl exhibited complete inhibition at a one-day incubation period after a 1-minute exposure, but time-dependent regrowth was observed at 7 and 14 days, reaching 33.3–46.7% for CHX and 33.3–40% for NaOCl. This regrowth suggests that short exposures to these agents may not provide prolonged antifungal protection. These findings align with a previous study indicating that CHX loses its efficacy over time due to protein binding and neutralization by organic tissue[22]. Similarly, NaOCl's antimicrobial activity reduces as chlorine is consumed[11].

In contrast, 5-minute exposures resulted in prolonged inhibition for 2% CHX, however, 5.25% NaOCl still showed modest regrowth at 14 days (13.3%), indicating that its antimicrobial effectiveness reduced over time. This supports the theory that prolonged exposure times improve disinfection but may not totally prevent bacterial regrowth[23].

HOCl (200 ppm) demonstrated complete and persistent antifungal activity at all exposure times and incubation intervals, with no regrowth observed. These results coincide with a study that exhibits HOCl's superior performance, which may be attributed to its strong oxidative properties and rapid microbial membrane disruption[24]. This confirms HOCl's stability and long-lasting efficacy, making it a more reliable alternative for preventing C. albicans from contributing to endodontic reinfection.

The present findings suggest that, when used for long periods of time, HOCl will be more effective than either CHX or NaOCl in their broad-spectrum antimicrobial activity with non-toxicity and stability, indicating it as the most appropriate alternative to conventional endodontic irrigation or adjunct agent[25].

The present findings indicate the promising impact of hypochlorous acid in root canal disinfection; however, its long-term effectiveness necessitates validation through rigorously designed in vivo and clinical studies. Investigating the effects of higher concentrations or the synergistic application with other disinfectants may further enhance the antimicrobial efficacy of endodontic protocols.

Conclusion

In summary, 200 ppm HOCl outperformed 2% CHX and 5.25% NaOCl in both immediate and residual antibacterial and antifungal efficacy against E. faecalis and C. albicans. Its consistent, long-lasting inhibition without regrowth establishes it as a viable disinfectant in endodontic therapy, necessitating additional clinical investigation.

References

1. Ahmad SM. Evaluation of Gutta-Percha Removal by Orange Oil Solvent and Eucalyptus Solvents Using Protaper Universal and XP-Endo® Rise

Retreatment Instrument (An Invitro Comparative Study). Sulaimani Dent J. 2024;11(3):50-8.
2. Abdulrahman SS, Faraj BM. Comparative analysis of conventional, sonic and laser activated irrigation methods on fracture resistance of endodontically treated roots: an in vitro study. Sulaimani Dent J. 2023;10(3):31-40.
3. Sundqvist G, Figdor D, Persson S, Sjögren U. Microbiologic analysis of teeth with failed endodontic treatment and the outcome of conservative re-treatment. Oral Surgery, Oral Medicine, Oral Pathol Oral Radiol Endodontol. 1998;85(1):86-93.
4. Stuart CH, Schwartz SA, Beeson TJ, Owatz CB. Enterococcus faecalis: its role in root canal treatment failure and current concepts in retreatment. J Endod. 2006;32(2):93-8.
5. Waltimo TMT, Sen BH, Meurman JH, Ørstavik D, Haapasalo MPP. Yeasts in apical periodontitis. Crit Rev Oral Biol Med. 2003;14(2):128-37.
6. Nair PNR. Pathogenesis of apical periodontitis and the causes of endodontic failures. Crit Rev Oral Biol Med. 2004;15(6):348-81.
7. Vishwanath V, Rao HM. Gutta-percha in endodontics-A comprehensive review of material science. J Conserv Dent. 2019;22(3):216-22.
8. Short RD, Dorn SO, Kuttler S. The crystallization of sodium hypochlorite on gutta-percha cones after the rapid-sterilization technique: an SEM study. J Endod. 2003;29(10):670-3.
9. de Almeida Gomes BPF, Vianna ME, Matsumoto CU, Zaia AA, Ferraz CCR, de Souza Filho FJ. Disinfection of gutta-percha cones with chlorhexidine and sodium hypochlorite. Oral Surg Oral Med Oral Pathol Oral Radiol Endod. 2005;100(4):512-7.
10. Valera MC, Silva KCG da, Maekawa LE, Carvalho CAT, Koga-Ito CY, Camargo CHR, et al. Antimicrobial activity of sodium hypochlorite associated with intracanal medication for Candida albicans and Enterococcus faecalis inoculated in root canals. J Appl Oral Sci. 2009;17(6):555-9.
11. Zehnder M. Root canal irrigants. J Endod. 2006;32(5):389-98.
12. Basrani B, Tjäderhane L, Santos JM, Pascon E, Grad H, Lawrence HP, et al. Efficacy of chlorhexidine-and calcium hydroxide–containing medicaments against Enterococcus faecalis in vitro. Oral Surg Oral Med Oral Pathol Oral Radiol Endod. 2003;96(5):618-24.
13. Rossi-Fedele G, Guastalli AR, Doğramacı EJ, Steier L, De Figueiredo JAP. Influence of pH changes on chlorine-containing endodontic irrigating solutions. Int Endod J. 2011;44(9):792-9.
14. Basrani BR, Manek S, Sodhi RNS, Fillery E, Manzur A. Interaction between sodium hypochlorite and chlorhexidine gluconate. J Endod. 2007;33(8):966-9.
15. Wang L, Bassiri M, Najafi R, Najafi K, Yang J, Khosrovi B, et al. Hypochlorous acid as a potential wound care agent: part I. Stabilized hypochlorous acid: a component of the inorganic armamentarium of innate immunity. J Burns Wounds. 2007;6:e5.
16. Sakarya S, Gunay N, Karakulak M, Ozturk B, Ertugrul B. Hypochlorous acid: an ideal wound care agent with powerful microbicidal, antibiofilm, and wound healing potency. Wounds. 2014;26(12):342-50.
17. Fukuzaki S. Mechanisms of actions of sodium hypochlorite in cleaning and disinfection processes. Biocontrol Sci. 2006;11(4):147–57.
18. Selkon JB, Cherry GW, Wilson JM, Hughes MA. Evaluation of hypochlorous acid washes in the treatment of chronic venous leg ulcers. J Wound Care. 2006;15(1):33-7.
19. Block MS, Rowan BG. Hypochlorous acid: a review. J Oral Maxillofac Surg. 2020;78(9):1461-6.
20. Siqueira Jr JF, Rôças IN, Favieri A, Lima KC. Chemomechanical reduction of the bacterial population in the root canal after instrumentation and irrigation with 1%, 2.5%, and 5.25% sodium hypochlorite. J Endod. 2000;26(6):331-4.
21. Zandi H, Rodrigues RC V, Kristoffersen AK, Enersen M, Mdala I, Ørstavik D, et al. Antibacterial effectiveness of 2 root canal irrigants in root-filled teeth with infection: a randomized clinical trial. J Endod. 2016;42(9):1307-13.
22. Basrani B, Santos JM, Tjäderhane L, Grad H, Gorduysus O, Huang J, et al. Substantive antimicrobial activity in chlorhexidine-treated human root dentin. Oral Surg Oral Med Oral Pathol Oral Radiol Endod. 2002;94(2):240-5.
23. Gomes BPFA, Vianna ME, Zaia AA, Almeida JFA, Souza-Filho FJ, Ferraz CCR. Chlorhexidine in endodontics. Braz Dent J. 2013;24(2):89-102.
24. Block SS. Disinfection, sterilization, and preservation. Lippincott Williams & Wilkins; 2001.
25. McDonnell G, Russell AD. Antiseptics and disinfectants: activity, action, and resistance. Clin Microbiol Rev. 1999;12(1):147-79.

Original Article

Comparative Analysis of FGFR2 Exon 8 and Exon 10 Sequences in Retrognathic Mandible Patients: A Case-Control Study

Shan S. Hamid[*1], *Mohammed A. Mahmood*[1], *Rana M. Al-Obaidi*[1]

Abstract

Objective: Class II malocclusion is associated with the gene FGFR2. Genotyping involved conducting genome linkage scans to identify mutations in various mandibular genes and loci associated with Class II malocclusion. The present study aimed to improve the current understanding of genetic factors involved in the development of a retrognathic mandible and to correlate genetic variations with phenotypic characteristics.

Methods: Two hundred patients with class II jaw relation have been examined; twenty patients with a retrognathic mandible and another twenty with normal mandibular size and position have been selected from the population by analyzing their lateral cephalometric radiographs. DNA was extracted from saliva samples collected from 40 individuals. FGFR2-8 and FGFR2-10 genes were amplified using the genomic DNA of patients' saliva by PCR. The results of sequenced samples were analyzed using a phylogenetic tree.

Results: Cephalometric readings indicated that patients with class II had a retrognathic mandible, while their maxilla was normally positioned. Genetically, when comparing FGFR2 exon 8 and exon 10, exon 10 is more promising for detecting class I and class II, because it mimics the results of clinical examination by cephalometric radiographs. In FGFR2-10 the controls were in one group of the phylogenetic tree.

Conclusions: This study concludes that FGFR2-10 may be promising for detecting class II malocclusion, while FGFR2-8 was not very specific. All found mutations were point mutations and can be considered new SNPs (Single Nucleotide Polymorphisms). FGFR2-10 showed clearer grouping patterns between cases and controls in the phylogenetic tree; these findings may serve as a diagnostic aid and require further validation.

Keywords: *FGFR2-8, FGFR2-10, Genetic Analysis, Retrognathic Mandible, Point Mutation.*

Submitted: October 29, 2025, Accepted: January 14, 2026, Published: April 1, 2026.

Cite this article as: Hamid SS, Mahmood MA, Al-Obaidi RM. Comparative Analysis of FGFR2 Exon 8 and Exon 10 Sequences in Retrognathic Mandible Patients: A Case-Control Study. Sulaimani Dent J. 2026;13(1):9-19.

DOI: https://doi.org/10.17656/sdj.10217

1. *Basic Sciences Department, College of Dentistry, University of Sulaimani, Sulaimani, Iraq.*

* *Corresponding author*: *shan.hamid@univsul.edu.iq*

Published by the College of Dentistry, University of Sulaimani

Introduction

Skeletal Class II malocclusion results from maxillary protrusion or mandibular retrognathism (hypoplasia)[1], characterized by decreased SNB angle (Sella-Nasion-B point angle), everted lower lip, reduced chin projection, and abnormal gonial angles. Cephalometrically, it demonstrates an increased mandibular plane angle, greater lower facial height, and an altered facial axis, all of which are correlated with mandibular length deficiency. Multiple factors, including heredity, environmental influences, and epigenetic modifications, impact how the craniofacial skeleton develops in humans. There are many different approaches to studying the diverse genetic components in a population. As genetic studies and facilities advanced quickly in recent years, a hereditary predisposition to a skeletal-facial profile was identified[2].

By providing a wide range of genetic markers for constructing genetic maps, advanced molecular techniques have supported the discovery of DNA mutations. This has allowed us to study the hereditary predisposition of diseases. Mutations in the nucleic acid sequence can be detected using DNA sequencing. To better anticipate the outcome of subsequent development or therapy, it can assist orthodontists in identifying and addressing the hereditary component in a particular malocclusion[3].

Class II malocclusion is associated with the genes FGFR2. Genotyping involved conducting genome linkage scans to identify mutations in various mandibular genes and loci associated with Class II malocclusion. PAX5, SNAI3, MYO1H, TWIST1, and PAX7 are linked to craniofacial skeletal variance in patients with malocclusion, whereas FGFR2, MSX1, MATN1, MYOH1, ACTN3, GHR, KAT6B, HDAC4, and AJUBA genes are connected with mandibular skeletal malocclusion[4].

Many cell types, including osteoblastic cells, are controlled in migration and proliferation by fibroblast growth factor (FGF). By activating tyrosine kinase receptors (FGFRs) on the surface of target cells, FGFs exert their effects. On the other hand, their precise action mechanism is still unclear[5]. During craniofacial development, FGFR2 is prominently expressed in the mesenchyme of the developing maxilla and mandible, serving a crucial function in osteogenesis and sutural homeostasis[6]. FGFR2 has been identified as a skeletal malocclusion risk gene, and FGFR2 polymorphisms regulate its transcriptional expression and then osteogenic differentiation[7]. Exons 10 and 8 of the FGFR2 gene encode a segment of the immunoglobulin-like domain III of the receptor, which is critical for ligand binding specificity. Mutations in exon10, particularly missense mutations such as S252W and P253R, are commonly associated with Apert syndrome. These mutations cause constitutive stimulation of FGFR2 signaling, resulting in modified osteogenic differentiation and premature suture fusion[8,9]. Mutations in exon 8, including C342Y and C342R, are frequently linked to Crouzon and Pfeiffer syndromes[10].

This research aims to further the understanding of FGFR2-8 and FGFR2-10 in the formation of retrognathic mandibles and to correlate genetic variants with phenotypic traits.

Patients and Methods

Study design

This study was designed as an unmatched case-control study, conducted at the postgraduate clinic at the College of Dentistry, University of Sulaimani, and laboratories at the College of Medicine, University of Sulaimani. The Ethical Committee at the College of Dentistry, University of Sulaimani, approved the research project with Code No. (COD-EC-25-0089) on August 11, 2025.

Participants

The purpose, procedures, potential risks, and benefits of the study were fully explained to all participants. Participant confidentiality and data anonymity were maintained throughout the study.

The datasets used/or analyzed during the current study are available from the corresponding author upon reasonable request.

Sample Size

During the research period, 200 individuals with class II jaw relations seeking orthodontic treatment were recruited for this study. Regarding ethnic variations, the presence of true mandibular retrognathism is not a common condition in the examined society[11]. G*Power sample size justification was applied; 20 individuals were classified and chosen according to the inclusion criteria for classes II, and another 20 individuals with normal mandibular size and position were selected from the population. Because the diagnosis of mandibular retrognathism was made early during the growth spurt, which starts at 10-11 years old, the participants' ages ranged from 11 to 32 years old. Patients with previous orthodontic treatment or orthognathic surgery, a history of mandibular trauma, or systemic disease, and retrognathic mandible patients belonging to the same family were excluded.

Data collection

Cephalometric Analysis

Lateral cephalometric radiographs were taken for every 40 individuals using the Vatech Computed Tomography X-ray System (model: PHT-30LFO). Radiographs were

taken with the head in a neutral position, the teeth in centric occlusion, and the lips relaxed. A head and neck radiologist took all radiographs, following standardized protocols to ensure consistency and minimize distortion. The subjects were positioned using ear rods and a nasion support to stabilize the head and maintain a constant distance between the X-ray source, the patient, and the detector. Exposure parameters were standardized for all images: 83 kVp, 10.0 mA, scan time 12.3 sec, and DAP 20.17 mGy*cm². All radiographs were assessed for quality and clarity. WebCeph™ performed cephalometric tracing and analysis **(**AI-powered cloud-based cephalometric analysis software). This software automatically identified anatomical landmarks, and all landmark positions were manually verified and adjusted where necessary to ensure accuracy. Standard cephalometric parameters, including SNA (Sella-Nasion-A point angle), SNB (Sella-Nasion-B point angle), and ANB (A point-Nasion-B point angle), were assessed based on Steiner analysis[12]. Repeated tracing of 20% of samples was conducted by a professional orthodontist and all clinical and cephalometric radiographs were double-checked. Inter-examiner reliability was assessed between the AI and manual analyses using Cohen's kappa coefficient. The kappa value was 0.84, indicating almost perfect agreement between examiners ($p < 0.001$).

Saliva Sample Collection

To prevent contamination and changes in salivary flow, participants were instructed to refrain from eating, drinking (apart from water), smoking, chewing gum, and engaging in oral hygiene practices (such as brushing their teeth) for at least 1 hour before saliva sample collection. Before collection, participants relaxed for 5 minutes and rinsed their mouths with distilled water to remove food particles. Next, participants were asked to sit comfortably and allow saliva to pool in the mouth. They passively drooled into a pre-weighed, sterile polypropylene tube for 5–10 minutes until a minimum volume of 2 mL was obtained. Finally, samples were transported on ice and stored at –20°C, and kept for 2 weeks to prevent degradation[13].

Genetic Analysis

DNA Extraction

For genomic DNA extraction, the Presto™ DNA Kit (100 Preps) (Geneaid, Taiwan) was used according to the manufacturer's instructions.

Agarose Gel Electrophoresis

According to Sambrook and Russell's instructions[14]. The agarose gel was prepared by dissolving two tablets of agarose powder (0.5g each) in 100 ml of 1X TBE to prepare 1% agarose. Next, 10 µL (10 mg/ml) of Ethidium bromide was added to the prepared agarose. The gel runs at 90 volts and 70 mA for 60 minutes. All 40 DNA samples were checked for DNA availability using a Nanodrop (Jenway Genova Nano, UK), then subjected to gel electrophoresis, and the PCR products were subjected to electrophoresis. The bands of extracted genomic DNA were detected using a UV Transilluminator (Major Science, Taiwan).

PCR for Confirming Genes

For gene detection, PCR was used to amplify FGFR2-8 and FGFR2-10 genes. The forward and reverse primers, along with the PCR programs for the genes, are shown in Table 1. B codes for FGFR2-8 PCR products and C codes for FGFR2-10 PCR products. The numbers before letters B and C indicate the number of patients. (10CFGFR2-10CI) and (C1 10-1 10 F) represent the positive control (class I), and other samples represent (class II). (10CFGFR2-10CI) and (C1 10-1 10 F) represent the positive control (class I), and other samples represent (class II)

Sequencing of Genes

PCR products were sent to Macrogen (Seoul, South Korea) for Sanger sequencing.

Statistical Analysis

Patient demographic data, along with cephalometric measurements, have been tabulated in Microsoft Excel© for patients with a normal and a retrognathic mandible. The data was subjected to statistical analysis using the IBM SPSS statistical package version 29, and the DATAtab Team (2025). DATAtab: Online Statistics Calculator. DATAtab, e.U. Graz, Austria. For each cephalometric angle, a t-test was used to assess differences between normal and retruded-mandible patients. P-value set at < 0.001 to be considered significant.

For Genetic comparison measurements, BioEdit, Mega 11, and NCBI BLAST were used for molecular analysis. For blasting, each sequence was added to confirm identity (normal and retrognathic patients). After confirmation, we used BioEdit and Mega 11 to align the sequences of patients and normal individuals for FGFR2-8 and FGFR2-10 to build phylogenetic trees for both genes.

Table 1: presents the forward and reverse primers, along with the PCR programs, for the FGFR2-8 and FGFR2-10 genes.

Gene	Forward primer			Reverse primer		
FGFR2-8	5'GGTCTCTCATTCTCCCATCCC3'			5' CCAACAGGAAATCAAAGAACC 3'		
FGFR2-10	5' CCTCCACAATCATTCCTGTGTC 3'			5' ATAGCAGTCAACCAAGAAAAGGG 3'		
PCR program	Initial temp	Denaturation	Annealing	extension	No. of cycles	Final extension
FGFR2-8 FGFR2-10	94°C-5 min	94°C-45 sec	61°C-40 sec	72ºC-45sec	40	72°C-10 min

Results

Cephalometric analysis

The sample comprises 40 participants, 50% of whom have a Class I skeletal relationship and 50% have a Class II skeletal relationship. The cephalometric analysis data have been subjected to a normality test. The Shapiro-Wilk test result indicated that none of the measurement parameters deviated significantly from normality (p-value > 0.001). The p-values are as follows for SNA, SNB, and ANB (0.781, 0.061, and 0.124); accordingly, parametric tests were applied.

The demographic distribution of the data is summarized by patients' jaw relationships: 20 patients with class I and 20 with class II (Table 2). No missing data has been reported.

Table 3 presents the cephalometric readings and the two-sided independent samples t-test results. The mean value of the SNA angle for class I patients is within the normal limit (81.02 ± 3.57), as well as for the class II patients (80.92 ± 2.23), which indicates that the class II patients showed no statistical difference from class I patients (p-value = 0.918); in other words, their maxilla is normally positioned. While the value of the SNB angle for class I patients was (77.95 ± 3.6) and (74.55 ± 2.09) for class II patients, the t-test showed a significant difference between them (p-value < 0.001). The same result has been reported for the ANB angle; the mean value for class I patients was (3.11 ± 1.16) and (6.38 ± 1.85) for class II patients, the t-test also showed a significant statistical difference between the two groups (p-value < 0.001) in the measurements of SNA and SNB angles that reflect the skeletal relationships, with significant differences between retrognathic mandible patients and normal individuals confirming that patients are true class II.

The extracted DNA from 40 saliva samples was checked by nanodrop; the nanodrop gave a concentration of 20 ng to 100 ng/ml. After that, they were run by gel electrophoresis, and then PCR was used to detect FGFR2-8 and FGFR2-10. The PCR results for the two genes were confirmed by gel electrophoresis. Figure 1 shows a sample for PCR product gel electrophoresis. All sequences were analyzed using Mega 11 to produce a phylogenetic tree. For FGFR2-8 sequences, all cases were compared against the NCBI database for exon 8. The result was that all cases were similar in sequence except for 9B, 8-2B, and 8-1B. In 9B and 8-2B, there are multiple mutations in different locations. In 8-1B, this case has a mutation at 166 bp of the gene: guanine has converted to Adenine. Figure 2 shows the alignment of the current study sequences compared to the USA exon 8 FGFR2 gene sequence in NCBI. For FGFR2-10 sequences, all cases were compared against the NCBI database for exon 10. The result was that all cases were similar in sequence, except that 6C had a mutation in position 119 bp of the gene, Adenine nucleotide has converted to Cytosine nucleotide. It may be a point mutation. Figure 3 shows the alignment of the current study sequences compared to the USA exon 10 FGFR2 gene sequence in NCBI. All found mutations were point mutations and can be considered new SNPs (Single Nucleotide Polymorphisms).

All sequences were analyzed using Mega 11 to produce a phylogenetic tree as shown in Figures 4 and 5. Figure 4 shows the phylogenetic tree for the FGFR2-8 gene. This phylogenetic tree demonstrates that the samples are divided into three main groups: the first group contains one class I individual and three class II patients, the second group contains one class I individual and two class II patients, and the third group contains five class II patients, which are genetically closer to the second

group than the first group. Figure 5 shows the phylogenetic tree for the FGFR2-10 gene. This phylogenetic tree demonstrates that the samples are divided into four groups. The first group contains two class I individuals and two class II patients that are genetically closest to class I.

The second group contains three class II patients; these eight patients are genetically further from the first group's class II. The third group contains two class II patients, who are the same distance from the class I cases. The last group consists of three class II patients, who are the furthest from group one.

Table 2: Demographic distribution of the data according to the sex of participants.

Sex	Class	Frequency	Minimum	Maximum	Mean ± Std.
Female	Class I	11	11	32	20 ± 6.56
	Class II	10	15	26	21.6 ± 2.88
Male	Class I	9	11	32	20.44 ± 7.37
	Class II	10	11	18	14.9 ± 2.47

Table 3: Cephalometric measurements.

		Frequency	Minimum	Maximum	Mean ± Std.	p-value
SNA	Class I	20	75.62	87.55	81.02 ± 3.57	0.918
	Class II	20	76.56	84.38	80.92 ± 2.23	
SNB	Class I	20	72.44	83.39	77.95 ± 3.6	>0.001
	Class II	20	69.67	78.36	74.55 ± 2.09	
ANB	Class I	20	0.6	4.81	3.11 ± 1.16	>0.001
	Class II	20	3.37	10.03	6.38 ± 1.85	

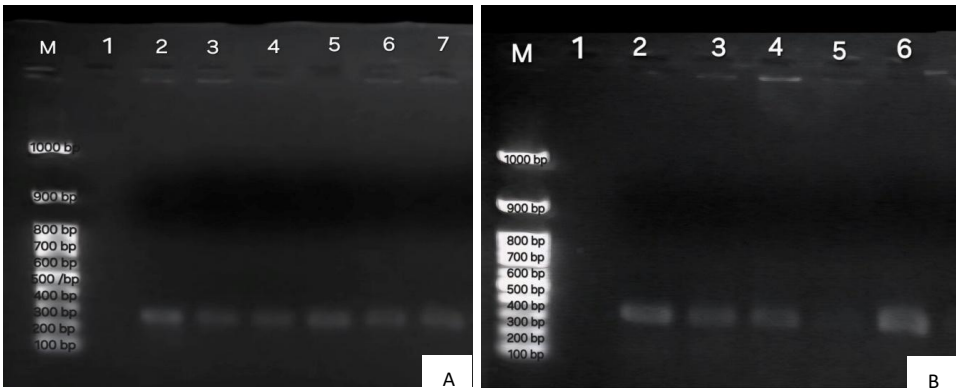

Figure 1: Shows the FGFR2-8 and FGFR2-10. (A): Lane M represent the DNA ladder (Marker 100-1000 bp), Lane 1 is negative control, Lane 2-7 represent DNA bands size 257 bp of FGFR2-10. (B): Lane M represent the DNA ladder (Marker 100-1000 bp), Lane 1 is negative control, Lane 2-6 represent DNA bands size 325 bp of FGFR2-8.

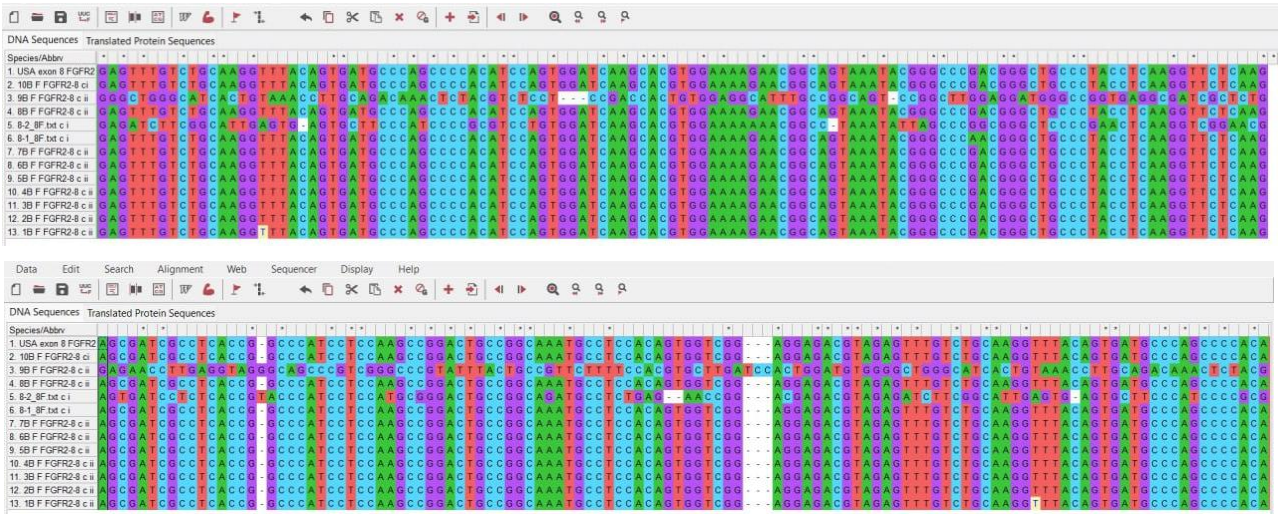

Figure 2: Shows the alignment of the current study sequences compared to USA exon 8 FGFR2 gene sequence in NCBI. Acc.No. Y17131.1.

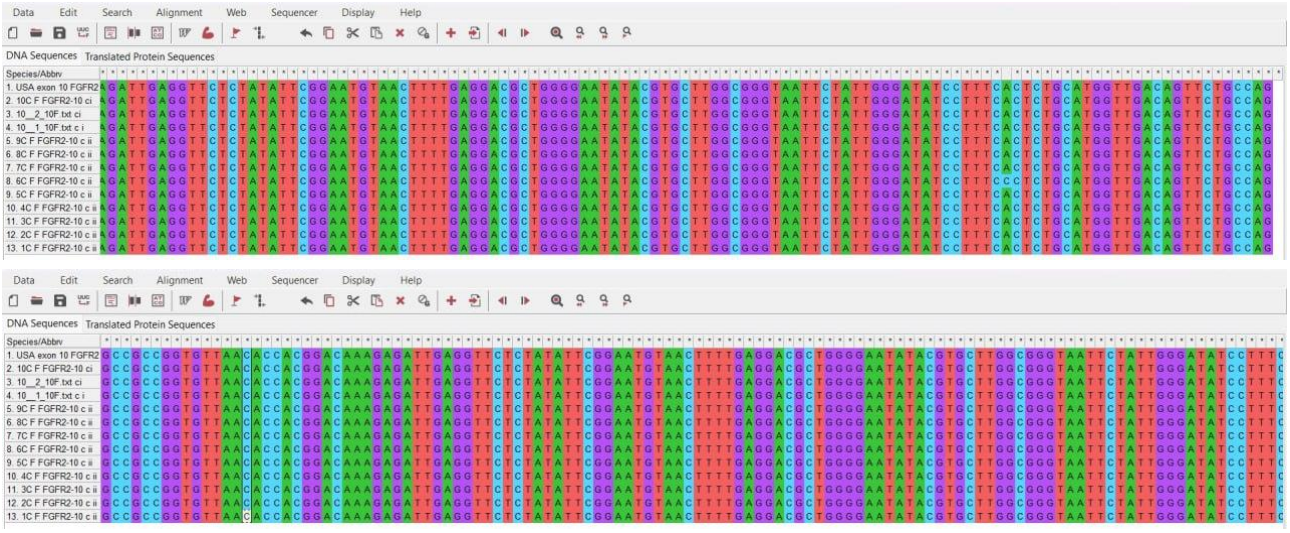

Figure 3: Shows the alignment of the current study sequences compared to USA exon 10 FGFR2 gene sequence in NCBI, Acc.No. AF169399.

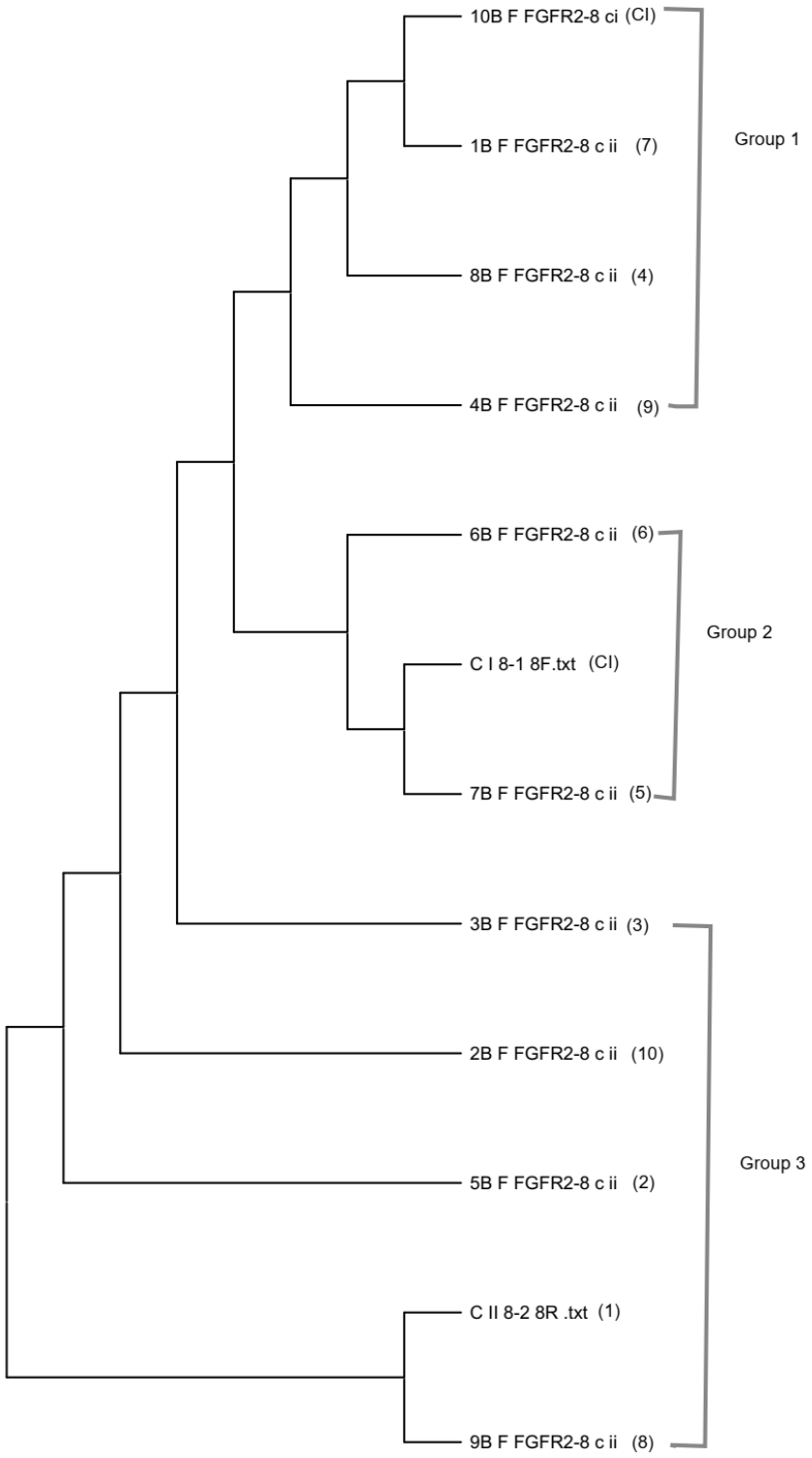

Figure 4: Phylogenetic tree for the FGFR2-8 gene. Compared with (10BFGFR2-8CI) and (C18-18F), which represent the positive control (class I), the other samples represent (class II). The phylogenetic tree shows three main groups: group (1), group (2), and group (3). group (1) includes (1) class I and (3) class II, group (2) includes (1) class I and (2) class II, and group (3) includes (5) class II. The brackets on the right side of the sample codes contain numbers indicating clinical severity as assessed by cephalometric radiography. Number (1) indicates the least severe, while 10 indicates the most severe.

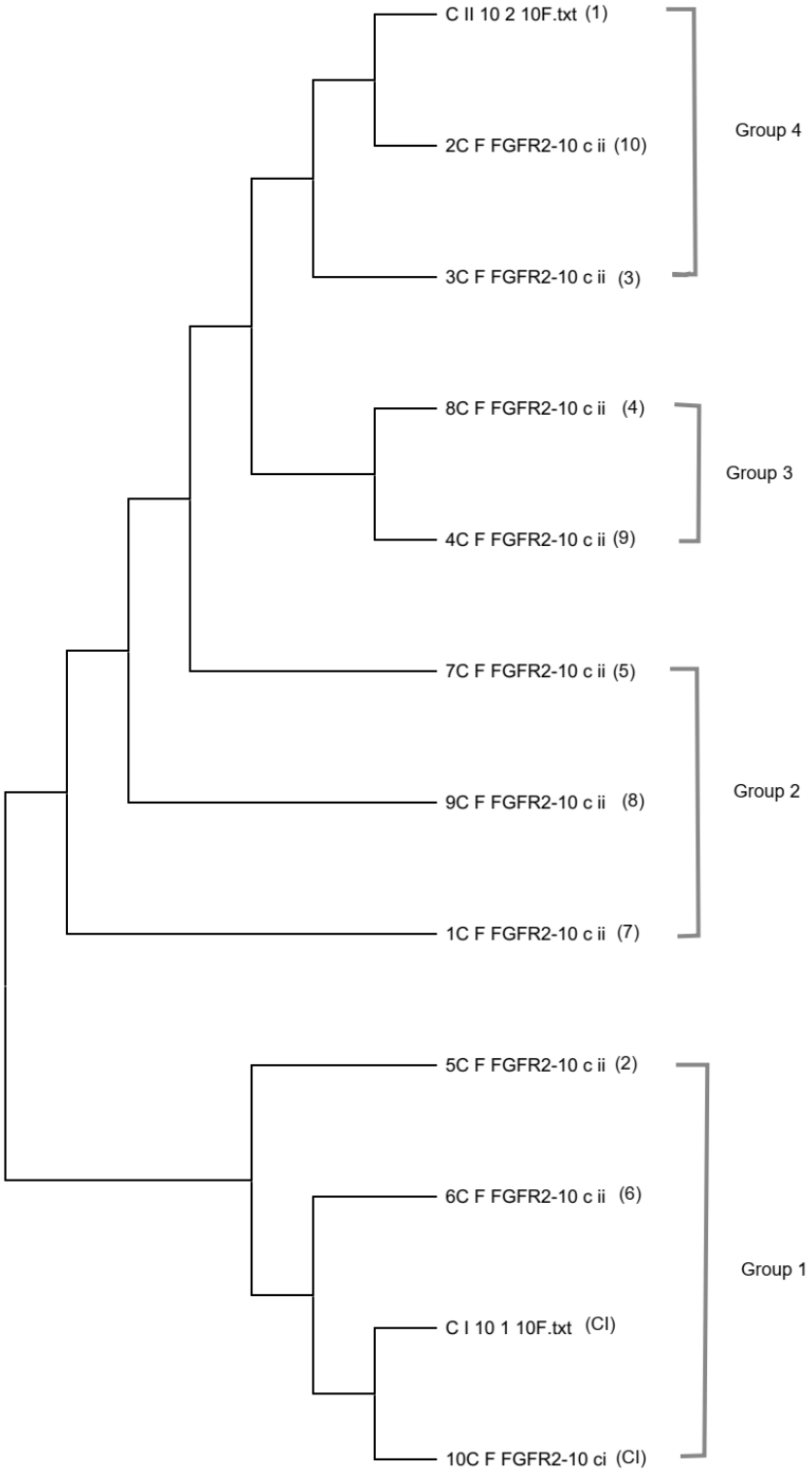

Figure 5: Phylogenetic tree for the FGFR2-10 gene. Compared with (10CFGFR2-10CI) and (C1 10-1 10 F), which represent the positive control (class I), the other samples represent (class II). The phylogenetic tree shows four main groups: group (1), group (2), group (3), and group (4). Group (1) includes (2) class I and (2) class II; group (2) includes class II, group (3) includes (2) class II, and group (4) includes (3) class II. The brackets on the right side of the sample codes contain numbers indicating clinical severity as assessed by cephalometric radiography. Number (1) indicates the least severe, while (10) indicates the most severe.

Discussion

According to the phylogenetic tree, this study found that the selected genes (FGFR2-10 and FGFR2-8) exhibit sequence variation between retrognathic mandibles and normal individuals. Thus, this result rejects the null hypothesis that there are no differences in the order of the selected genes between retrognathic mandibles and normal individuals. Also, it answers the question, "Is it possible to predict mandibular retrognathism by genetic analysis?" The results reveal that yes, it is possible. This research is a novel genetic study of the selected genes (FGFR2-10 and FGFR2-8) in patients with retrognathic mandibles of Kurdish nationality in the Kurdistan region of Iraq. It is hoped that this variation in the sequence of these genes could be used to detect mandibular retrognathism early, enabling interceptive orthodontic therapy or preparation for orthognathic surgery to shorten treatment time and achieve more stable results.

All sequences were analyzed using Mega 11 to produce a phylogenetic tree. For FGFR2-8 sequences, all cases were compared against the NCBI database for exon 8. All cases were similar in sequence except for 9B, 8-2B, and 8-1B. In 9B and 8-2B, multiple mutations occur at different locations. In 8-1B, this case has a mutation at 166 bp of the gene: guanine has converted to Adenine. Figure 2 shows the alignment of the current study sequences with the USA exon 8 FGFR2 gene sequence from NCBI. For FGFR2-10 sequences, all cases were compared against the NCBI database for exon 10. The result was that all cases were similar in sequence, except that 6C had a mutation in position 119 bp of the gene, Adenine nucleotide has converted to Cytosine nucleotide. It may be a point mutation. Figure 3 shows the alignment of the current study sequences with the USA exon 10 FGFR2 gene sequence from NCBI. All found mutations were point mutations and can be considered new SNPs (Single Nucleotide Polymorphisms).

As shown in Figure 4, the phylogenetic tree of FGFR2-8 divides the samples into three groups: group (1), group (2), and group (3). Numbers on the right side indicate clinical severity, which is assessed using cephalometric radiographs; number (1) is the least severe, and number (10) is the most severe class II. The first group contains four clades: one class I and three class II. 10B has been proven to be genetically and clinically class I, with an ANB of 1.4°. 1B is proved to be genetically and in cephalometric analysis class II, with ANB of 5.47° and SNB of 74.650°; it has a level (7) of severity. 1B genetically is the closest class II case as compared to 10B, which is class I of this group. 8B, which is class II genetically and clinically, with ANB 7.75 and SNA 74.57°, has level (4) of severity. 4B is proven to be class II clinically and genetically, with an ANB of 8.14 and SNB of 76.03°, and it has a level (9) of severity. Genetically, 8B is positioned further away than both 1B and 10B, while 4B is the most distant class II in this group. The second group consists of three clades: one class I and two class II. The lateral cephalometric radiograph indicates that (C1 8-1) is class I with an ANB of 4.0°, which agrees with the genetic result, as confirmed by the phylogenetic tree. 7B is proved to be class II both genetically and clinically, with ANB 3.82° and SNB 72.75°; it has a level (5) of severity. It is the closest class II of this group to (C1 8-1), which is class I of this group. 6B is proved to be class II both genetically and clinically, with an ANB of 7.72° and SNB of 76.63°; it has a level (6) of severity; it is further classified as more class II than 7B. The third group consists of five clades of class II. 3B is the closest sample of the third group to the second group; it is genetically and clinically class II, with an ANB of 5.31° and SNB of 78.36°, and it has a level (3) of severity. 2B is further than 3B, which is also genetically and clinically class II, with an ANB of 10.03° and an SNA of 74.34°; it has a level (10) of severity. 5B is at a further distance than 3B; 5B is class II genetically and clinically, with an ANB of 6.26° and with SNB of 80.95°, it has level (2) of severity. (C II 8-2) and 9B are both at the same distance, the furthest samples of the third group, and are both proven to be class II genetically and clinically. (C II 8-2), with ANB of 3.37° and SNB of 78.24°, has a severity level (1). 9B, with ANB of 3.45° and SNB of 73.94°, has a level (8) of severity.

As shown in Figure 5, when the FGFR2-10 gene sequences of class II patients are compared with those of class I individuals, four groups (1-4) are identified. Numbers on the left indicate clinical severity, assessed on a cephalometric radiograph; number 1 is the least severe, and number 10 is the most severe class II. In group (1), there are four clades, two of which indicate class I; the furthest clade is 5C, and the nearest is 6C. In the first group, the lateral cephalometric radiograph shows a class I (C1 10 1) with ANB 4.0°, which agrees with the genetic result, as confirmed by the phylogenetic tree. Based on the lateral cephalometric radiograph, 10C was class I with an ANB of 1.4°, which also agreed with the genetic result, as confirmed by the phylogenetic tree. These two normal samples are in the same clade. 6C is a class II, shown genetically to be closest to the class I clade, but clinical results from cephalometric radiographs showed an ANB of 7.72° and an SNB of 76.63°; it has a level (6) of severity. The 5C is class II genetically and clinically, with an ANB of 6.26° and

with SNB of 80.95°; it has a level (2) of severity and is further from class I individuals in comparison to 6C. The following three samples are grouped into group (2) genetically according to the phylogenetic tree of Figure 3. 1C has proven to be class II both genetically and clinically, with ANB of 5.47° and SNB of 74.65°; it has a level (7) of severity. 9C is proven to be class II both genetically and clinically, with ANB of 3.45° and SNB of 73.94°; it has a level (8) of severity. 7C has been proven to be class II both genetically and clinically, with ANB 3.82° and SNB 72.75°, and it has a level (5) of severity. 1C is the nearest clade to group 1, while 7C is the furthest clade of this group. The third group is formed by two cases: 4C, which is proven to be class II both genetically and clinically, with ANB of 8.14° and SNB of 76.03°, has level (9) of severity, and 8C, which is class II both genetically and clinically, with ANB of 7.75° and SNA 74.57°, has level (4) of severity; they are genetically closest to each other and the same distance from group 1. The fourth group consists of three samples. 3C is genetically class II with ANB of 5.31° and SNB of 78.36°; it has a level (3) of severity. 3C is the closest one to group 1. 2C and (C II 10 2) are genetically at the same distance, and they are the furthest samples from group 1 samples, with 2C having an ANB of 10.03° and SNA of 74.34°; it has a level (10) of severity, which is the most severe class II case clinically. (C II 10 2) has an ANB of 3.37° with SNB of 78.24° and level (1) of severity, which means it is the least severe class II case clinically.

Many studies have been done on FGFR2 in Iraq[15], Iran[16], Turkey[17], and Saudi Arabia[18]. These studies examined the contribution of FGFR2 to breast cancer and Craniosynostosis, but no study has examined the use of these genes for detecting class I, class II, and class III in this area. Other researchers who have studied skeletal class I, class II, and class III have found SNPs in FGFR2[19]. A systematic review has stated that, through reviewing and reanalyzing available human studies, 19 genes were found to be associated with skeletal class II malocclusion, FGFR2 being one of these genes[20]. However, the existing literature predominantly reports associations involving intronic regions of the FGFR2 gene.

Finally, when comparing FGFR2 exon 8 and exon 10, exon 10 is more promising for detecting class I and class II, because the controls of FGFR2-10 were in the same group on the phylogenetic tree, while controls of FGFR2-8 formed two different groups, so it is recommended to conduct further study on FGFR2-8 to inspect its specificity. None of the genes were specific for detecting the severity of class II cases compared to clinical and radiographic analysis. According to the results of this study, exon 10 of the FGFR2 gene can serve as a biomarker to identify patients with retrognathic mandibles.

The primary outcome of this study was the genetic comparison between class I and class II individuals; the secondary outcome was the relationship between lateral cephalometric radiographs and genetic results. This study found that FGFR2-10 is a diagnostic marker for class II patients, which strengthens this study's findings.

This study had several limitations. First, regarding sample size, there were few cases of true retrognathic mandibles. In a study conducted by Nadir and Amin 2024 in Sulaimani city[11], the facial angle and Frankfort mandibular plane angle FMA showed a statistically significantly higher value in Class II patients than in Class I patients. Finding the perfect individual was difficult because our inclusion criteria required that all participants in this study have sought orthodontic treatment for a retruded mandible and decreased facial height. A second limitation of this study was the lack of laboratory standardization. Cost and time constraints, which limited the use of cutting-edge technology and the duration of data collection, may have affected the generalizability and comprehensiveness of the findings. Despite these limitations, the findings of this study provide valuable information and lay a base for future studies in the area.

Conclusion

This study indicates that FGFR2-10 may be specific for detecting class II malocclusion, whereas FGFR2-8 lacks specificity. The differences in the sequence of these genes are suggested for the early detection of mandibular retrognathism, enabling interceptive orthodontic therapy or preparation for orthognathic surgery to reduce treatment duration and enhance stability. In this study, a point mutation was identified in two patients; further studies are required to confirm that this mutation is an SNP.

References

1. Oueis R, Waite PD, Wang J, Kau CH. Orthodontic-Orthognathic Management of a patient with skeletal class II with bimaxillary protrusion, complicated by vertical maxillary excess: A multi-faceted case report of difficult treatment management issues. Int Orthod. 2020;18(1):178-90.
2. Nanci A. Ten Cate's Oral Histology-E-Book: Ten Cate's Oral Histology-E-Book. Elsevier Health

Sciences; 2024.
3. Sharma P, Patil A, Sharma S, Rout T, Hemgude P, Sabane A. Presence of single nucleotide polymorphisms in transforming growth factor β and insulin-like growth factor 1 in class II malocclusions due to retrognathic mandible. Folia Med (Plovdiv). 2024;66(2):243-9.
4. George AM, Felicita AS, Milling Tania SD, Priyadharsini JV. Systematic review on the genetic factors associated with skeletal Class II malocclusion. Indian J Dent Res. 2021;32(3):399-406.
5. Novais A, Chatzopoulou E, Chaussain C, Gorin C. The potential of FGF-2 in craniofacial bone tissue engineering: a review. Cells. 2021 Apr 17;10(4):932.
6. Zhao X, Erhardt S, Sung K, Wang J. FGF signaling in cranial suture development and related diseases. Front Cell Dev Biol. 2023;11:1112890.
7. Jiang Q, Mei L, Zou Y, Ding Q, Cannon RD, Chen H, et al. Genetic polymorphisms in FGFR2 underlie skeletal malocclusion. J Dent Res. 2019;98(12):1340-7.
8. Al-Namnam NM, Jayash SN, Hariri F, Rahman ZAA, Alshawsh MA. Insights and future directions of potential genetic therapy for Apert syndrome: A systematic review. Gene Ther. 2021;28(10-11):620-33.
9. Li F, Meyer AN, Peiris MN, Nelson KN, Donoghue DJ. Oncogenic fusion protein FGFR2-PPHLN1: Requirements for biological activation, and efficacy of inhibitors. Transl Oncol. 2020;13(12):100853.
10. Liu J, Nam HK, Wang E, Hatch NE. Further analysis of the Crouzon mouse: effects of the FGFR2(C342Y) mutation are cranial bone-dependent. Calcif Tissue Int. 2013;92(5):451-66.
11. Nadir HH, Amin AA. Cephalometric assessment of skeletal class II malocclusion in a sample of kurdish population in Sulaimani city (Retrospective Study). Sulaimani Dent J. 2025;11(1):18-26.
12. Mohammed SA, Ali TM, Rashid ZJ. Evaluation of Skeletal Jaw Relation by Different Cephalometric Angles for Sample of Kurdish Young Adults in Sulaimani City-A Cephalometric Study. Sulaimani Dent J. 2022;9(1):21-30.
13. Yu KM, Lee AM, Cho HS, Lee JW, Lim SK. Optimization of DNA extraction and sampling methods for successful forensic microbiome analyses of the skin and saliva. Int J Legal Med. 2023;137(1):63-77.
14. Wittmeier P, Hummel S. Agarose gel electrophoresis to assess PCR product yield: comparison with spectrophotometry, fluorometry and qPCR. Biotechniques. 2022;72(4):155–8.
15. Slman ZA, Umran MA, Alwachi HK. Polymorphism of FGFR2 gene in breast cancer of Iraqi patients. Onkologia I Radioterapia. 2023;17(11):1.
16. Hosseini Mojgan, Houshmand Massoud, Froozan Shima. Association of FGFR2 and TOX3 genetic variants with the risk of breast cancer in Iranian women. Arch Breast Cancer. 2018;5(3):118-21
17. Nur BG, Pehlivanoğlu S, Mıhçı E, Çalışkan M, Demir D, Alper ÖM, et al. Clinicogenetic study of turkish patients with syndromic craniosynostosis and literature review. Pediatr Neurol. 2014;50(5):482-90.
18. Alghamdi M, Alhumsi TR, Altweijri I, Alkhamis WH, Barasain O, Cardona-Londoño KJ, Ramakrishnan R, Guzmán-Vega FJ, Arold ST, Ali G, Adly N. Clinical and genetic characterization of craniosynostosis in Saudi Arabia. Frontiers in Pediatrics. 2021;9:582816.
19. Ardani IGAW, Budipramana M, Rachmawati E, Nugraha AP, Ardana IKKG, Budhy TI, et al. COL1A1 and FGFR2 single-nucleotide polymorphisms found in class II and class III skeletal malocclusions in Javanese population. Eur J Dent. 2023;17(1):183-90.
20. Gershater E, Li C, Ha P, Chung CH, Tanna N, Zou M, et al. Genes and pathways associated with skeletal sagittal malocclusions: a systematic review. Int J Mol Sci. 2021;22(23):13037.

Original Article

Comparative Evaluation of Three Electronic Apex Locators in Determining Working Length: An In-Vitro Study

Adil O. Abdullah[1,2*], *Aso M. Abdulkarem*[1], *Zana A. Hamadameen*[1]

Abstract

Objective: The purpose of this in-vitro study was to determine the precision of three electronic apex locators (AppleDent AL, Eighteeth AL, and Coxo AL) in determining the working length (WL) of root canals using extracted human teeth. Although several new apex locator models have recently become commercially available, independent evidence regarding their measurement accuracy remains limited, underscoring the need for objective evaluation.

Methods: A total of 90 freshly extracted human permanent single-rooted teeth with mature apices were standardized. Access cavities were prepared and canal patency was controlled (with a 10 K file) and AWL (with size 15 K file at ×25 magnification) were detected by the stereomicroscope. After embedding them in alginate to recreate the periodontium, teeth were randomly divided into 3 groups (n = 30). The average of 3 repeated measurements was used for the calculation of the EWL in each group. The value of AWL and EWL have been calculated. The accuracy was measured under ±0.5 mm and ±1.0 mm. Data were statistically treated with Shapiro-Wilk test (to assess data normality), Levene´s test, one-way ANOVA and Tukey's post hoc testing (α = 0.05).

Results: In comparison with Eighteeth AL (0.41 ± 0.27 mm), the mean deviations of AppleDent AL and Coxo AL from AWL were by a lower level (by 0.24 ± 0.58 mm and by 0.24 ± 0.33 mm, respectively). Precision within ±0.5 mm was 50.0%, 86.7%, and 73.3% for AppleDent, Coxo, and Eighteeth models, respectively. All devices achieved a 90% or greater accuracy within ±1.0 mm. The ANOVA analysis confirmed that Eighteeth was different from AppleDent and Coxo (p = 0.012), which the Tukey's test also confirmed.

Conclusions: All 3 electronic foramen locators showed clinical accuracy. Coxo AL performed far better, while AppleDent AL showed similar mean scores, but had higher variability, and Eighteeth overestimated the working length.

Keywords: *Endodontics, Dental instruments, Root canal preparation, Dental pulp test, Tooth apex.*

Submitted: October 17, 2025, Accepted: January 12, 2026, Published: April 1, 2026.

Cite this article as: Abdullah AO, Abdulkarem AM, Hamadameen ZA . Comparative Evaluation of Three Electronic Apex Locators in Determining Working Length: An In-Vitro Study. Sulaimani Dent J. 2025;13(1):20-27.

DOI: https://doi.org/10.17656/sdj.10218

1. *Dental Assistant Department, Erbil Technical Medical Institute, Erbil Polytechnic University, Erbil, Iraq.*
2. *Endodontics Department, Faculty of Dentistry, Tishk International University, Erbil, Iraq*

** Corresponding author*: *adil.abdullah@epu.edu.iq.*

Introduction

Effective endodontic treatment depends on complete debridement, shaping, and obturation of the root canal system with minimal disturbance to periapical structures[1]. It is important to establish the working length (WL), defined as the distance from a coronal reference point to the apical constriction beyond which preparation and obturation do not extend[1]. Both under-instrumentation and over-instrumentation may be detrimental to the outcome of treatment: apical trauma leading to impaired healing through over-instrumentation and infected material remaining as a nidus for infection within canal dimensions[2-3].

Working length confirmation was based on tactile sensation and radiographic evidence[13]. Conventional radiographs are useful, but they are two-dimensional, suffer from distortion and superimposition due to overlying structures, and contribute to cumulativeexposure for the patient[4-6]. When canals are curved, when they have apical resorption, or when they diverge[5-6], the reliability of these measurements decreases. Later, in the middle of the 20th century, with an attempt to overcome these shortcomings, electronic apex locators (EALs) were introduced and became indispensable[6-7].

Current devices use multifrequency impedance ratios, allowing for a better localization of the apical constriction even in irrigant-filled conditions[2,7-8]. Clinical tests also show that the root canal length at which new EALs can detect is within 0.5 mm from the apical constriction in more than 95%[9-10] and the measuring accuracy of most vendors′ models is ±0.5 mm. The Root ZX, Raypex, and Apex ID are commercially validated devices that serve as standards[11-12].

There is a need for independent confirmation[12], since gadgetry keeps rolling out. Power generation: owing to pressure from manufacturers, power generators strive for cheapness, convenience of use or technical innovation even when evidence supporting alternative development models is weak[13]. Evaluation should be conducted for new instruments such as AppleDent AL, Eighteeth AL and Coxo AL.

Developments in apex locator technology mirror this idea, with devices designed to address biological conditions within the root canal system 13. Studies on Multi-Frequency Impedance Analysis MFA technology indicate that by analyzing electric signals at multiple frequencies more accurate readings can be achieved, especially in the presence of irrigants and complex canal shapes[12-13]. The importance of accurately recording the presence of a signal and adapting to biological variation, as described with regard to apex locators, underscores the need for dentists to have a precise method for measuring working length (WL) in endodontics[13].

The purpose of this study was to assess the accuracy of three electronic apex locators (AppleDent AL, Eighteeth AL, and Coxo AL) in determining working length for extracted human teeth under controlled in vitro conditions. The null hypothesis was that there would be no differences in precision among the devices.

Materials and methods

Sample selection

The sample selection was performed using 90 freshly extracted human permanent single-rooted teeth (N = 90) with fully developed apices. Teeth that had caries into the root, fractures, resorption, calcifications or previous endodontic treatment were excluded. Following extraction, the attached calculus and soft tissue residues were removed with an ultrasonic scaler, and the teeth were stored in 0.1% thymol at room temperature until use. The teeth were examined under a stereomicroscope (×25 magnification) before the start of the experiment to verify that no fissures, fractures, or open apices existed.

The Ethical Committee at the Erbil Polytechnic University approved the research project with Code No. (25 / 0081 HRE) on February 20, 2025.

Preparation of samples

Standard access preparations were performed in all specimens using a high-speed diamond bur (ISO 014 size, Dentsply, Ballaiges, Switzerland) under constant water irrigation. A size 10 K-file (Dentsply Maillefer, Ballaigues, Swiss) was inserted in the canal for patency test. Actual working length (AWL) through the penetration of a size 15 K-file to be barely visible at the apical foramen determined and observed into a stereomicroscope. The measured length was adjusted by subtracting 0.5 mm to obtain the AWL as the control standard.

The canals were irrigated with 2.5% NaOCl and saline alternately during instrumentation to remove debris. Before EAL measurement, canals were gently dried with paper points to remove excess irrigant while maintaining slight moisture, as completely dry or overly wet canals may compromise electronic length readings. The shape of the coronal third was achieved by flaring with Gates-Glidden drills (numbers 2 and 3) and preparing the canals to a size 25 K-file in all specimens.

Embedding process

Each tooth was embedded in fresh-mixed alginate within a plastic mold to simulate the periodontium and provide an electrically conductive medium for electronic measurements. The upper segment of the root was entirely encapsulated in alginate to ensure conductivity. Alginate was reconstituted prior to each test session to ensure consistent moisture and conductivity.

Research cohorts and digital working length measurements

The 90 teeth were evenly and randomly distributed among 3 experimental groups (n = 30): Group 1–-AppleDent electronic apex locator (AppleDent, Hong Kong, China), Group 2–Eighteeth electronic jusapex locator (Changzhou Sifary Medical Technology Co., Ltd., Jiangsu, China), and Group 3—Coxo electronic apex finder Coxo (Foshan Coxo Medical Instrument Co., Ltd., Guangdong, China) Figure 1. The suffix "AL" used in this study corresponds to the model designation found on the product labels and instruction manuals of the tested devices, although it may not consistently appear in all online listings.

The three electronic apex locators tested in the present study were AppleDent AL (left), Eighteeth AL (middle), and Coxo AL (right) (Figure 1).

A size 15 K-file was attached to the file holder for each EAL in all groups. The instrument was carefully inserted into the canal up to the point where the apical constriction was indicated (0. 0 or an apex mark in the read-out on display). The silicone stopper was placed at the reference point of the coronal (crown), and the file was withdrawn. The length was measured with a digital caliper (Mitutoyo Corporation, Kawasaki, Japan) with 0.01 mm precision, as shown in Figure 2.

All measurements were repeated 3 times for each sample, and the mean value was used as the electronic working length (EWL). A complete overview of the study process is illustrated in Figure 3.

Figure 3 is a flowchart of the experimental design, including how samples were selected, prepared, and divided into groups, the measurement method, and data collection/analysis.

Data acquisition and precision evaluation

The difference between the EWL achieved with each device and the AWL (reference standard) was calculated for each sample. A tolerance of Â±0.5 mm from the AWL was considered clinically acceptable, while a larger tolerance (Â±1.0 mm) was also investigated later.

Quantitative analysis

All statistical analyses were performed using SPSS for Windows, Version 25.0 (IBM Corp., Armonk, NY). Normality of the data distribution was tested using the Shapiro–Wilk test. To evaluate homoscedasticity of variance between groups, Levene's test for equality of variances was used. Sample size was estimated in advance using G*Power software (version 3.1.9.7; Heinrich-Heine-Universität Düsseldorf, Germany), considering the effect size of f = 0.25 (medium effect) with $\alpha = 0.05$ and statistical power $(1–\beta)=0.80$, suggesting a minimum of 30 samples for each group to be appropriate.

Parametric testing assumptions were met, and the average difference among the three groups was compared using one-way ANOVA. Post hoc pairwise comparisons were carried out using Tukey's HSD (honestly significant difference) test. Statistical significance was defined as a p-value < 0.05.

Figure 1: The three electronic apex locators assessed in this study are AppleDent AL (left), Eighteeth AL (center), and Coxo AL (right).

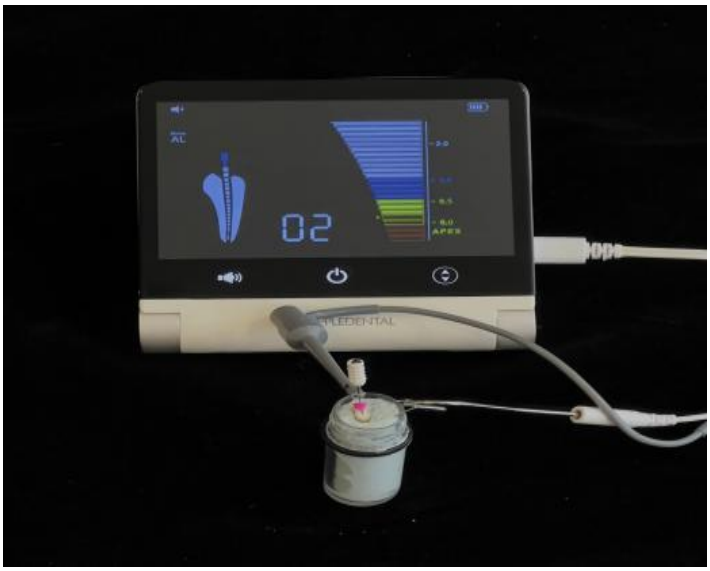

Figure 2: Experimental configuration illustrating the AppleDent electronic apex finder linked to a tooth encased in alginate for the purpose of ascertaining working length.

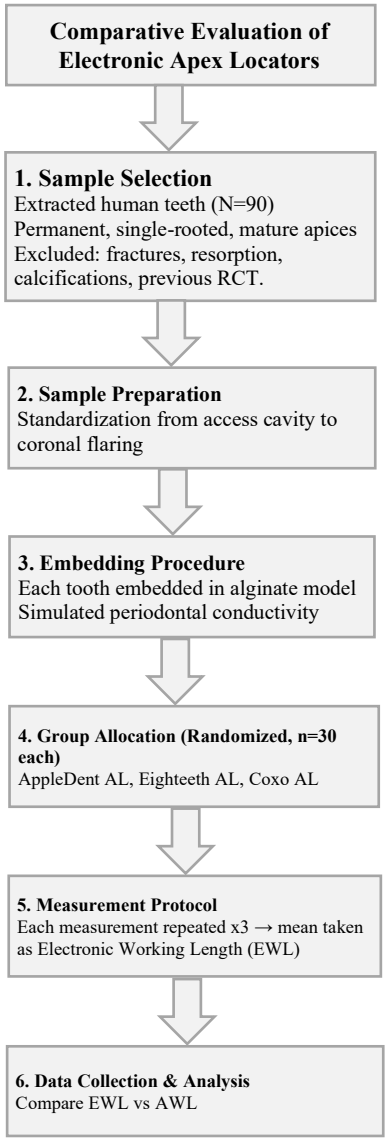

Figure 3: Flow diagram illustrating the study design, encompassing sample selection, preparation, grouping, measurement methodology, and data collection/analysis.

Results

Analysis was based on 90 measurements (N = 90, n = 30 per group). The AWL, determined under magnification, was used as the final reference standard for comparing with the EW length (EWL) acquired by three EALs: Eighteeth AL (Changzhou Sifary Medical Technology Co., Ltd., Jiangsu, China), Coxo AL (Foshan Coxo Medical Instrument Co., Ltd., Guangdong, China), and AppleDent AL (AppleDent, Hong Kong, China).

Mean differences (EWL – AWL) and standard deviations are summarized in Table 1. Eighteeth AL had a tendency to overestimate canal length, with the highest mean positive deviation (0.41 mm). The absolute mean deviations of Coxo AL and AppleDent AL were lower (0.24 mm). For Coxo AL, variability was lower (SD = 0.33 mm) than in AppleDent AL (SD = 0.58 mm). The accuracy of all 3 EALs tested was clinically acceptable at determining the working length. Coxo AL presented the best compromise between accuracy and precision, AppleDent AL displayed similar mean values but a higher variance; Eighteeth AL made overestimations of working length points that were significantly greater than recorded by the other two devices.

Table 2 summarizes the percentage of measurements within an acceptable clinical tolerance (±0.5 mm and ±1.0 mm) limits. AppleDent AL showed the least proportion at ±0.5 mm (50.0%) but reached 90% at 1.0 mm. Coxo AL presented a higher precision of 0.5 mm (86.7%), and Eighteeth AL showed an intermediate value (73.3%). When the matching tolerance was increased to 1.0 mm, both Coxo AL and Eighteeth AL achieved 100% accuracy.

The One-way ANOVA showed that mean deviations differed significantly between the nine subjects ($p = 0.012$). Post hoc analysis by Tukey's multiple comparisons test disclosed significant difference between Eighteeth AL and Coxo AL ($p < 0.018$), as well as between Eighteeth AL and AppleDent AL ($p < 0.027$), while the difference observed in Coxo AL vs. AppleDent AL was not statistically significant with $p = 0.64$ (Table 3).

Table 1: Mean differences (EWL – AWL) accompanied by standard deviations (mm) for the three electronic apex locators.

Apex locator	Mean difference (mm) ± SD
Eighteeth AL	0.41 ± 0.27
Coxo AL	0.24 ± 0.33
AppleDent AL	0.24 ± 0.58

Table 2: The precision of the three apex locators falls within acceptable tolerance limits.

Apex locator	≤ ±0.5 mm (n/30, %)	≤ ±1.0 mm (n/30, %)
Eighteeth AL	22/30 (73.3%)	30/30 (100%)
Coxo AL	26/30 (86.7%)	30/30 (100%)
AppleDent AL	15/30 (50.0%)	27/30 (90.0%)

Table 3: Results of one-way ANOVA and Tukey's post hoc pairwise comparisons for mean differences (EWL – AWL).

Pairwise comparison	Result
Eighteeth AL vs AppleDent AL	p = 0.027 (significant)
Eighteeth AL vs Coxo AL	p = 0.018 (significant)
Coxo AL vs AppleDent AL	p = 0.640 (NS)

NS = non-significant; AWL = actual working length; EWL = electronic working length.

Discussion

The purpose of this study was to evaluate the precision of 3 EALs: AppleDent AL, Eighteeth AL, and Coxo, in determining the working length of extracted teeth. The findings showed that Coxo AL was the most accurate within ±0.5 mm, AppleDent AL exhibited more dispersion than the other groups, and Eighteeth AL predominantly overestimated WL. All devices achieved clinically acceptable accuracy when in their optimal position (±1.0 mm). The rationale behind this research was the growing uncertainty surrounding the accuracy of newer, commercially available EALs, many of which enter the market without strong independent evaluation. Because clinicians depend on precise WL determination for predictable outcomes, comparing these devices under similar conditions was necessary to clarify their reliability. This study provides missing evidence and helps contextualize how each EAL performs in practice.

Accordingly, the null hypothesis of no significant differences among the three devices was partially rejected. There was a significant difference between Eighteeth AL and both AppleDent AL and Coxo AL, but no significant difference between AppleDent AL and Coxo AL.

Regarding Eighteenth AL, the overestimation is of clinical importance through causing apical perforation and removal of irrigation or filling materials, followed by periapical tenderness[14-15]. Similar results have been found in previous in-vitro studies highlighting the device-specific differences in impedance algorithms[16-19]. The high accuracy of Coxo AL is in accordance with other laboratory evaluations of next-generation EALs. AppleDent AL was inconsistent in performance, though mean values were similar; a shortfall was identified in other studies involving new devices[19-22].

The results are consistent with the previous studies showing that there is a general reliability of ±1.0 mm for most electronic apex locators[23-26]. Although significant differences were reported in different models by standardized protocols, with most adopting technological improvements, independent validation is still essential before implementing them into clinical settings[27-28].

From the treatment viewpoint, Coxo AL appears to be the most reliable for apical precision. Eighteenth AL is acceptable within ±1.0 mm but should be verified by radiograph to avoid iatrogenic errors of over-instrumentation. AppleDent AL may perform adequately in simple canals; however, its high variability limits its suitability for complex canal anatomies.

The in-vitro design of this study, while controlled, cannot fully replicate the complex biological conditions present in vivo, where periapical tissue resistance, irrigant dynamics, and ongoing structural changes can influence EAL performance. Our sample was limited to single-rooted teeth with fully developed apices, so the findings may not translate seamlessly to multi-rooted teeth or immature root forms. These factors should be considered when extrapolating the results to real-world clinical scenarios.

Further study should include controlled clinical trials, evaluation in difficult conditions (curvatures, resorption), and comparison with standard devices such as root ZX or raypex across different centres.

Conclusion

All three electronic apex locators evaluated in this in-vitro study—AppleDent AL, Eighteeth AL, and Coxo AL—demonstrated clinically acceptable accuracy within ±1.0 mm. Coxo AL exhibited the most reliable overall performance, showing high accuracy and the lowest variability, with 86.7% of measurements falling within ±0.5 mm. AppleDent AL produced mean values comparable to Coxo AL but showed substantially greater variability, indicating less consistent measurement stability. Eighteeth AL achieved 100% accuracy within ±1.0 mm but consistently overestimated the working length and demonstrated significantly higher mean deviation compared with the other two devices. Within the limitations of this in-vitro design, Coxo AL appears to provide the most predictable measurements, whereas readings from AppleDent AL and Eighteeth AL may require greater clinical caution due to variability and overestimation, respectively.

References

1. Ricucci D, Langeland K. Apical limit of root canal instrumentation and obturation, part 2: A histological study. Int Endod J. 1998;31(6):394-409.
2. Tsesis I, Blazer T, Ben-Izhack G, Taschieri S, Del Fabbro M, Corbella S, et al. The precision of electronic apex locators in working length

determination: A systematic review and meta-analysis of the literature. J Endod. 2015;41(11):1818-23.
3. Pirani C, Camilleri J. Effectiveness of root canal filling materials and techniques for treatment of apical periodontitis: A systematic review. Int Endod J. 2023;56 Suppl 3:436-54.
4. Broon NJ, Palafox-Sánchez CA, Estrela C, Camarena DCS, Uribe M, Ceja I, et al. Analysis of electronic apex locators in human teeth diagnosed with apical periodontitis. Braz Dent J. 2019;30(6):550-4.
5. Patel S, Durack C, Abella F, Shemesh H, Roig M, Lemberg K. Cone beam computed tomography in endodontics: A review. Int Endod J. 2015;48:3-15.
6. Przesmycka A, Tomczyk J. Differentiation of root canal morphology: A review of the literature. Anthropol Rev. 2016;79(3):221-39.
7. Mourão PS, Fernandes IB, Moreira LV, Machado GF, Falci SG, de Souza GM, et al. Conventional methods and electronic apical locator in determining working length in different primary teeth: Systematic review and meta-analysis of clinical studies. Evid Based Dent. 2025;26(2):116.
8. Golkar S, Khademi A, Saatchi A, Ghorani A, Iranmanesh P. Factors influencing the accuracy of electronic apex locators: A scoping review. Dent Res J. 2025;22:26.
9. Santhosh L, Raiththa P, Aswathanarayana S, Panchajanya S, Reddy JT, Susheela SR. Influence of root canal curvature on the accuracy of an electronic apex locator: An in vitro study. J Conserv Dent Endod. 2014;17(6):583-6.
10. Jha P, Nikhil V, Raj S, Ravinder R, Mishra P. Accuracy of electronic apex locator in the presence of different irrigating solutions. Endodontology. 2021;33(4):232-6.
11. Yolagiden M, Ersahan S, Suyun G, Bilgec E, Aydin C. Comparison of four electronic apex locators in detecting working length: An ex vivo study. J Contemp Dent Pract. 2018;19(12):1427-33.
12. Mahmoud O, Awad Abdelmagied MH, Dandashi AH, Jasim BN, Tawfik Kayali HA, Al Shehadat S. Comparative evaluation of accuracy of different apex locators: Propex IQ, Raypex 6, Root ZX, and Apex ID with CBCT and periapical radiograph-In vitro study. Int J Dent. 2021;2021:5563426.
13. Baruah Q, Sinha N, Singh B, Reddy PN, Baruah K, Augustine V. Comparative evaluation of accuracy of two electronic apex locators in the presence of contemporary irrigants: an in vitro study. J Int Soc Prev Community Dent. 2018;8(4):349-53.
14. Monteiro Czornobay LF, de Oliveira Rocha A, Leite CC, Menezes Dos Anjos L, Ribeiro JS, Pacheco de Castro Henriques BA, et al. A global overview on electronic apex locator use from 1968 to 2023: a bibliometric analysis. J Endod. 2024;50(7):925-33.
15. Abdullah AO. A survey of root canal treatment in Kurdish community: A pilot study. Polytech J. 2024;14(2):8.
16. Mosleh H, Khazaei S, Razavian H, Vali A, Ziaei F. Electronic apex locator: A comprehensive literature review, part I: Different generations, comparison with other techniques and different usages. Dent Hypotheses. 2014;5(3):84-97.
17. Dutlu D, Yilmaz A. Apex locators and apical resorption. Int Dent J. 2024;74:S310.
18. Venturi M, Breschi L. A comparison between two electronic apex locators: an in vivo investigation. Int Endod J. 2005;38(1):36-45.
19. Shirazi ZA, Saleh AR. Electronic apex locators and their implications in contemporary clinical practice: A review. Open Dent J. 2023;17(1):1-10.
20. Mancini M, Palopoli P, Iorio L, Conte G, Cianconi L. Accuracy of an electronic apex locator in the retreatment of teeth obturated with plastic or cross-linked gutta-percha carrier-based materials: an ex vivo study. J Endod. 2014;40(12):2061-5.
21. Chogle S, Zuaitar M, Sarkis R, Saadoun M, Mecham A, Zhao Y. The Recommendation of cone-beam computed tomography and its effect on endodontic diagnosis and treatment planning. J Endod. 2020;46(2):162-8.
22. D'Assunção FL, Silva JR, Arnaud KC, Leite TB, dos Santos JP, de Almeida AC. Evaluation of the effect of irrigants on the accuracy and repeatability of three electronic apex locators: An ex vivo study. Res Soc Dev. 2021;10(3):1-8.
23. de Morais AL, de Alencar AH, Estrela CR, Decurcio DA, Estrela C. Working length determination using cone-beam computed tomography, periapical radiography and electronic apex locator in teeth with apical periodontitis: A clinical study. Iran Endod J. 2016;11(3):164-8.
24. Ahmad IA, Pani SC. Accuracy of electronic apex locators in primary teeth: a meta-analysis. Int Endod J. 2015;48(3):298-307.
25. Khandewal D, Ballal NV, Saraswathi MV. Comparative evaluation of the accuracy of 2 electronic Apex locators with conventional radiography: An ex vivo study. J Endod. 2015;41(2):201-4.
26. ElAyouti A, Dima E, Ohmer J, Sperl K, von Ohle C, Löst C. Consistency of apex locator function: a clinical study. J Endod. 2009;35(2):179-81.
27. Çalışkan MK, Kaval ME, Tekin U. Clinical accuracy of two electronic apex locators in teeth

with large periapical lesions. Int Endod J. 2014;47(10):920-5.

28. D'Assunção FL, Silva JR, Arnaud KC, Leite TB, dos Santos JP, de Almeida AC. Comparative evaluation of the accuracy of electronic apex locator and digital radiography for working length determination in primary teeth: A systematic review. J Dent (Shiraz). 2024;25(13):203-14.

Original Article

Antibacterial and Antibiofilm Activity of Lavandula angustifolia Essential Oil for Inhibiting Primary Biofilm Colonizers: An In Vitro Study

Lara S. Mohammed Raouf[*1], *Faraedon M. Zardawi*[2]

Abstract

Objective: The present study aimed to assess the effectiveness of Lavandula angustifolia (L. angustifolia) essential oil (EO) in inhibiting bacterial growth and biofilm formation of primary colonizers, such as Streptococcus sanguinis (S. Sanguinis), Streptococcus mitis (S. mitis), and Streptococcus oralis (S. oralis), in an in vitro setting.

Methods: Gas chromatography-mass spectrometry (GC–MS) analysis was used to examine the oil extracted from L. angustifolia EO by hydrodistillation. Agar well diffusion and broth dilution techniques were performed to evaluate antibacterial activity and Minimum Inhibitory Concentrations (MICs) and Minimum Bactericidal Concentrations (MBCs), respectively, against the three American Type Culture Collection (ATCC) strains. In contrast, the qualitative tube method was performed to assess the antibiofilm effect. Chlorhexidine 0.12% was used as a positive control, and all experiments were performed in triplicate (n = 3). Data were analyzed using SPSS (version 26), with $p \leq 0.05$ considered statistically significant.

Results: GC–MS identified 25 constituents in L. angustifolia EO, with linalool (20.99%) predominant. The EO (5–20%) showed dose-dependent antibacterial activity, producing inhibition zones up to 16.2 mm compared with 16–18 mm for chlorhexidine. MIC/MBC values (µL/mL) were 1.56/3.125 for S. mitis, 0.39/0.781 for S. oralis, and 0.156/3.12 for S. sanguinis. For the mixed-species consortium, MIC and MBC were 0.156 and 3.12 µL/mL, respectively. The EO demonstrated moderate to weak antibiofilm activity.

Conclusions: L. angustifolia EO showed concentration-dependent antibacterial activity against primary oral colonizers. While chlorhexidine 0.12% produced larger inhibition zones overall, L. angustifolia EO at higher concentrations, especially 15%, demonstrated comparable efficacy against S. mitis. These findings suggest its potential as a supplementary therapeutic natural adjunct for preventing early plaque formation.

Keywords: *Lavandula angustifolia, Antibacterial effect, Antibiofilm activity, Primary biofilm colonizers.*

Submitted: October 25, 2025, Accepted: January 10, 2026, Published: April 1, 2026.

Cite this article as: Raouf LS, Zardawi FM. Antibacterial and Antibiofilm Activity of Lavandula angustifolia Essential Oil for Inhibiting Primary Biofilm Colonizers: An In Vitro Study. Sulaimani Dent J. 2026;13(1):28-39.

DOI: https://doi.org/10.17656/sdj.10219

1. *Periodontics Department, College of Dentistry, University of Sulaimani, Sulaimani, Iraq.*
2. *Dean of Faculty of Dentistry, Qaiwan International University, Sulaymaniyah 46001, Iraq.*

** Corresponding author*: *Lara.mohammedraouf@univsul.edu.iq.*

Introduction

Periodontal diseases, such as gingivitis and periodontitis, are chronic, multifactorial inflammatory diseases that primarily result from an immune response that is exacerbated by dysbiotic, diverse bacterial biofilms. These diseases and conditions affect the supporting structures of the teeth[1]. Investigations of the oral cavity, especially the dental biofilm, have found more than 700 different species of bacteria living in a very organized yet very diverse microbial community that plays a crucial role in periodontal health and disease[2,3].

Initial biofilm colonizers, including *Streptococcus oralis, Streptococcus mitis,* and *Streptococcus sanguinis*, which make up the yellow complex of the typical oral flora, are proposed to be crucial in forming the initial biofilm matrix and account for around 80% of the nascent biofilm. These species form an attachment framework for later colonizers such as *Fusobacterium nucleatum*, *Prevotella intermedia*, and *Porphyromonas gingivalis* to colonize gingival pockets and firmly establish themselves, ultimately causing disease. These streptococci facilitate bacterial adherence and enhance biofilm stability through the production of extracellular polysaccharides, making them key targets for strategies aimed at preventing biofilm-induced periodontal diseases[4, 5].

Although mechanical methods such as brushing and flossing are effective for removing biofilms, they are often insufficient, particularly in inaccessible areas. Furthermore, individual differences in oral hygiene practices, dexterity, and compliance often lead to the persistence of pathogenic biofilms, necessitating antimicrobial agents as an adjunct[6,7].

Chlorhexidine mouthwash has long been considered the benchmark for chemical plaque control because of its broad-spectrum antimicrobial action. Its cationic molecules bind to bacterial cell walls, alter membrane permeability, and cause leakage of intracellular components, ultimately leading to cell death. However, prolonged use is associated with undesirable side effects, such as dental staining, taste alteration, mucosal irritation, and the risk of bacterial resistance, prompting continuous interest in safer and more biocompatible alternatives[7-9].

In this context, natural plant-derived products, particularly essential oils, have attracted considerable attention due to their diverse bioactive components, favorable safety profile, and lower cost.

Several *in vitro* investigations have indicated that herbal mouthrinses can achieve antibacterial effects comparable to chlorhexidine. Among these, *Lavandula angustifolia* (lavender) essential oil (EO) has been recognized for its analgesic, anti-inflammatory, and antimicrobial activities against both Gram-positive and Gram-negative organisms, primarily attributed to its key constituents, linalool and linalyl acetate[10-12].

The chemical composition of *L. angustifolia* EO varies widely depending on factors such as chemotype, climate, geography, and harvest conditions, as reflected in GC–MS analyses from different regions, including studies from Iraq and the Kurdistan Region. Reported profiles often show notable shifts in the relative abundance of major constituents such as linalool, linalyl acetate, and terpinen derivatives, emphasizing the importance of chemical characterization when interpreting biological activity[13-15].

In studies, lavender EO has shown antibacterial properties against periodontal pathogens like *P. gingivalis, P. intermedia,* and *F. nucleatum*[16,17]. However, they examined oils from different regions, cultivars, or chemotypes, making direct comparisons difficult. Moreover, these studies have focused on established periodontal pathogens rather than early oral streptococcal colonizers. The antibacterial and antibiofilm properties of *L. angustifolia* EO against *S. mitis*, *S. oralis*, and *S. sanguinis* have not been investigated.

Understanding its capacity to suppress bacterial growth and impede early biofilm development could introduce a promising natural approach to periodontal disease prevention. Accordingly, this study aimed to evaluate the antibacterial and biofilm-inhibiting effects of *L. angustifolia* EO on *S. mitis, S. oralis,* and *S. sanguinis* in an *in vitro* setting. These findings could support the development of plant-based antimicrobial formulations aimed at preventing initial biofilm formation and minimizing the onset of biofilm-associated oral diseases.

Materials and Methods

Study design and setting

This experimental study was conducted in the Microbiology Laboratory of the College of Dentistry at the University of Sulaimani, College of Agricultural Engineering Sciences for plant identification, and the Bahar factory for essential oil extraction.

Plant collection and identification

Fresh stems and flowers of *L. angustifolia* were supplied by Bahar Factory (Sulaymaniyah, Kurdistan Region of Iraq), which collected the plants in March from cultivated lavender fields in the Sulaymaniyah governorate (Figure 1). Assistant Professor Dr. Lanja

Hewa Khal (PhD, Plant Taxonomist, College of Agricultural Engineering Sciences, University of Sulaimani) confirmed the plant species and its cultivation status based on standard morphological characteristics. The Ethical Committee at the College of Dentistry, University of Sulaimani, approved the research project with Code No. (COD-EC-24-0020) on December 16, 2024.

Essential oil extraction

The EO was extracted using the hydrodistillation method at the Bahar factory in Sulaymaniyah, following the standard process[18,19]. The aerial parts of *L. angustifolia* were collected in mid-July and air-dried under shade at ambient indoor conditions until constant weight was achieved. Approximately 1 kg of the dried plant material was loaded into a Novin stainless-steel hydrodistillation unit (Tehran, Iran). For each kilogram of dried plant material, 5 L of water was added, and hydrodistillation was performed for 8 hours. During distillation, steam carried the volatile compounds through the plant matrix, after which the vapor was condensed and collected in a separation vessel. Because of density differences, the essential oil separated naturally from the aqueous phase and was collected from the upper layer, yielding approximately 2-3% EO per 100g of dried plant material. The extracted oil was immediately transferred into tightly sealed amber-glass bottles and stored in the dark at a controlled room temperature of 20-25 °C. The interval between extraction and subsequent antimicrobial testing did not exceed four weeks (Figure 1).

Gas Chromatography–Mass Spectrometry (GC-MS) analysis

Gas Chromatography–Mass Spectrometry (GC-MS) analysis revealed the unique chemical profiles of the EO. The volatile compounds were separated and identified using an Agilent (7890A) gas chromatography-mass spectrometry system (Santa Clara, CA, USA) with high resolution and sensitivity. All analyses were conducted at the Central Laboratory – Chemistry Division, Islamic Azad University (Sanandaj Branch).

The essential oil was diluted 1:100 in n-hexane, and 1 µL of the solution was injected in split mode (1:50) onto a DB-35MS capillary column (30 m × 0.32 mm). Helium was used as carrier gas at a flow rate of 2 mL/min. The oven program began at 35 °C (5 min hold), increased to 280 °C at 10 °C/min, with a final 5-min hold at 280 °C. The injector temperature was 250 °C, and the MS detector operated in electron-ionization mode (70 eV) with a scan range of 50–500 m/z[20].

Compound identification was achieved by comparing mass spectra with the NIST 11 library, supported by Kovats retention indices calculated from a homologous series of n-alkanes run under identical conditions. Only compounds meeting all three criteria (high-quality library match, RI agreement with published data for *L. angustifolia*, and characteristic fragmentation patterns) were accepted. Relative abundances were reported as percentages of the total ion chromatogram (TIC)[21].

Bacterial strains preparation

The three bacterial strains were reference strains of *S. mitis* (ATCC 49456), *S. oralis* (ATCC 35037), and *S. sanguinis* (ATCC 10556), purchased from the American Type Culture Collection (ATCC, Manassas, VA, USA). Lyophilized cultures were reanimated under sterile conditions using the features described in ATCC protocols. Subsequently, each strain was plated and cultured onto Blood Agar and Brain Heart Infusion (BHI) broth (HiMedia, India) and incubated at 37 °C for 24 hours under CO_2-enriched microaerophilic conditions generated using a candle jar. Stock cultures were preserved in 20% glycerol (Unimedic Pharma, Sweden) at −80 °C for subsequent use. All experimental procedures were conducted using fresh subcultures from the frozen stocks to ensure consistency and viability (Figure 2). Gram staining confirmed the presence of Gram-positive cocci in chains[22].

Preparation of essential oil solutions

Owing to the limited water solubility of EOs, a single standardized vehicle composed of 0.5% Tween 80 (Biochem-France) and 10% dimethyl sulfoxide (DMSO) (Merck, Germany) was employed consistently for all assays, including the agar well diffusion test, MIC, and MBC to facilitate their dissolution while maintaining methodological uniformity. This solution allowed for antimicrobial testing of various EO concentrations against the three streptococcal strains[23]. Vehicle controls (10% DMSO alone, 0.5% Tween 80 alone, and the combined 0.5% Tween 80 + 10% DMSO mixture) were included in all assays to verify that the solvent system had no intrinsic antimicrobial activity.

Antibacterial efficacy evaluation

Mueller–Hinton agar (MHA) without blood supplementation was used for the agar well diffusion assay, a qualitative method for assessing the sensitivity of bacterial strains to the tested essential oil. This medium provides standardized conditions that allow reliable diffusion of hydrophobic compounds and is widely applied in essential-oil antimicrobial testing. Although viridans streptococci are clinically fastidious, all ATCC strains showed consistent, reproducible growth on MHA[24-26].

Suspensions of bacteria were standardized to ≈1.5×10^8 CFU/mL through comparison with the 0.5 McFarland

standard in phosphate-buffered saline (PBS) (Central Drug House, India). From this suspension, 100 µL of the bacterial inoculum was applied to Mueller–Hinton agar plates (HiMedia, India) and evenly spread using a sterile cotton swab, followed by a drying period of approximately 5 minutes.

Wells of 6 mm diameter were aseptically created using a sterile stainless-steel borer. Essential oil concentrations (5%, 10%, and 15% for *S. mitis* and *S. oralis*; 10%, 15%, and 20% for *S. sanguinis*) were prepared by making 5 mL working solutions in which the required percentage of EO was added, followed by 10% DMSO and 0.5% Tween 80, and the remaining volume completed with sterile distilled water. This standardized vehicle ensured complete solubilization of the EO and consistent preparation across all assays. From each prepared EO dilution, 20 µL was dispensed into the wells. Chlorhexidine gluconate 0.12% (CHX) served as the positive control.

Plates were left at room temperature for 15 minutes to facilitate diffusion of the test agents and then incubated at 37 °C for 24 h in a candle jar. Inhibition zones were measured using a digital Vernier caliper, recording the total diameter (clear zone + 6-mm well), a commonly used method in essential-oil diffusion assays where hydrophobic compounds exhibit variable diffusion patterns[24] (Figure 3). All tests were performed in triplicate across three independent experiments (n = 9 per concentration per strain).

Determination of the MIC and MBC

The macrodilution broth method was utilized to determine the MIC of the EO tested[27]. Stock solutions were prepared by dissolving the EO in 10% dimethyl sulfoxide (DMSO; Merck, Germany) and 0.5% Tween 80 (Biochem-France). Positive (bactericidal) control was chlorhexidine gluconate 0.12% (CHX; KIN, SA, Spain), while Mueller–Hinton broth (MHB; HiMedia, India) served as the negative control.

The stock concentrations for MIC testing were selected based on the agar well diffusion results. For *S. mitis* and *S. oralis*, antibacterial activity began at 5% EO; therefore, a 50 µL/mL stock solution was prepared, and two-fold serial dilutions using 10 glass tubes were generated to obtain final test concentrations ranging from 25 to 0.048 µL/mL, using the same vehicle system (10% DMSO + 0.5% Tween 80), which showed no intrinsic antimicrobial activity in control assays. Because *S. sanguinis* demonstrated inhibition zones at 10% EO, a 100 µL/mL stock solution was used to prepare serial dilutions ranging from 50 to 0.0975 µL/mL. For each MIC tube, 900 µL of Mueller–Hinton broth (MHB; HiMedia, India) was dispensed into sterile glass tubes, followed by 100 µL of the standardized bacterial inoculum (0.5 McFarland ≈ 1.5×10^8 CFU/mL), resulting in a final test volume of 1 mL. The essential oil concentrations described above were incorporated into the tubes via the prepared dilution series according to standard macrodilution methodology. Tubes were gently vortexed, sealed with cotton plugs, and incubated for 24 h at 37 °C in a candle jar. After incubation, tubes were examined for visible growth, manifested as turbidity or pellet formation[28]. Figure 4 illustrates this process. The MIC was defined as the lowest EO concentration that inhibited visible bacterial growth, as indicated by the absence of cloudiness or particle formation.

During MIC evaluation, the concentration showing no bacterial growth was judged to be the MBC. In accordance with standard CLSI macrodilution procedures, only the tubes that showed no visible growth at the MIC reading (i.e., absence of turbidity or pellet formation) were selected for subculture. A sample was gathered from the contents of these growth-negative tubes using a sterile wire loop, then plated onto agar plates and incubated at 37 °C within a candle jar for 24 hours. After incubation, plates were examined for the presence or absence of bacterial colonies, and the MBC was defined as the lowest concentration that yielded no growth. All assays for MIC and MBC determination were performed in triplicate[29].

Antibiofilm activity assay

This test was carried out using a standardized tube adhesion assay to assess the anti-biofilm activity of the extracts[30]. After the MIC of the EO was determined, the inoculated culture medium was removed aseptically. The test tubes were washed three times with phosphate-buffered saline (PBS, pH 7.3) to remove any planktonic and non-adherent cells, then inverted and left to dry for 45 minutes. Then, for each tube, 1 mL of 1% crystal violet solution was added and left at room temperature for 15 minutes. Subsequently, the tubes were washed three times with sterile distilled water to remove excess stain. Crystal violet staining of the tubes was used to assess biofilm formation by the presence of a violet-stained layer on the inner walls and base of the tubes. Staining intensity was visually evaluated qualitatively (examiner's vision) according to standard interpretive categories: weak (+), moderate (++), or strong (+++) biofilm formation, based on the density and uniformity of the violet film on the wall and bottoms of the tubes[31,32]. A negative control (bacterial inoculum in MHB without EO) and a positive control (0.12% chlorhexidine) were included in every run. All

procedures were conducted in triplicate, and the experimental protocol was consistently applied across the three bacterial species tested.

Statistical analysis

The statistical analyses were performed with SPSS software version 26.0 (IBM Corp., Armonk, NY, USA). Kolmogorov–Smirnov and Shapiro–Wilk tests were used to assess the normality of the data distribution. An independent sample t-Test was used to compare the antibacterial and antibiofilm activities of L. angustifolia essential oil (0.05, 0.1, and 0.2 mg/mL) and chlorhexidine mouthwash (0.01, 0.02, 0.04, and 0.08mg/mL). Results are expressed as mean ± SD (standard deviation) and with $p \leq 0.05$ considered statistically significant.

Results

Bacterial strains assessment and identification

The bacterial cultures were obtained from the ATCC (Manassas, VA, USA). The initial assessment involved visual examination of colony attributes under magnification, staining methods to discern cell structure and arrangement, growth characteristics, and Gram staining. After 24 hours of incubation, the S. mitis and S. oralis colonies displayed a greenish halo, indicating alpha-hemolysis with red blood cells, distinguishing them as streptococci. Separately, *S. sanguinis* colonies emerged as tiny grayish or colorless microscopic clusters (Figure 2).

Analysis of bioactive compounds

GC-MS analysis of L. angustifolia

Gas chromatography–mass spectrometry (GC–MS) analysis of *L. angustifolia* EO using the Agilent 7890A system revealed twenty-five phytochemical constituents, with six major compounds dominating the profile.

Linalool (20.99%) and linalyl anthranilate (14.20%) were the most abundant, followed by 1,3,6-octatriene, 3,7-dimethyl-, (E) (7.06%), L-caryophyllene (5.80%), 4-terpineol (5.65%), and 1,6,10-dodecatriene, 7,11-dimethyl-3-methylene-, (E) (5.11%), as presented in Table 1. The essential oil used in this study was tested within 4 weeks of extraction to ensure chemical stability.

The Antibacterial Activity

The Antibacterial Activity of L. angustifolia. EO

The sensitivity of the tested oral streptococcal strains to *L. angustifolia* essential oil was assessed using the agar well diffusion method, and the results are summarized in Table 2. In this study, inhibition zones greater than the 6-mm well diameter were interpreted as evidence of antibacterial activity, consistent with the essential-oil diffusion assay methodology, in which hydrophobic compounds often diffuse minimally beyond the well. The tested bacterial strains, *S. mitis*, *S. sanguinis*, *S. oralis*, and a mixed-species consortium, exhibited varying degrees of sensitivity to *L. angustifolia* EO across concentrations of 5%, 10%, 15%, and 20%. Vehicle controls (10% DMSO, 0.5% Tween 80, and their mixture) consistently produced 0-mm inhibition zones, confirming the absence of intrinsic antimicrobial activity.

For *S. mitis*, inhibition zones ranged from 9.33 ± 1.15 mm at 5% to 15.77 ± 1.39 mm at 15%, with statistically significant differences compared to CHX 0.12% at lower concentrations ($p < 0.05$), but not at 15% ($p = 0.487$). *S. oralis* showed a concentration-dependent response, with inhibition zones increasing from 8.21 ± 1.02 mm at 5% to 16.21 ± 1.02 mm at 15%, all significantly lower than CHX ($p \leq 0.05$).

S. sanguinis demonstrated modest susceptibility, with inhibition zones of 8.00 ± 0.00 mm, 9.55 ± 0.39 mm, and 11.00 ± 0.58 mm at 10%, 15%, and 20% EO concentrations, respectively. These were significantly smaller than those produced by CHX 0.12% ($p < 0.05$). The mixed-species group showed minimal inhibition at 5% EO (0.00 ± 0.00 mm), but responded at higher concentrations, reaching 12.00 ± 0.00 mm at 15% ($p < 0.05$).

Across all bacterial strains and concentrations, CHX 0.12% consistently produced larger inhibition zones, ranging from 14.22 ± 0.38 mm to 18.00 ± 0.67 mm, with statistically significant superiority over *L. angustifolia* EO ($p < 0.05$) as shown in Table 2. All results represent median (IQR) values from n = 3 replicates × 3 independent experiments.

MIC and MBC of L. angustifolia EO against the bacterial strain

The MICs of *L. angustifolia* EO against the tested bacterial strains, as measured by the broth macro dilution method, were 1.56 µL/mL and 0.39 µL/mL for *S. mitis* and *S. oralis*, respectively, and 0.156 µL/mL for both *S. sanguinis* and the mixed-species consortium, as shown in Table 3.

Corresponding MBC values, as seen in Figure 3, were 3.125 µL/mL *for S. mitis*, 0.781 µL/mL for *S. oralis*, and 3.120 µL/mL for both *S. sanguinis* and the mixed-species group. The larger MIC–MBC gap observed for S. sanguinis (0.156 vs. 3.120 µL/mL) is consistent with essential oils, in which bacteriostatic inhibition often occurs at much lower concentrations than bactericidal killing due to hydrophobicity, slower kill kinetics, and

reduced penetration into cellular structures. Additionally, the loop-based subculture method used for MBC determination has limited plating sensitivity, which may contribute to the wider separation between inhibitory and bactericidal concentrations[24,27].

The relatively low MIC and MBC values observed for *S. oralis* suggest that L. angustifolia EO exhibits potent bacteriostatic and bactericidal activity against this strain. In contrast, *S. mitis* required higher concentrations to achieve complete bacterial eradication, reflecting its comparatively reduced susceptibility.

Antibiofilm activity of L. angustifolia EO

The antibiofilm activity of *L. angustifolia E. oil* was evaluated using the test-tube adherence method, wherein biofilm formation was qualitatively assessed based on the intensity of crystal violet staining on the inner walls and bottoms of the tubes. Compared to the negative control (Mueller–Hinton broth with bacterial inoculum), which exhibited strong biofilm formation (+++), *L. angustifolia* EO demonstrated variable inhibitory effects across the tested strains.

As shown in Table 4, *L. angustifolia* EO exhibited weak biofilm formation in *S. mitis* (+) and S. *sanguinis* (+), moderate adherence in *S. oralis* (++), and strong biofilm persistence in the mixed-species consortium (+++). These results suggest that *L. angustifolia* EO possesses strain-specific antibiofilm properties, with greater efficacy against individual strains than against polymicrobial communities.

In contrast, the positive control (0.12% chlorhexidine mouthwash) completely inhibited visible biofilm formation in *S. oralis*, *S. sanguinis*, and the mixed-species group, while *S. mitis* remained weakly adherent (+). These findings highlight the partial antibiofilm potential of *L. angustifolia E. oil* and support its role as a natural adjunct in biofilm management, particularly in mono-species oral infections.

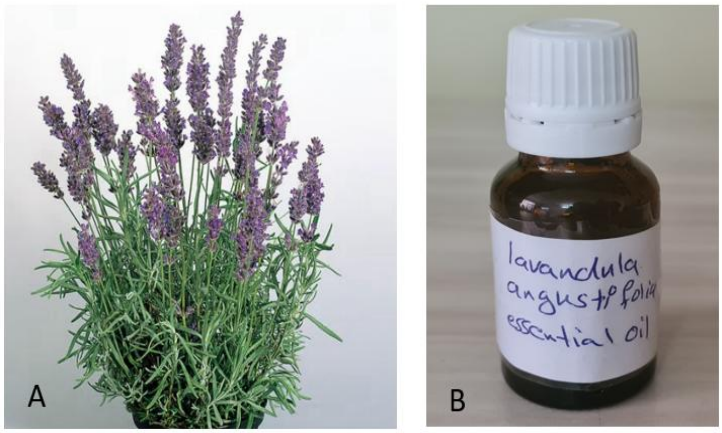

Figure 1: (A) *L. angustifolia* plant, (B) *L. angustifolia* essential oil.

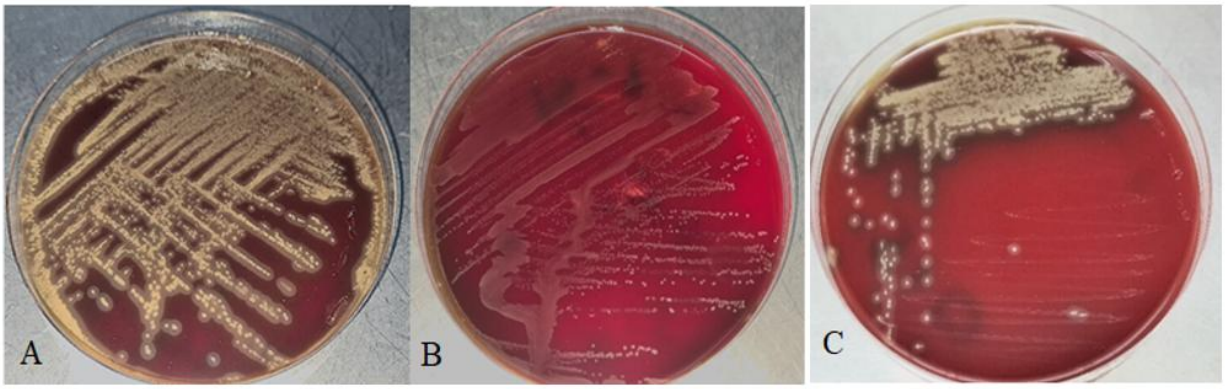

Figure 2: Presents the colony morphology of alpha-hemolytic streptococcal strains cultured on blood agar: (A) *Streptococcus mitis* shows dense, brownish colonies with diffuse spread; (B) *Streptococcus sanguinis* exhibits less dense, reddish colonies with focal growth zones; and (C) *Streptococcus oralis* displays moderately dense colonies with mixed brownish-red pigmentation, reflecting subtle variations in hemolytic activity.

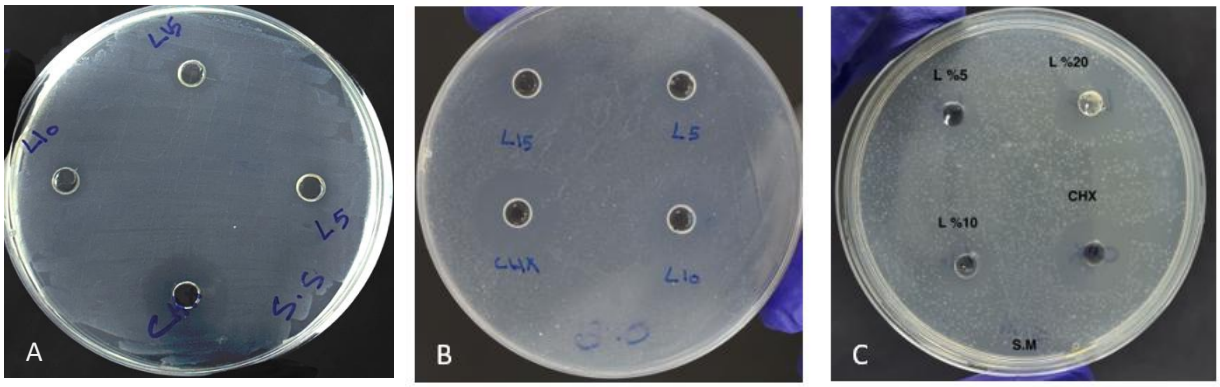

Figure 3: Mueller–Hinton agar plates showing the results of the agar well diffusion method used to evaluate antibacterial susceptibility. (A) Streptococcus sanguinis; (B) Streptococcus oralis; (C) Streptococcus mitis.

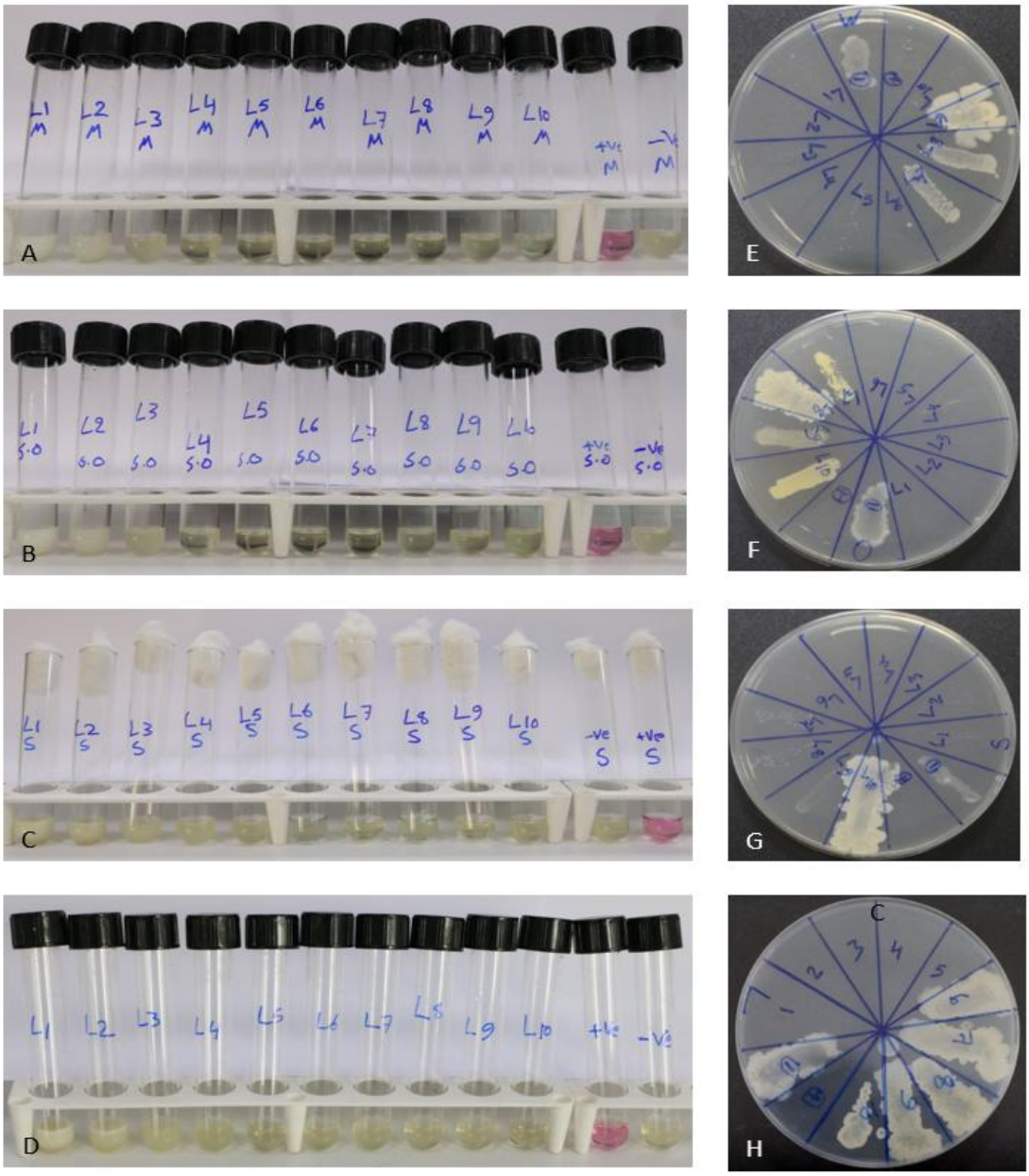

Figure 4: Determination of MIC and MBC values of L. angustifolia essential oil against primary biofilm colonizers and mixed species. (A–D) Broth macrodilution assay showing the MIC of L. angustifolia essential oil against S. mitis, S. oralis, S. sanguinis, and the mixed-species consortium, respectively. (E–H) Agar culture assay confirming the MBC of L. angustifolia against the same bacterial strains in the same order.

Table 1: Results of GC-MS analysis of L. angustifolia.

Peak	R. T	Area%	MW	MF	CAS#	Compound name[1]
25	4.398	0.682	136	C10H16	7785-70-8	1R-α-Pinene
16	5.687	1.545	136	C10H16	18172-67-3	Bicyclo[3.1.1]heptane, 6,6-dimethyl-2-methylene-, (1S)-
22	6.04	0.874	128	C8H16O	3391-86-4	1-Octen-3-ol
21	6.235	0.89	130	C8H18O	589-98-0	3-Octanol
11	6.361	2.369	128	C8H16O	106-68-3	3-Octanone
15	6.458	1.546	136	C10H16	5989-27-5	D-Limonene
12	6.59	1.708	136	C10H16	555-10-2	β-Phellandrene
3	6.729	7.058	136	C10H16	3779-61-1	1,3,6-Octatriene, 3,7-dimethyl-, (E)-
10	6.799	2.393	154	C10H18O	470-82-6	Eucalyptol
8	6.861	3.594	136	C10H16	13877-91-3	1,3,6-Octatriene, 3,7-dimethyl
1	8.247	20.994	154	C10H18O	78-70-6	Linalool
13	9.27	1.687	154	C10H18O	58461-27-1	4-Hexen-1-ol, 5-methyl-2-(1-methylethenyl)-
20	9.364	0.944	172	C10H20O2	2639-63-6	Butanoic acid, hexyl ester
14	9.476	1.584	156	C10H20O	2216-51-5	1-Menthol
5	9.604	5.647	154	C10H18O	562-74-3	4-Terpineol
9	9.962	2.53	154	C10H18O	98-55-5	α-Terpineol
2	10.392	14.198	154	C10H18O	7149-26-0	Linalyl anthranilate
24	10.532	0.817	138	C9H14O	500-02-7	Crypton
19	10.688	1.081	154	C10H18O	106-24-1	Lemonol
7	10.918	4.069	196	C12H20O2	25905-14-0	(±)-Lavandulol, acetate
23	12.05	0.859	196	C12H20O2	141-12-8	2,6-Octadien-1-ol, 3,7-dimethyl-, acetate, (Z)-
17	12.156	1.316	204	C15H24	512-61-8	α-Santalene
4	12.45	5.803	204	C15H24	87-44-5	L-Caryophyllene
6	12.738	5.108	204	C15H24	18794-84-8	1,6,10-Dodecatriene, 7,11-dimethyl-3-methylene-, (E)-
18	13.386	1.163	204	C15H24	13744-15-5	1H-Cyclopenta [1,3] cyclopropa[1,2]benzene, octahydro-7-methyl-3-methylene-4-(1-methylethyl)-, [3aS-(3aα,3bβ

[1] Compound identification was performed by matching mass spectra with the NIST/EPA/NIH Mass Spectral Library (NIST 14) and by comparison with published retention indices.

Area%: Compound percentage; **CAS#:** Registry number; **MW:** Molecular weight (g/mol); **MF:** Molecular formula, **R. T:** Retention time

in periodontal disease progression[33].

Table 2: Mean and standard deviations of inhibition zones of L. angustifolia at different concentrations against S. mitis, S. sanguinis, S. oralis, and mixed species together.

Oil%	Inhibition zone (*S. mitis*)			Oil%	Inhibition zone (*S. oralis*)		
	L. angustifolia	CHX 0.12%	*p*-value		*L. angustifolia*	CHX 0.12%	*p*-value
5%	9.33 ± 1.15	15.99 ± 1.15	0.043 *	5%	8.21 ± 1.02	18.00 ± 0.67	0.05 *
10%	10.66 ± 0.66	15.33 ± 1.15	0.046 *	10%	10.22 ± 0.38	17.78 ± 0.39	0.043 *
15%	15.77 ± 1.39	16.66 ± 0.00	0.487 ns	15%	16.21 ± 1.02	18.00 ± 0.67	0.05 *
	Inhibition zone (*S. sanguinis*)				**Inhibition zone (mixed species)**		
10%	8.0 ± 0.0	17.77 ± 1.02	0.037 *	5%	0.00 ± 0.00	14.22 ± 0.38	0.034 *
15%	9.55 ± 0.39	17.55 ± 0.39	0.043 *	10%	8.66 ± 0.67	14.66 ± 0.67	0.05 *
20%	11.00 ± 0.58	17.78 ± 0.39	0.043 *	15%	12.00 ± 0.00	14.22 ± 0.38	0.034 *

Ns: No significant difference; *: Significant difference; Independent sample t-Test.

Table 3: The MIC and MBC values of L. angustifolia EO on bacterial strains.

Streptococcus species	*L. angustifolia* EO	
	MIC	MBC
S. mitis	1.56 µL/mL	3.125 µL/mL
S. oralis	0.39 µL/mL	0.781 µL/mL
S. sanguinis	0.156 µL/mL	3.12 µL/mL
Bacterial strains together	0.156 µL/mL	3.12 µL/mL

Table 4: Qualitative biofilm formation of the L. angustifolia EO.

Streptococcus species	*L. angustifolia* EO	CHX (Positive control)	MHB (Negative control)
S. mitis	+	+	+++
S. oralis	++	0	+++
S. sanguinis	+	0	+++
Mixed Species together	+++	0	+++

Discussion

Periodontitis is a chronic, biofilm-mediated inflammatory disease initiated by the adhesion and proliferation of early colonizers such as *S. mitis, S. oralis*, and *S. sanguinis*. These species form the foundational layer of supragingival and subgingival biofilms, facilitating the subsequent attachment and maturation of late colonizers, including *Porphyromonas gingivalis*, *Tannerella forsythia*, and *Treponema denticola*, which are recognized as keystone pathogens

The transition from health to disease is marked by microbial dysbiosis, where commensal streptococci lose dominance and pathogenic anaerobes thrive, triggering host immune dysregulation and tissue destruction[34].

The present study demonstrates that *L. angustifolia* essential oil (EO) exhibits antimicrobial and antibiofilm activity against these primary oral colonizers. GC–MS analysis revealed linalool (20.99%) and linalyl anthranilate (14.20%) as the dominant constituents, both

known to disrupt bacterial membranes, increase permeability, and interfere with enzymatic and metabolic processes[11]. Their high abundance likely underlies the observed antibacterial efficacy. Lavender EO is also highly volatile, and this property may influence diffusion outcomes, since rapid evaporation or uneven dispersion can alter the measured inhibition zones. This limitation is inherent to agar diffusion assays and has been widely documented in EO research.

Growth inhibition was concentration-dependent, with *S. oralis* showing the highest sensitivity and *S. sanguinis* the lowest, possibly due to structural and metabolic variations among species. Inhibition of biofilm formation further suggests interference with bacterial adhesion and extracellular matrix synthesis, key events in early plaque development[32].

These findings are consistent with the literature. Stamova et al.[13] reported that linalool and linalyl acetate from lavender EO disrupted bacterial membranes and exhibited synergistic effects with antibiotics, particularly against *E. coli* and *S. aureus*. Similar results were observed by Husian and Zardawi[17] against *P. gingivalis* and *P. intermedia*, and by Salavati Hamedani et al.[35], who highlighted strong antimicrobial and antioxidant properties. Other studies confirmed synergistic activity when lavender EO was combined with other therapeutic oils[25] and noted inhibition zones exceeding 25 mm against *E. coli* and *S. aureus*[36], reinforcing its broad-spectrum efficacy.

The EO demonstrated bacteriostatic and bactericidal activity across all tested strains. Notably, *S. oralis* and *S. sanguinis* showed greater susceptibility than *S. mitis*, requiring lower concentrations for growth inhibition and killing. Similar antimicrobial patterns have been reported for Bulgarian lavender essential oil, which exhibited potent activity against a range of pathogens such as *S. aureus* and *C. albicans*[37]. The activity of lavender EO against Gram-positive cocci has also been validated in studies showing synergistic or additive effects when combined with other essential oils[25].

The antibiofilm assessment revealed stronger inhibition in mono-species cultures of *S. mitis* and *S. sanguinis* than in mixed-species biofilms, indicating greater resistance in polymicrobial communities. This observation aligns with de Alteriis et al.[38], who showed that both free and liposome-encapsulated lavender EO eradicated *Candida auris* biofilms, and with Khanem et al.[39], who reported inhibition rates of 6–89% against *E. coli* biofilms through oxidative stress and membrane disruption. Together, these results affirm lavender EO's ability to penetrate biofilm structures and impair their stability.

Despite these promising outcomes, several limitations should be noted. Standardized ATCC strains cannot fully represent the genetic and phenotypic diversity of clinical isolates, and the in vitro model does not reproduce the complex host factors, such as immune response, nutrient gradients, and shear forces, present *in vivo*. Variability in the chemical composition of lavender EO by chemotype, geography, and harvest time may also influence reproducibility.

In conclusion, *L. angustifolia* EO demonstrated concentration-dependent antibacterial and antibiofilm efficacy against primary biofilm colonizers. Although chlorhexidine remains more potent, lavender EO presents a safe, natural alternative for controlling early dental biofilm formation. However, the volatile nature of EO, compositional variability, and the need for cytotoxicity and *in vivo* studies underline that these findings should be considered preliminary. Future studies should aim to standardize its chemical profile, optimize formulations for oral administration, assess its biocompatibility and cytotoxicity at higher concentrations, and confirm its safety and clinical effectiveness through *in vivo* and randomized trials.

Conclusion

This *in vitro* study showed that *L. angustifolia* EO possesses antibacterial and antibiofilm activity against *S. mitis*, *S. oralis*, *S. sanguinis*, and their mixed-species consortium. The oil displayed a concentration-dependent effect, with *S. oralis* most susceptible, *S. sanguinis* less responsive, and mixed-species biofilms showing greater resistance.

Although chlorhexidine consistently outperformed lavender oil, the results indicate its potential as a safe, natural adjunct for controlling early colonizers and delaying biofilm maturation.

References

1. Hajishengallis G, Chavakis T. Local and systemic mechanisms linking periodontal disease and inflammatory comorbidities. Nat Rev Immunol. 2021;21(7):426-40.
2. Kilian M, Chapple ILC, Hannig M, Marsh PD, Meuric V, Pedersen AML, et al. The oral microbiome – an update for oral healthcare professionals. Br Dent J. 2016;221(10):657-66.

3. Marsh PD, Zaura E. Dental biofilm: Ecological interactions in health and disease. J Clin Periodontol. 2017;44 Suppl 18:S12-S22.
4. Kreth J, Merritt J, Qi F. Bacterial and Host Interactions of Oral Streptococci. DNA Cell Biol. 2009;28(8):397-403.
5. Bloch S, Hager-Mair FF, Andrukhov O, Schaffer C. Oral streptococci: Modulators of health and disease. Front Cell Infect Microbiol. 2024;14:1357631.
6. De Almeida J, Ervolino E, Bonfietti LH, Novaes VC, Theodoro LH, Fernandes LA, et al. Adjuvant therapy with sodium alendronate for the treatment of experimental periodontitis in rats. J Periodontol. 2015;86(10):1166-75.
7. James P, Worthington HV, Parnell C, Harding M, Lamont T, Cheung A, et al. Chlorhexidine mouthrinse as an adjunctive treatment for gingival health. Cochrane Database Syst Rev. 2017;(3):CD008676.
8. Thosar N, Basak S, Bahadure RN, Rajurkar M. Antimicrobial efficacy of five essential oils against oral pathogens: An in vitro study. Eur J Dent. 2013;7(Suppl 1):S071-S7.
9. Prasad KA, John S, Deepika V, Dwijendra KS, Reddy BR, Chincholi S. Anti-plaque efficacy of herbal and 0.2% chlorhexidine gluconate mouthwash: A comparative study. J Int Oral Health. 2015;7(8):98-102.
10. Di Vito M, Smolka A, Proto MR, Barbanti L, Gelmini F, Napoli E, et al. Is the antimicrobial activity of hydrolates lower than that of essential oils? Antibiotics. 2021;10(1):88.
11. Todorova D, Yavorov N, Lasheva V, Damyanova S, Kostova I. Lavender essential oil as antibacterial treatment for packaging paper. Coatings. 2022;13(1):32.
12. Betlej I, Andres B, Cebulak T, Kapusta I, Balawejder M, Jaworski S, et al. Antimicrobial properties and assessment of bioactive compounds in Lavandula angustifolia Mill cultivated in southern Poland. Molecules. 2023;28(17):6416.
13. Stamova S, Ermenlieva N, Tsankova G, Georgieva E. Antimicrobial activity of lavender essential oil from lavandula angustifolia mill.: In vitro and in silico evaluation. Antibiotics (Basel). 2025;14(7):656.
14. Alhasan AS, Alrawi MSh, Al-Ameri DT, Almehemdi AF. Effect of distillation duration on essential oil yield and composition of Lavandula angustifolia grown in Iraq. Anbar J Agric Sci. 2025;23(1):339-53.
15. Ciocarlan A, Lupascu L, Aricu A, Dragalin I, Popescu V, Geana E-I, et al. Chemical composition and assessment of antimicrobial activity of lavender essential oil and by-products. Plants. 2021;10(9):1829.
16. Rosner O, Livne S, Bsharat M, Dviker S, Jeffet U, Matalon S, et al. Lavandula angustifolia essential oil inhibits the ability of fusobacterium nucleatum to produce volatile sulfide compounds, a key components in oral malodor. Molecules. 2024;29(13):2982.
17. Husian SG, Zardawi FM. Antibacterial and antibiofilm profiles of Lavandula angustifolia essential oil on clinically isolated Porphyromonas gingivalis and Prevotella intermedia: an in vitro study. J Oral Dent Res. 2022;9(2):9-20.
18. Elyemni M, Louaste B, Nechad I, Elkamli T, Bouia A, Taleb M, et al. Extraction of essential oils of Rosmarinus officinalis L by two different methods: hydrodistillation and microwave-assisted hydrodistillation. Sci World J. 2019;2019:3659432.
19. Wainer J, Thomas A, Chimhau T, Harding KG. Extraction of essential oils from Lavandula × intermedia 'Margaret Roberts' using steam distillation, hydrodistillation, and cellulase-assisted hydrodistillation: experimentation and cost analysis. Plants. 2022;11(24):3479.
20. Adams RP. Identification of Essential Oil Components by Gas Chromatography/Mass Spectrometry. 4th ed. Carol Stream, IL: Allured Publishing; 2007.
21. Mondello L, Herrero M, Kumm T, Marriott PJ. Comprehensive gas chromatography in essential oil analysis. TrAC Trends Anal Chem. 2018;103:1-12.
22. Thairu Y, Nasir IA, Usman Y. Laboratory perspective of gram staining and its significance in investigations of infectious diseases. Sub-Sahar Afr J Med. 2014;1(4):168-74.
23. Rasheed AH, Gul SS, Azeez HA. Antibacterial and antibiofilm profiles of Thymus Vulgaris essential oil on clinically isolated Porphyromonas Gingivalis and Prevotella Intermedia: An in vitro study. Sulaimani Dent J. 2022;9(2):53-63.
24. Balouiri M, Sadiki M, Ibnsouda SK. Methods for in vitro evaluating antimicrobial activity: a review. J Pharm Anal. 2016;6(2):71-9.
25. De Rapper S, Kamatou G, Viljoen A, Van Vuuren S. The in vitro antimicrobial activity of Lavandula angustifoliaessential oil in combination with other aromatherapeutic oils. Evid Based Complement Altern Med. 2013;2013(1):852049.
26. Epifani F, Latronico M, Di Stefano MG, Notarnicola M, Bruni G, Mastronardi M, et al. Antimicrobial activity of essential oils: A review

on applications. Antibiotics (Basel). 2021;10(1):12.
27. Rao J, Chen B, McClements DJ. Improving the efficacy of essential oils as antimicrobials in foods: mechanisms of action. Annu Rev Food Sci Technol. 2019;10(1):365-87.
28. Sha AM, Garib BT. Antibacterial effect of curcumin against clinically isolated Porphyromonas gingivalis and connective tissue reactions to curcumin gel in the subcutaneous tissue of rats. Biomed Res Int. 2019;2019:6810936.
29. Pellegrini M, Ricci A, Serio A, Chaves-Lopez C, Mazzarrino G, D'amato S, et al. Characterization of essential oils obtained from abruzzo autochthonous plants: Antioxidant and antimicrobial activities assessment for food application. Foods. 2018;7(2):19.
30. Hukić M, Seljmo D, Ramovic A, Ibrišimović MA, Dogan S, Hukic J, et al. The effect of lysozyme on reducing biofilms by Staphylococcus aureus, Pseudomonas aeruginosa, and Gardnerella vaginalis: an in vitro examination. Microb Drug Resist. 2018;24(4):353-8.
31. Gonzalez-Moles M, Scully C, Gil-Montoya J. Oral lichen planus: controversies surrounding malignant transformation. Oral Dis. 2008;14(3):229-43.
32. Eladawy M, El-Mowafy M, El-Sokkary MMA, Barwa R. Effects of lysozyme, proteinase k, and cephalosporins on biofilm formation by clinical isolates of pseudomonas aeruginosa. Interdiscip Perspect Infect Dis. 2020;2020(1):6156720.
33. ohnston W, Rosier BT, Artacho A, Paterson M, Piela K, Delaney C, et al. Mechanical biofilm disruption causes microbial and immunological shifts in periodontitis patients. Sci Rep. 2021;11(1):9796.
34. Paul L. Microbial dysbiosis in periodontitis: a paradigm shift in understanding oral health. J Dent Sci Med. 2024;7(4):253-60.
35. Salavati Hamedani M, Rezaeigolestani M, Mohsenzadeh M. Chemical composition, antimicrobial and antioxidant activities of Lavandula angustifolia essential oil. J Nutr Fast Health. 2020;8(4):273-9.
36. Arshad B, Shaheen SIMK. Essential oils extraction and identification of phytochemical compounds from Lavandula angustifolia Mill: unveiling their antibacterial potential against selected strains. Pak J Bot. 2025;57(5):1517-24.
37. Mladenova A et al. In vitro antimicrobial activity of Bulgarian lavender essential oil. Acta Microbiol Bulg. 2024;40:252-7.
38. De Alteriis E, Maione A, Falanga A, Bellavita R, Galdiero S, Albarano L, et al. Activity of free and liposome-encapsulated essential oil from lavandula angustifolia against persister-derived biofilm of candida auris. Antibiotics (Basel). 2021;11(1):26.
39. Khanem A, Karim N, Ullah I, Younas F. Essential oils of Citrus limon, Cymbopogon citratus, and Lavandula officinalis disrupt Escherichia coli biofilms by inducing cellular damage. Biol Futura. 2025;76(3):343-58.

Original Article

Comparison of the gingival phenotype in diabetic and non-diabetic subjects among patients suffering from periodontal diseases

Aram M. Sha[1*]

Abstract

Objective: This study aimed to compare the gingival phenotype (GP) in subjects with periodontal disease and type 2 diabetes mellitus (DM) with that in subjects without diabetes mellitus.

Methods: A cross-sectional study was performed involving 182 subjects with periodontal diseases (102 with type 2 DM, 80 without DM), aged 40 to 65 years. Clinical parameters were assessed, including keratinized gingival width (KGW) and gingival thickness (GT), plaque index (PI), bleeding index (BI), probing depth (PD), and clinical attachment loss (CAL).

Results: Diabetic patients displayed significantly higher KGW (5.58 ± 0.90 mm vs. 5.12 ± 0.58 mm, p = 0.006), PI (41.19 ± 19.71% vs. 28.38 ± 13.53%, p = 0.001), and BI (42.49 ± 18.16% vs. 28.19 ± 13.80%, p = 0.0001) in comparison to non-DM individuals. There were no significant differences in GT, PD, and CAL between the groups. Sex-based comparisons indicated no significant differences between any of the examined parameters. Correlation analysis and chi-square testing demonstrated substantial relationships between PI and BI (p = 0.0001), BI and CAL (p = 0.04), and PD with CAL (p = 0.0001).

Conclusions: Diabetes significantly alters the GP by increasing KGW, plaque, and bleeding indices, whereas other clinical parameters, such as GT, PD, and CAL, remain predominantly unchanged. These findings underscore the importance of managing inflammation and closely monitoring treatment outcomes in individuals with diabetes with periodontal disease.

Keywords: *Gingival phenotype, Keratinized gingival width, Gingival thickness, Diabetes mellitus, Periodontal disease.*

Submitted: December 19, 2025, Accepted: January 21, 2026, Published: April 1, 2026.

Cite this article as: Sha AM. Comparison of the gingival phenotype in diabetic and non-diabetic subjects among patients suffering from periodontal diseases. Sulaimani Dent J. 2026;13(1):40-50.

DOI: https://doi.org/10.17656/sdj.10220

1. *Periodontics Department, College of Dentistry, University of Sulaimani, Sulaimani, Iraq.*

** Corresponding author*: *aram.hamad@univsul.edu.iq.*

Published by the College of Dentistry, University of Sulaimani

Introduction

Periodontal diseases (gingivitis and periodontitis) are chronic, multifactorial inflammatory diseases of the tooth-supporting structures. They result from the interaction between pathogenic bacterial biofilms and host immune-inflammatory responses and are influenced by systemic diseases[1,2]. Among systemic diseases, diabetes mellitus (DM) is considered a major risk factor for periodontal diseases. Periodontitis and DM have a bidirectional relationship: periodontitis can affect glycemic control and lead to diabetic complications; similarly, DM is associated with the increased prevalence and severity of periodontitis[3].

The term "periodontal phenotype", suggested by the 2017 classification of periodontal and peri-implant diseases and conditions, refers to the combination of gingival phenotype (GP) that includes both three-dimensional gingival volumes, such as keratinized gingival width (KGW) and gingival thickness (GT), as well as bone morphotype (the thickness of the buccal or labial bony plate)[4]. Clinically, GP is frequently classified as either thick or thin. Gingival recession, periodontal attachment loss, and compromised esthetics are more likely to occur in a thin GP, which is typically associated with thin tooth morphologies and narrow keratinized tissue[5,6]. On the other hand, a thick GP offers better treatment outcomes by being more resistant to trauma and inflammation, and better outcomes following periodontal surgical procedures[7]. Additionally, a thick GP has conventionally been considered fundamental for preserving periodontal health and improving plaque control. However, it has been reported that even with a minimal KGW, periodontal health may be maintained with proper oral hygiene measures[8].

GP can be evaluated by direct visual inspection, transgingival probing, dental probe transparency, ultrasonic transducer, parallel profile periapical radiography, and cone-beam computed tomography (CBCT)[9]. Nevertheless, more than 50% of patients with the thin-scalloped GP are misclassified, suggesting that thick and thin GPs cannot be distinguished by direct visual evaluation[10]. Although trans gingival probing is a straightforward procedure, it requires local anesthesia to distort the soft tissues. On the other hand, despite being non-invasive, ultrasonic instruments are unable to detect subtle variations in gingival tissues[11]. Recently, CBCT has become a more common method to evaluate the type of GP. However, in addition to the risk of high-dose radiation exposure, it requires technical expertise and is usually part of the cost-benefit analysis[12]. Finally, a straightforward technique for evaluating the GP based on the transparency of the periodontal probe throughout the gingival margin has been introduced. This approach is considered the "gold standard" because it has been used in numerous clinical studies[6,13].

In diabetes, the structure and healing capacity of gingival tissues can be adversely affected by hyperglycemia-induced microvascular changes, impaired collagen metabolism, increased inflammatory responses, and altered neutrophil activity[14, 15]. Reduced GT and KGW may occur in individuals with DM due to these metabolic and circulatory alterations. Many studies have focused on the effects of GPs on periodontal health and disease[16-19]. However, research specifically comparing GP in DM and non-DM individuals with periodontal diseases has not yet been conducted. Therefore, this cross-sectional study was conducted to compare GPs in individuals with DM and those without DM with periodontal disease.

Materials and methods

Ethical Approval

Ethical approval for the current cross-sectional clinical study was obtained from the Ethical Committee of the College of Dentistry, University of Sulaimani (ethical approval code: COD-EC-25-0112, on December 14, 2025). Accordingly, a sample of 182 individuals with periodontal diseases, comprising both males and females, was selected from the College of Dentistry-Periodontics Department and the Diabetes and Endocrine Center in Sulaimani city, Kurdistan Region, Iraq, between 21 December 2022, and 25 November 2024. All participants signed written informed consent before participating in the study.

Study design

A total of 182 individuals with periodontal diseases were classified into type 2 DM (80 subjects) and non-DM (102 subjects) groups (Figure 1). Periodontal disease subjects recruited were defined by the presence of bleeding on probing at >10% of sites for gingivitis or "the presence of interproximal clinical loss of attachment (CAL) at ≥2 teeth or the presence of CAL ≥3 mm at the facial/oral surfaces associated with probing pocket depths (PPDs) ≥4 mm for periodontitis"[20]. DM was verified by HbA1c readings ≥ 6.5% and medical records. To be eligible, diabetic patients had to have had type 2 DM for at least a year and have moderate glycemic control, as indicated by HbA1c levels between 7.0 and 9.0%[21].

Study criteria

The inclusion criteria for the study were an age range of 40-65 years, individuals with upper and lower anterior teeth, diagnosed as periodontal disease, and those with

diabetes, confirmed as type 2 DM for at least 1 year, with an HbA1c level within the last three months of 7.0–9.0%. Meanwhile, the criteria for exclusion from the study were individuals with long-term use of drugs that influence gingival tissues, such as cyclosporine, calcium channel blockers, and phenytoin, history of periodontal therapy during the previous six months, pregnancy or lactation, smoking or a history of smoking during the previous five years, orthodontic appliances, systemic diseases other than diabetes that are known to impact periodontal health.

Clinical Periodontal Parameters

BI and PI were measured to evaluate gingival inflammation and dental hygiene, respectively[22]. Bleeding observed after 20 seconds was recorded as 1, while its absence was 0. Dental plaque presence was coded as 1 and absence as 0. At the same time, PD and CAL were measured as the distances from the gingival margin and cementoenamel junction to the base of the sulcus/pocket, respectively[20].

Twelve teeth per patient, six maxillary anterior (FDI numbers: 11, 12, 13, 21, 22, 23), and six mandibular anterior teeth (FDI numbers: 31, 32, 33, 41, 42, 43), were examined for the clinical examination of GT and KGW.

The UNC-15 probe was used to evaluate the KGW, and its evaluation was performed by measuring the distance from the gingival margin to the mucogingival junction at the mid-labial aspect of all anterior teeth[23].

Based on the visibility of the periodontal probe through the gingival sulcus, a clinical examination was conducted to assess GT. “Colorvue TM Biotype Probe (Hu-Friedy®, Chicago, IL, USA)” was used in the probe transparency method to detect the GP. GT can be classified as thin, medium, thick, or very thick, with the probe's three different-colored resin tips (white, green, and blue)[13]. This technique involved inserting the probe 1 mm into the gingival sulcus of the maxillary and mandibular anterior teeth through the mid-labial surface (Figure 2). The phenotype was considered thin if the white tip was visible, medium if the green tip was visible, and the phenotype was labeled as thick if the blue tip was present, and as extremely thick if neither the green nor the blue tip was discernible[24].

Examiner Calibration

A single calibrated examiner performed all clinical examinations. A kappa value of > 0.85 was obtained for intra-examiner reliability for B after calibration on ten subjects not included in the study for the clinical parameters, suggesting strong repeatability[25].

Statistical Analysis

Data were compiled in Microsoft Excel and analyzed using SPSS version 26. The Shapiro-Wilk test assessed normality, while descriptive statistics, including mean ± SD and frequency, were calculated. Independent samples t-tests compared mean values of KGW, PD, and CAL between groups, and the Chi-square test examined distributions of GT, PI, and BI. Pearson's correlation was used to assess the correlation between the means of clinical parameters. Statistical significance was defined as a p-value of ≤ 0.05.

Results

The study population consisted of 182 patients, among whom 80 (43.95%) were non-DM and 102 (56.04%) were DM**.** The distribution of participants by sex showed that 132 (72.5%) were female and 50 (27.5%) were male. The average age of patients with DM was 52.04 ± 7.2 years, whereas in those without diabetes, the mean age was 46.54 ± 6.37 years.

Comparison of clinical parameters between diabetic and non-diabetic patients

The mean of GT in DM was 1.81± 0.85 mm, while in non-DM, it was 1.91± 0.89 mm, with no statistically significant difference (p = 0.5). DM subjects had a statistically significantly higher KGW (5.58± 0.9 mm) than non-DM subjects (5.12 ± 0.58 mm, p < 0.006).

Likewise, individuals with DM had a greater PI (41.19±19.71%) than those without DM (28.38 ± 13.53%, p = 0.001). Additionally, there was a significant difference in the BI in DM (42.49 ± 18.16%) when compared to non- DM (28.19 ±13.80, p = 0.0001).

No statistically significant differences in mean PD between DM subjects (1.75 ± 0.75 mm) and non-DM subjects (1.38 ± 0.65mm) were detected (p = 0.07). Similarly, no statistically significant differences in mean CAL of DM (1.48 ± 0.33 mm) and non-DM (1.40 ± 0.28 mm) were observed (p = 0.8).

Overall, these results show that DM patients had considerably higher KGW, PI, and BI values than non-DM subjects. Whereas no statistically significant differences in GT, PD, and CAL were detected between the studied groups (Figure 3).

Tooth-by-tooth comparison of keratinized gingival width between diabetic and non-diabetic patients

As mentioned earlier, DM individuals had a mean KGW of 5.58 ± 0.90 mm, while non-DM individuals showed a mean KGW of 5.12 ± 0.58 mm. In DM subjects, the mean KGW per tooth ranged from 4.13 ± 1.18 mm to

6.79 ± 1.18 mm. While in non-DM patients, the range was 4.06 ± 1.09 mm to 6.28 ± 1.09 mm. No statistically significant differences between groups at any tooth site ($p > 0.05$) were detected, and KGW distribution across the dentition was found to be similar for both groups, as shown in Figure 4.

Tooth-by-tooth comparison of gingival thickness between diabetic and non-diabetic patients

Again, as presented in Figure 3, DM patients had a mean GT of 1.81 ± 0.85 mm, and non-DM patients showed a mean GT of 1.91 ± 0.89 mm. When evaluated by individual tooth, DM patients had average GT values ranging from 1.74 ± 0.03 mm to 1.84 ± 0.03 mm. In non-DM subjects, average GT values ranged from 1.78 ± 0.11 mm to 2.09 ± 0.11 mm. Although some tooth sites showed numerical differences, statistical analysis found no significant differences in GT between DM and non-DM groups across all teeth ($p > 0.05$ for each tooth position). Thus, GT was similarly distributed in both DM and non-DM subjects, with no significant tooth-specific changes (Figure 5).

Comparison of clinical parameters between males and females

A comparison of clinical periodontal parameters between male (n = 50) and female (n = 132) participants indicated no statistically significant differences in any of the parameters examined, as shown in Figure 6.

Correlation of clinical periodontal parameters

The darker shading in Figure 7 distinctly highlights the strong correlations (e.g., PI–BI, PD–CAL, KGW–CAL, and age-related correlations), while lighter tones indicate negligible or weaker correlations. Several significant relationships were identified among clinical parameters in the correlation analysis. Age showed a weak but statistically significant positive correlation with KGW ($r = 0.22$, $p = 0.003$), PI ($r = 0.20$, $p = 0.007$), and BI ($r = 0.27$, $p = 0.0001$). However, no statistically significant associations were found between age and GT, PD, or CAL ($p > 0.05$). Regarding the association among periodontal clinical parameters, GT showed no statistically significant correlations with KGW, PI, BI, PD, or CAL ($p > 0.05$). KGW displayed a statistically significant negative correlation with CAL ($r = –0.27$, $p = 0.0001$), while its correlations with PI, BI, and PD were not statistically significant.

Further, the study demonstrated a strong positive association between PI and BI. There was also a strong positive association between PD and CAL ($P \leq 0.01$). BI was moderately correlated with CAL ($P \leq 0.05$). However, there were no statistically significant associations among GT, KGW, and other parameters.

These findings suggest that increased age is associated with higher KGW, PI, and BI. In contrast, the correlations with other parameters showed that inflammatory indices (PI and BI) are strongly associated with periodontal breakdown markers (CAL and PD).

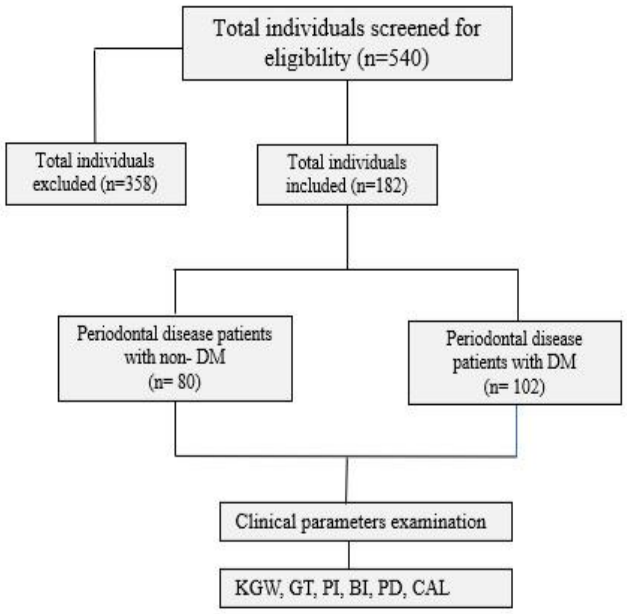

Figure 1: Design of the study.

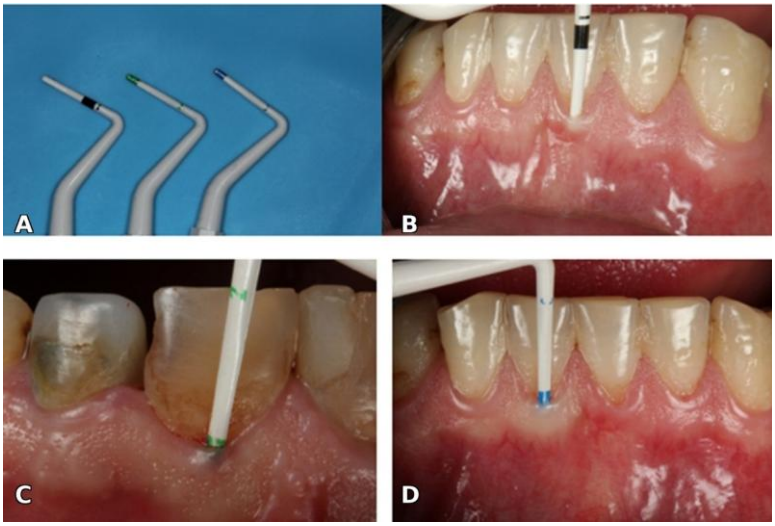

Figure 2: Probe transparency method using Hu-Friedy's Colorvue Biotype Probe for the evaluation of GT (A). The probe was inserted 1 mm into the gingival sulcus at the mid-labial surface (B). The GT was considered thin if the white tip was visible, medium if the green tip was visible, and thick if the blue tip was present, and as extremely thick if neither the green nor the blue tip was discernible (B, C, and D).

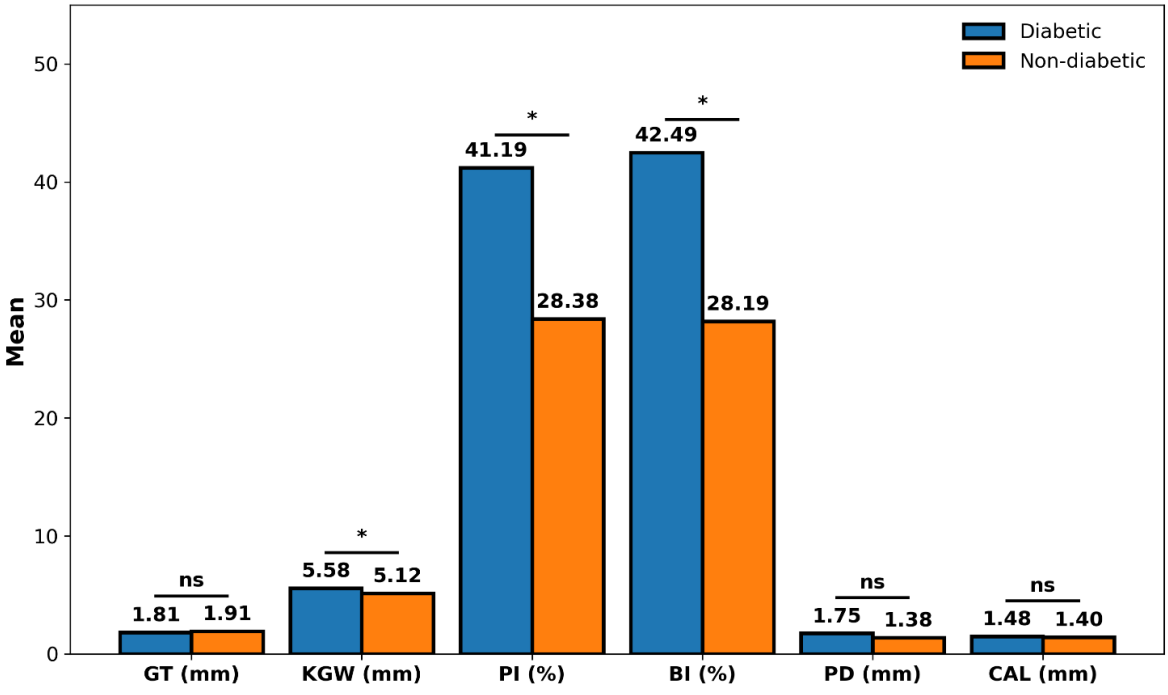

Figure 3: Comparison of clinical parameters between diabetic and non-diabetic patients. ns: non-significant.

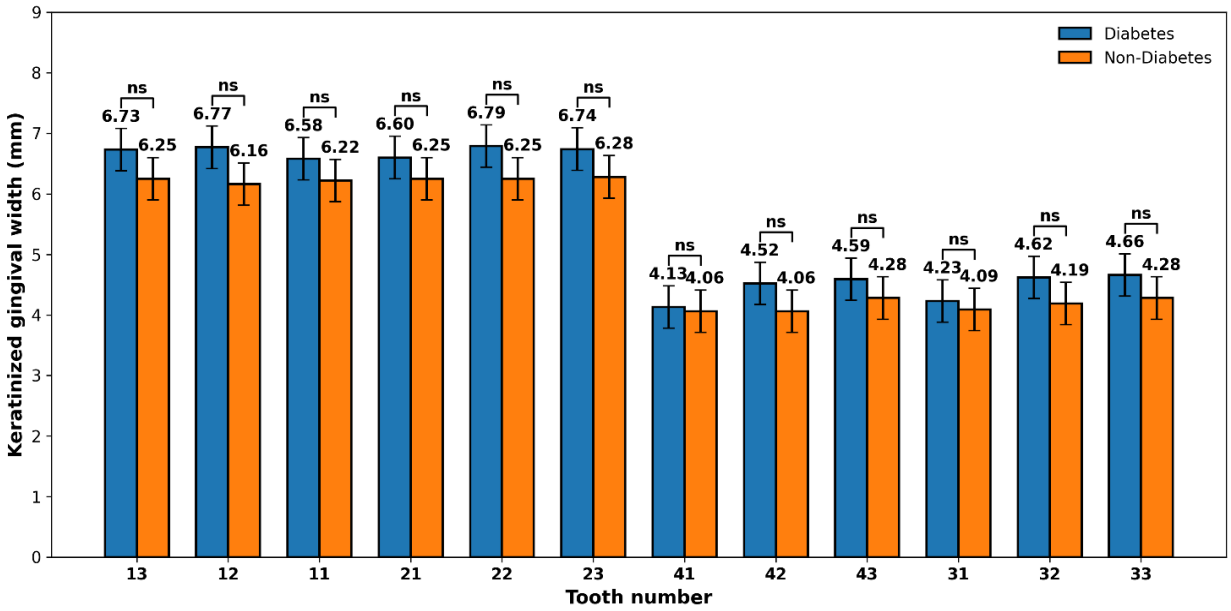

Figure 4: Keratinized gingival width in diabetic versus non-diabetic patients (tooth-by-tooth comparison).

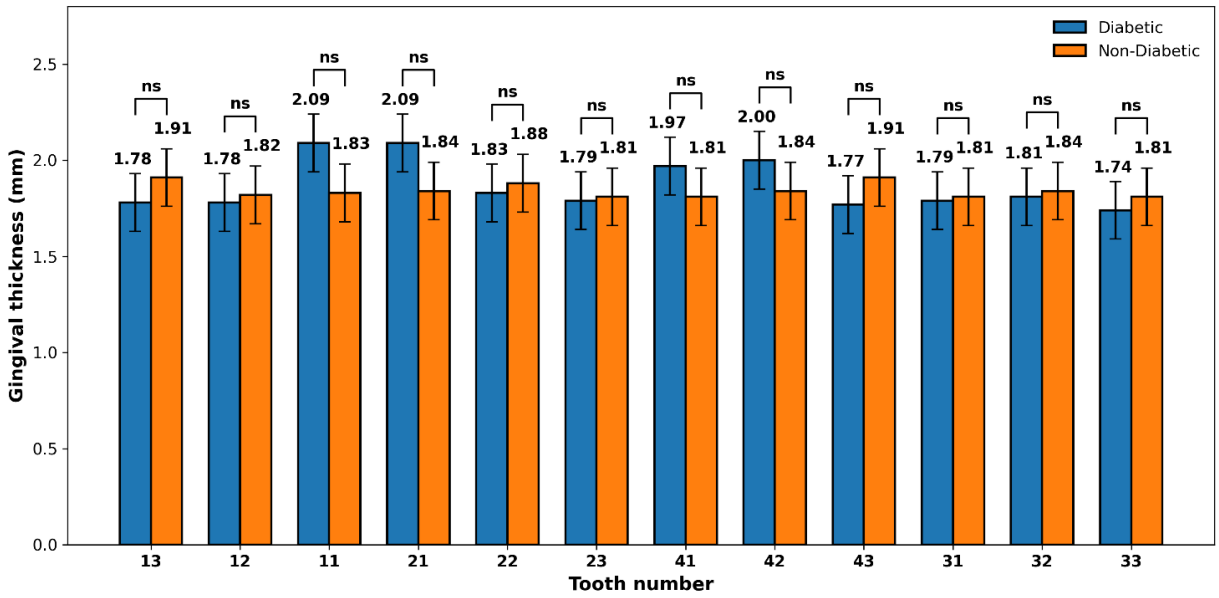

Figure 5: Gingival thickness in diabetic versus non-diabetic patients (tooth-by-tooth comparison).

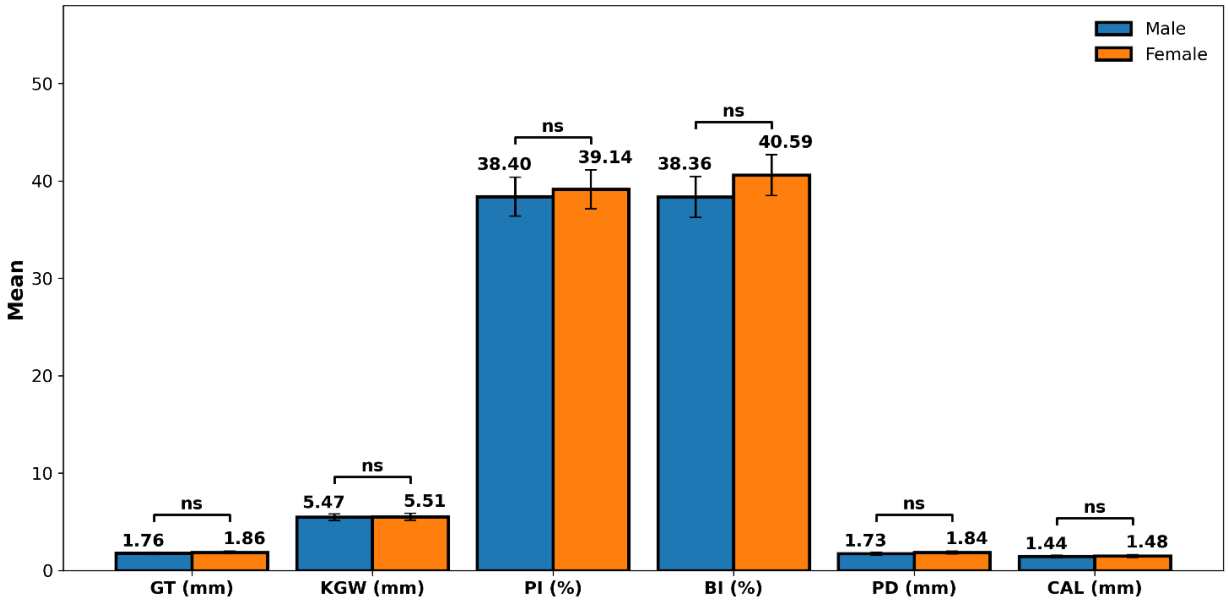

Figure 6: Comparison of clinical parameters between males and females.

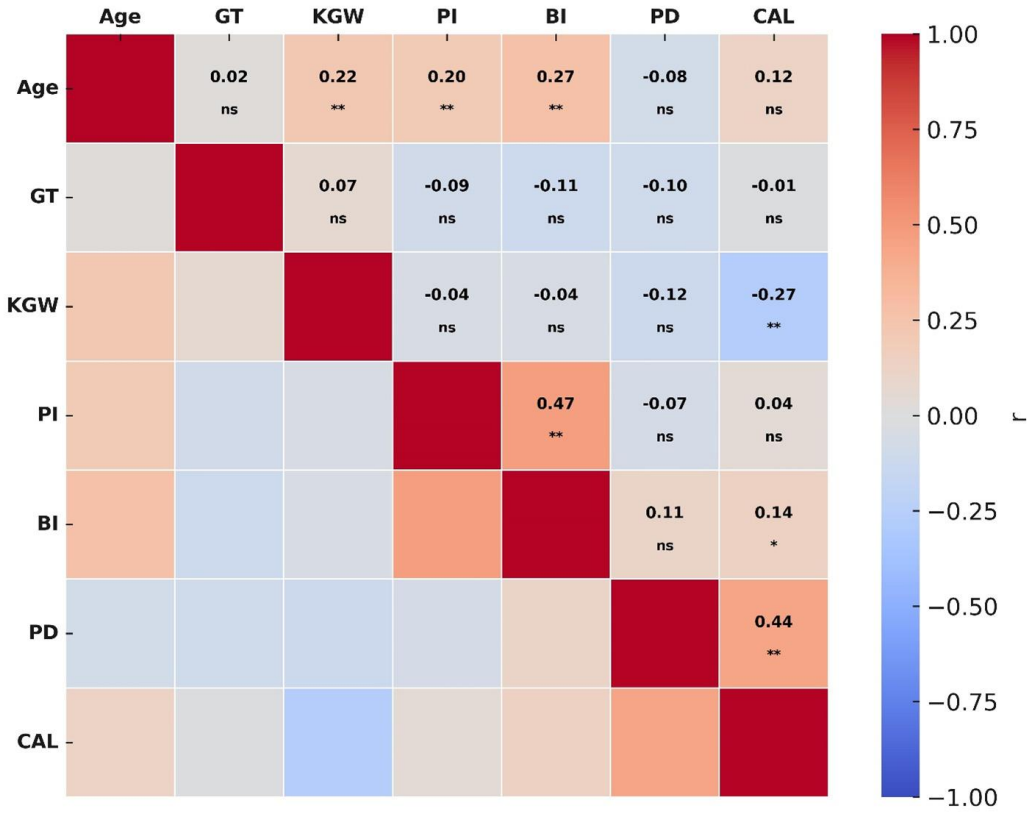

Figure 7: Correlations between clinical parameters.

r: Pearson Correlation; **Correlation is significant at the 0.01 level; *Correlation is significant at the 0.05 level; ns: non-significant

Discussion

The GP is pivotal in periodontal health and disease progression, as it induces liability to inflammation, tissue response to bacterial biofilm, and outcomes of periodontal treatment[19]. In patients with DM, modifications in the immune-inflammatory response, disrupted collagen metabolism, and microvascular complications contribute to a thinner and more fragile GP, potentially leading to more severe periodontal destruction than in non-diabetic individuals[26,27]. Numerous studies have demonstrated that individuals with DM often have diminished KGW and altered GT. This negatively affects periodontal stability and regenerative capacity[28,29]. In contrast, non-DM individuals usually have a more robust GP. This offers better protection against microbiological and mechanical challenges[9]. Comparing the GP of DM and non-DM individuals gives significant insights. It helps understand the relationship between systemic diseases and the characteristics of periodontal tissues.

The current study demonstrated that DM impacts GP and periodontal health, with the characteristics of these effects differing across clinical and biological parameters.
The rise in KGW among DM individuals contradicts the belief that DM compromises gingival tissue heights. Multiple mechanisms may explain this observation.

Chronic hyperglycemia affects collagen metabolism and microvascular function. This may lead to fibrotic remodeling or an adaptive increase in keratinized tissues[14]. Adaptive reaction may explain the increased width of keratinized gingiva in people with DM. However, Tooth-by-tooth comparisons showed no statistically significant differences. This means the overall rise in KGW may not apply to all anterior teeth.

Recent research shows that GT measurements are sensitive to the specific locations tested. Yildirim Bolat and Lutfioglu[30] found that measuring GT at several vertical levels (sulcus base, 1 mm, and 2 mm apical) gives different results. They demonstrated that averaging multiple points offers a more dependable classification of GP. This may explain the non-significant GT differences between DM and non-DM. The finding also aligns with research showing that GT is more affected by local anatomical features and tooth morphology than by systemic disease[5,6]. Tooth-by-tooth comparisons demonstrated no statistically significant variations in GT. This finding corroborates the notion that GT is a relatively stable parameter, whereas KGW may be more vulnerable to systemic metabolic changes[31].

DM individuals showed significantly higher PI and BI. Contemporary pathogenesis models indicate that periodontal inflammation alters the subgingival environment, promoting a dysbiotic shift. In turn, dysbiosis perpetuates inflammation, creating a circular feed-forward loop. This framework suggests that elevated BI and PI reflect an altered host–biofilm relationship rather than increased plaque quantity alone [32]. This aligns with findings that hyperglycemia triggers heightened inflammatory responses and weakens immune regulation[15]. The strong association between PI and BI highlights the role of biofilm-induced inflammation in periodontal disease. Biomarker research has found increased concentrations of MMP-8, MMP-9, IL-6, and AGE in patients with DM and periodontitis. This supports a molecular link between systemic hyperglycemia and local periodontal inflammation[33,34]. Gregorczyk-Maga, Kania[35] reported changes in the gingival crevicular fluid microbiota and metabolome in people with type 1 DM on continuous insulin therapy. These changes correlated with mild gingival inflammation. The findings support that hyperglycemia and its systemic effects trigger molecular changes. These include microbial dysbiosis, elevated inflammatory mediators, and AGEs, which can affect GP and disease progression[33].

KGW, PI, and BI vary between DM and non-DM individuals. However, many studies, including this one, have not found significant differences in PD and CAL. It may depend on glycemic control, disease duration, and methodological differences[3,36]. These results suggest that inflammatory indices (PI, BI) may be more sensitive predictors of early periodontal risk in individuals with DM than destructive measures such as CAL or PD.

The positive associations observed among PI and BI, PD and CAL, and BI and CAL underscore the interrelationships among inflammatory and destructive periodontal disease. Moreover, age exhibited weak yet significant correlations with KGW, PI, and BI, indicating that aging may progressively affect GP and inflammatory load. These findings align with a previous study indicating cumulative age-related periodontal alterations[1].

There were no significant differences between DM and non-DM subjects by sex. This suggests that systemic metabolic status and behavioral risk factors have a greater impact on periodontal status than sex[9]. This

highlights DM status as a more critical determinant of periodontal health outcomes than sex.

Several limitations should be considered when interpreting these results. The cross-sectional design precludes establishing a cause-and-effect relationship between diabetes status and changes in gingival phenotype or periodontal characteristics. Assessment of the gingival phenotype was limited to anterior teeth, excluding posterior teeth, which may exhibit greater morphological variation. The diabetic cohort comprised only individuals with moderate glycemic control, limiting the generalizability of findings to those with well-controlled or poorly controlled diabetes. Gingival thickness was measured using the probing transparency method, a semi-quantitative approach that may not detect subtle tissue differences despite its clinical utility. Behavioral and socioeconomic factors were not systematically evaluated. Additionally, because the research was conducted at a single center, the findings may not generalize to other populations, underscoring the need for multicenter longitudinal studies.

The clinical implications of these results underscore the need to tailor periodontal care techniques for DM patients by providing tailored oral hygiene measures and treatment. Standardized assessment techniques, including multi-point GT measures, improve accuracy and comparability across studies and clinical settings[30]. Although GT may not be substantially influenced by DM, the persistently high PI and BI values underscore the importance of accurate biofilm management, reinforcement of oral hygiene, and routine professional maintenance to prevent periodontal disease. Future studies should incorporate salivary or GCF biomarkers, such as AGEs, cytokines, and microbiota profiles, that can serve as essential instruments for early identification and customized treatment strategies[37]. The increase in KGW among individuals with DM contradicts established assumptions, raising important questions regarding whether this adaptation serves a protective or pathological role. This observation underscores the need for a prospective longitudinal study to further investigate its implications.

Conclusion

DM clearly affects GP and periodontal health, primarily increasing KGW, PI, and BI. GT, PD, and CAL appear to be less affected under moderate glycemic control. These findings underscore the need for inflammatory control and thorough oral hygiene in individuals with DM. Future research should explore whether increased KGW is a protective adaptation or a pathogenic response to metabolic stress.

References

1. Kinane DF, Stathopoulou PG, Papapanou PN. Periodontal diseases. Nat Rev Dis Primers. 2017;3(1):1-14.
2. Zardawi F, Gul S, Abdulkareem A, Sha A and Yates J. Association between periodontal disease and atherosclerotic cardiovascular diseases: revisited. Front. Cardiovasc. Med. 2021; 7:625579.
3. Preshaw PM, Alba AL, Herrera D, Jepsen S, Konstantinidis A, Makrilakis K, et al. Periodontitis and diabetes: a two-way relationship. Diabetologia. 2012; 55(1):21-31.
4. Jepsen S, Caton JG, Albandar JM, Bissada NF, Bouchard P, Cortellini P, et al. Periodontal manifestations of systemic diseases and developmental and acquired conditions: Consensus report of workgroup 3 of the 2017 world workshop on the classification of periodontal and peri-implant diseases and conditions. J Clin Periodontol. 2018;45: S219-S229.
5. De Rouck T, Eghbali R, Collys K, De Bruyn H, Cosyn J. The gingival biotype revisited: transparency of the periodontal probe through the gingival margin as a method to discriminate thin from thick gingiva. J Clin Periodontol. 2009: 36(5):428-33.
6. Kan JY, Morimoto T, Rungcharassaeng K, Roe P, Smith DH. Gingival biotype assessment in the esthetic zone: visual versus direct measurement. Int J Periodontics Restorative Dent. 2010;30 (3)237-43.
7. Fu JH, Yeh CY, Chan HL, Tatarakis N, Leong DJ, Wang HL. Tissue biotype and its relation to the underlying bone morphology. J Periodontol. 2010;81(4):569-74.
8. Wennström J, Lindhe J. Role of attached gingiva for maintenance of periodontal health: healing following excisional and grafting procedures in dogs. J Clin Periodontol. 1983;10(2):206-21.
9. Kim DM, Bassir SH, Nguyen TT. Effect of gingival phenotype on the maintenance of periodontal health: An American Academy of Periodontology best evidence review. J. Periodontol. 2020;91(3):311-38.
10. Lee SP, Kim TI, Kim HK, Shon WJ, Park YS. Discriminant analysis for the thin periodontal biotype based on the data acquired from three-dimensional virtual models of Korean young adults. J Periodontol. 2013;84(11):1638-45.
11. Bednarz W. The thickness of periodontal soft tissue ultrasonic examination—current possibilities and perspectives. Dent Med Probl. 2011;48(3):303-10.

12. Fu JH, Lee A, Wang HL. Influence of tissue biotype on implant esthetics. Int J Oral Maxillofac Implants. 2011;26(3):499-508.
13. Tofiq RK, Hamad AM. Assessment of Gingival Phenotype in Type 2 Diabetic Patients in Sulaimani City. Sulaimani Dent J. 2023;10 (1):11-19.
14. Lalla E, Papapanou PN. Diabetes mellitus and periodontitis: a tale of two common interrelated diseases. Nat Rev Endocrinol. 2011;7(12):738-748.
15. Polak D, Shapira L. An update on the evidence for pathogenic mechanisms that may link periodontitis and diabetes. J Clin Periodontol. 2018;45(2):150-66.
16. Pashova-Tasseva Z, Mlachkova A, Tosheva E. Impact of gingival phenotype on the periodontal disease. Folia Med. 2023;65(3):468-75.
17. Moosa Y, Samaranayake L, Pisarnturakit PP. The gingival phenotypes and related clinical periodontal parameters in a cohort of Pakistani young adults. Heliyon. 2024;10(2):e24219.
18. Alasiri MM, Almalki A, Alotaibi S, Alshehri A, Alkhuraiji AA, Thomas JT. Association between gingival phenotype and periodontal disease severity-a comparative longitudinal study among patients undergoing fixed orthodontic therapy and Invisalign treatment. Healthcare (Basel). 2024;12(6):656.
19. Nagate RR, Chaturvedi S, Al-Ahmari MMM, Al-Qarni MA, Gokhale ST, Ahmed AR, et al. Importance of periodontal phenotype in periodontics and restorative dentistry: a systematic review. BMC Oral Health. 2024;24(1):1-10.
20. Tonetti MS, Greenwell H, Kornman KS. Staging and grading of periodontitis: Framework and proposal of a new classification and case definition. J Periodontol. 2018;89(12):S159-S72.
21. Ainamo J, Bay I. Problems and proposals for recording gingivitis and plaque. Int Dent J. 1975;25(4):229-25.
22. Lang NP, Löe H. The relationship between the width of keratinized gingiva and gingival health. J Periodontol. 1972;43(10):623-27.
23. Kloukos D, Koukos G, Doulis I, Sculean A, Stavropoulos A, Katsaros C. Gingival thickness assessment at the mandibular incisors with four methods: a cross-sectional study. J Periodontol. 2018; 89(11):1300-09.
24. Bland JM, Altman D. Statistical methods for assessing agreement between two methods of clinical measurement. Lancet. 1986;327(8476):307-310.
25. Mealey BL, Oates TW. Diabetes mellitus and periodontal diseases. J Periodontol. 2006;77(8):1289-303.
26. Botero JE, Yepes FL, Roldan N, Castrillon CA, Hincapie JP, Ochoa SP, et al. Tooth and periodontal clinical attachment loss are associated with hyperglycemia in patients with diabetes. J Periodontol. 2012;83(10):1245-50.
27. Păunică I, Giurgiu M, Dumitriu AS, Păunică S, Pantea Stoian AM, Martu M.A, et al. The bidirectional relationship between periodontal disease and diabetes mellitus—a review. Diagn. 2023;13(4):681.
28. Zhang Z, Ji C, Wang D, Wang M, Song D, Xu X, Zhang D. The burden of diabetes on the soft tissue seal surrounding the dental implants. Front Physiol. 2023;14:1136973.
29. Yildirim Bolat S, Lutfioglu M. Evaluation of gingival phenotype: the role of gingival thickness measurements from different vertical gingival levels. Clin Oral Investig. 2025;29(1):87.
30. Barootchi S, Tavelli L, Di Gianfilippo R, Shedden K, Oh TJ, Rasperini G. et al. Soft tissue phenotype modification predicts gingival margin long-term (10-year) stability: longitudinal analysis of six randomized clinical trials. J Clin Periodontol. 2022;49(7):672-83.
31. Abdulkareem AA, Al-Taweel FB, Al-Sharqi AJB, Gul SS, Sha A, Chapple ILC. Current concepts in the pathogenesis of periodontitis: from symbiosis to dysbiosis. J Oral Microbiol. 2023;15(1):2197779.
32. Chen J, Wang H, Bu S, Cheng X, Hu X, Shen M, Zhuang H. Alterations in subgingival microbiome and advanced glycation end-products levels in periodontitis with and without type 1 diabetes mellitus: a cross-sectional study. BMC Oral Health. 2024;24(1):1344.
33. Ebersole JL, Kirakodu SS, Zhang XD, Dawson III D, Miller CS. Salivary features of periodontitis and gingivitis in type 2 diabetes mellitus. Sci Rep. 2024;14(1):30649.
34. Gregorczyk-Maga I, Kania M, Dąbrowska M, Samborowska E, Żeber-Lubecka N, Kulecka M, Klupa T. The interplay between the gingival crevicular fluid microbiome and metabolomic profile in intensively treated people with type 1 diabetes, combined metagenomic/metabolomic approach, cross-sectional study. Front Endocrinol. 2024;14:1332406.

35. Xiang Dd, Sun Yx, Jiao C, Guo Yq, Fei Yx, Ren Bq, et al. Diabetes and periodontitis: the role of a high-glucose microenvironment in periodontal tissue cells and corresponding therapeutic strategies. Stem cell res ther. 2025;16(1),366.
36. Sanz M, Ceriello A, Buysschaert M, Chapple I, Demmer RT, Graziani F, et al. Scientific evidence on the links between periodontal diseases and diabetes: Consensus report and guidelines of the joint workshop on periodontal diseases and diabetes by the International Diabetes Federation and the European Federation of Periodontology. Diabetes Res Clin Pract. 2018;137:231-41.

Original Article

Mandibular Asymmetry in Cleft Lip and Palate Versus Class I Malocclusion: A Panoramic Radiographic Study in Mosul

Omar S. Mohammed Ali[*1], *Mohammed A. Mohammed*[1]

Abstract

Objective: This study aimed to evaluate the mandibular asymmetry between patients with Unilateral and Bilateral Cleft Lip and Palate in Mosul city by using panoramic radiographs and mandibular asymmetry index to compare with Class I malocclusion controls for selecting the type of treatment in future.

Methods: A retrospective cross-sectional study was performed on 150 orthodontic patients (75 with CLP and 75 controls with Class I anterior relationship) visiting a dental hospital in Mosul city. Patients between 12 and 18 years of age who had not been previously treated orthodontically were included in the study. Digital orthopantomograms were analyzed for vertical ramus and condylar heights using Habets' method. The mandibular asymmetry index for each patient was calculated as the percentage difference between right and left ramus or condylar heights. A $p \leq 0.05$ was considered significant.

Results: The CLP and Class I groups showed no statistically significant differences in mandibular asymmetry indices. The mean ramus asymmetry index was 2.61% in Class I vs 3.88% in CLP, and the mean condylar asymmetry index was 7.68% vs 8.99%, respectively (both comparisons, $p>0.05$). Within each group, the right and left ramus and condylar heights were symmetric (no significant side-to-side differences, $p>0.1$). Age was associated with increased asymmetry: older adolescents exhibited higher ramus asymmetry, significantly in the Class I group ($p<0.01$). Sex had no significant influence on asymmetry in either group ($p>0.05$).

Conclusions: Both groups had vertical mandibular asymmetry, with no difference in asymmetry between CLP subjects and Class I malocclusion controls. The average asymmetry indices for both groups were greater than 3%, implying that mild vertical mandibular asymmetry was present in both boys and girls.

Keywords: *Mandibular asymmetry, Cleft lip and palate, Class I malocclusion, Habets index.*

Submitted: December 12, 2025, Accepted: March 3, 2026, Published: April 1, 2026.

Cite this article as: Mohammed Ali OS, Mohammed MA. Mandibular Asymmetry in Cleft Lip and Palate Versus Class I Malocclusion: A Panoramic Radiographic Study in Mosul. Sulaimani Dent J. 2026;13(1):51-58.

DOI: https://doi.org/10.17656/sdj.10221

1. *Orthodontics Department, College of Dentistry, Tishk International University, Erbil, Iraq.*

* *Corresponding author*: *omar.sabah@tiu.edu.iq*.

Introduction

Facial symmetry and proportionality are key components of craniofacial esthetics, while mandibular asymmetry is defined as a discrepancy in form or size between the right and left sides of the mandible and is one of the most common asymmetrical features encountered in orthodontics[1]. Multiple factors, such as age, growth pattern, occlusion, parafunctional habits, trauma, and developmental defects, can influence the development of mandibular asymmetry. Indeed, epidemiological studies have reported that up to one-third of orthodontic patients may have noticeable facial or mandibular asymmetries 2.

Maxillary deficiencies are associated with Cleft lip and palate (CLP) and there is interest in whether CLP also contributes to mandibular growth disturbances or asymmetry[3]. The mandible of unilateral CLP patients has been observed to grow in a complex manner due to functional shifts and occlusal compensations[4]. Some longitudinal studies indicate that unilateral CLP patients manifest mandibular asymmetry that increases during growth and parallels the maxillary asymmetry, underscoring the intertwined development of the jaws. This has led to recommendations for early evaluation and intervention addressing both the nasomaxillary complex and the mandible in CLP patients[5]. The literature on mandibular asymmetry in CLP has reported inconsistent findings, which may be attributable to differences in sample characteristics, imaging techniques, and measurement methods across studies[6]. Non-syndromic CLP patients have a wide spectrum of growth outcomes, and while some studies have found significant differences in mandibular ramal or condylar heights between CLP patients and non-cleft controls, others have found no significant differences[7].

Clinically, panoramic radiography (orthopantomogram, OPG) is a common imaging modality used in the initial orthodontic assessment of CLP patients[8]. Prior studies have validated panoramic measurements of condylar and ramus height asymmetries as having acceptable reproducibility and accuracy for screening purposes[9,10,11]. We are looking for any significant relationship between mandibular asymmetry and cleft patients with class I malocclusion. We hypothesized that adolescents with CLP would demonstrate greater vertical mandibular asymmetry than Class I controls.

Materials and Methods

Study Design and Ethical Clearance

This was a retrospective, cross-sectional study in which available patient records were reviewed at the College of Dentistry, University of Mosul. The protocol was presented to the Institutional Research Ethics Committee of the University of Mosul, and approval was granted (Approval No. MOS-OD/2025/001).

Sample Selection

The sample comprised 150 subjects (75 with cleft lip and/or palate and 75 with Class I malocclusion) treated in the Department of Orthodontics in Mosul. Inclusion criteria for the CLP group were non-syndromic unilateral or bilateral cleft lip and palate patients aged 12–18 years who had pre-treatment panoramic radiographs of diagnostic quality. The Class I malocclusion group consisted of

orthodontic patients ages 12–18 with skeletal and dental Class I relationships (ANB ≈ 2–4°) and no crossbites or significant asymmetries noted clinically. Mild dental crowding or spacing was permitted in the Class I group (as these are common and not expected to affect mandibular symmetry), but cases with any anterior or posterior crossbite were excluded. Additional exclusion criteria for both groups were: history of previous orthodontic treatment or jaw surgery, any systemic conditions or syndromes affecting growth, and trauma or pathologies of the jaw. From an initial pool of 180 eligible records (95 CLP, 85 Class I), we applied the above criteria and randomly selected 75 individuals per group for analysis. A power calculation was performed using G*Power 3.1 to determine the sample size: based on an effect size of 0.5 for asymmetry index difference, a total of ~138 subjects (69 per group) was required for 80% power at $\alpha = 0.05$. Our final sample of 150 exceeded this requirement, providing adequate power to detect moderate group differences.

Imaging and Measurements

All subjects had pre-treatment panoramic radiographs (orthopantomograms) taken as part of their orthodontic records. The radiographs were acquired using a digital panoramic X-ray unit (Planmeca ProMax, Helsinki, Finland) set at standard exposure parameters and 1.3× magnification.

Panoramic images were exported to digital imaging software (EzDent-i, Vatech, Korea) for measurement. Before analysis, each image was calibrated to account for the machine's known magnification factor. The technique described by Habets *was* used to measure the vertical height of the mandibular ramus and condyle on each side. Briefly, a horizontal reference line (line “A”) was drawn as a tangent to the inferior border of the mandible (at the gonial region). A perpendicular line was constructed from this tangent to the highest point of the condylar process, defining the condylar height (CH). The ramus height (RH) was defined as the distance from the most superior condylion point to the intersection

with the tangent at the mandibular angle (i.e., the distance between points O1 and O2 as per Habets' method). Each measurement was performed for the left and right sides of the mandible. Figure 1 illustrates the reference points and measurements on a sample panoramic radiograph (O1: lateral condylar point; O2: lateral ramus point; AC: condylar height; AR: ramus height). The condylar asymmetry index (CAI) and ramus asymmetry index (RAI) were then calculated for each subject using the formula:

$$Asymmetry\ Index\ (AI) = \frac{Right\ side - Left\ side}{Right\ side + Left\ side} \times 100\%$$

where the absolute difference in heights is normalized to the average of both sides. An asymmetry index of 0% indicates perfect symmetry, whereas higher values indicate greater asymmetry. We considered an index >3% as the threshold for clinically notable vertical asymmetry, based on the original validation by Habets[11], who reported that a 3% index corresponds to ~6% linear discrepancy due to minor head positioning differences.

All radiographic measurements were made by a single calibrated examiner (an orthodontist). To assess intra-observer reliability, 15 radiographs (10% of the sample) were randomly selected and re-measured by the same examiner after a 3-week interval. Furthermore, a second orthodontist measured 10 radiographs to assess inter-examiner reliability. Intraclass correlation coefficients for measurements of ramus and condyle height were 0.93 and 0.91, indicating excellent repeatability. Small differences (≤ 1 mm) in duplicate measurements were resolved by consensus, and the average was used.

Statistical analysis

SPSS 26.0 (IBM, Armonk, NY) was used to process the data. Age was presented as a continuous variable (years). Continuous variables were tested for normal distribution using the Shapiro–Wilk test. For each group (CLP and Class I), paired t-tests were applied to compare the means of right vs left ramus height and condylar height. Comparisons between CLP and Class I groups were assessed using independent samples t-tests for normally distributed variables (e.g., age). Comparison between groups of the nonnormally distributed asymmetry indices was made using the Mann–Whitney U test. Categorical data (percentage with >3% prevalence of asymmetry, gender) were compared using the chi-square test (or Fisher's exact test if expected counts were <5). Furthermore, we used Spearman's rank correlation analysis to examine the association between age and AsysCs within each group. The criterion for statistical significance was $p \leq 0.05$ in all analyses.

Results

Sample Characteristics

Table 1 presents the demographic distribution of the two groups. The mean age of the Class I group was slightly higher than that of the CLP group (15.8 ± 1.8 vs 14.9 ± 1.9 years, respectively), and this difference was statistically significant (p = 0.010). The CLP sample included 38 males (50.7%) and 37 females (49.3%), whereas the Class I sample had 27 males (36.0%) and 48 females (64.0%). Although the CLP group had a higher proportion of males than the Class I group, the difference in sex distribution did not reach statistical significance (chi-square, p = 0.073). Overall, the combined sample comprised 43.3% males and 56.7% females.

Side-to-Side Comparisons of Mandibular Dimensions

Table 2 summarizes the vertical ramus and condylar height measurements on the right and left sides for each group. In the Class I group, the mean ramus height was 38.5 mm on the right and 39.0 mm on the left, a difference that was not statistically significant (paired t-test p = 0.68). The mean condylar process height in Class I patients was 5.7 mm (right) vs 5.9 mm (left), and the difference was not statistically significant (p = 0.21). Similarly, in the CLP group, the mean ramus heights were 40.6 mm (right) and 42.0 mm (left), with no significant side difference (p = 0.33). The mean condylar heights in CLP patients were 5.9 mm (right) and 5.5 mm (left); although the left condyle tended to be slightly shorter on average, this difference was not statistically significant (p = 0.17). Figure 2 illustrates an example panoramic radiograph from a CLP patient, demonstrating the measurement of right and left ramus and condylar heights using the reference lines (the left condylar height is marginally less than the right in this case, consistent with the trend in group means).

Asymmetry Indices and Group Comparison

Table 3 shows the condylar and ramus asymmetry indices of two groups. For ramus asymmetry, the median asymmetry index was 2.0% in Class I as well as CLP groups. The mean ramus asymmetry index tended to be greater in CLP (3.5% ± 3.8%) than in Class I subjects (2.9% ± 2.4%), but the difference was not significant (Mann–Whitney U = 2648, p = 0.538). Regarding condylar height asymmetry, the median of the CLP group was 9.0% for the asymmetry index (mean 9.5% ± 7.5%), and this value in the Class I group was 6.5% (mean = 7.2% ± 6.5%). The condylar asymmetry was statistically higher in the CLP patients, although the inter-group difference did not reach the usual level of significance (p = 0.067). Accordingly, the cleft sample trended towards greater condylar asymmetry, although

there remained significant overlap between samples. Significantly, both groups had mean values well above the 3% threshold for both ramus and condylar asymmetry indices, indicating that mild vertical asymmetries are frequently observed even in Class I individuals.

The mean condylar height differences were in the range of 5–10%, and the mean ramus height differences were smaller (~3%) for this group of adolescent patients. There was a large inter-individual variation: for example, in the CLP group, the condylar asymmetry indices ranged from nearly 0% (i.e., almost perfectly symmetrical condyles) to about 25%. In the Class I sample, the maximum observed condylar asymmetry index was approximately 21%. Despite CLP patients including some of the most asymmetric cases, the overall distribution did not differ significantly from that of the Class I group.

From a clinical standpoint, we also evaluated the prevalence of notable asymmetry in each group using the 3% cutoff. In the Class I group, 27 out of 75 patients (36%) had a ramus asymmetry index >3%, compared to 15 out of 75 (20%) in the CLP group; this difference was not significant ($\chi^2 = 0.41$, $p = 0.523$). For condylar asymmetry, 60 of 75 Class I patients (80%) and 62 of 75 CLP patients (82.7%) had an index >3% ($\chi^2 = 0.07$, $p = 0.799$). Figure 3 illustrates the prevalence of ramus asymmetry >3% in each group, and Figure 4 shows the prevalence of condylar asymmetry >3%; both figures demonstrate the similarity between groups (no significant group differences).

Association of Asymmetry with Age and Sex

We investigated whether mandibular asymmetry was related to patient age or sex within each group. Because age was treated as a continuous variable, a correlation approach was used. In those with Class I malocclusions, a significant positive correlation was observed between age and the ramus asymmetry index (Spearman $\rho = +0.28$, $p = 0.018$), indicating that older patients show greater vertical ramus asymmetry.

For instance, for Class I subjects, the average RAI was 1.8% in the youngest subset (12–14 years old) and 4.0% in the oldest subset (18 years old). This was also evident in the categorical analysis: 60% of Class I patients at age 18 had an "abnormal" asymmetry (>3% of the ramus, whereas ages 12–17 had only 20–40% (this age-group comparison was significant, $p = 0.037$). On the other hand, no significant age-dependence was found for ramus asymmetry in the CLP group ($\rho = +0.13$, $p = 0.24$); neither could the previously noted difference between those aged 18 (50% prevalence of ramus asymmetry >3%) and aged 12–17 (26%) be attributed to chance (not statistically significant).

For condylar asymmetry, neither group showed a significant age correlation (Class I $\rho \approx -0.10$, $p = 0.40$; CLP $\rho \approx +0.08$, $p = 0.51$). An interesting pattern in Class I was that the oldest patients (18 years) actually had *lower* condylar asymmetry on average than mid-adolescents, but given the high overall prevalence of condylar asymmetry, this inverse trend was not significant (prior age- group analysis in Class I found 66.7% of 18-year-olds vs ~87–90% of younger teens had condylar asymmetry >3%, $p = 0.406$, not significant). In CLP patients, condylar asymmetry remained high (75–89% prevalence >3%) across all age subgroups with no significant age effect ($p = 0.547$).

Regarding sex, we found no significant differences in asymmetry indices between males and females in either group. In the Class I group, the mean RAI was 3.1% in males vs 2.8% in females ($p = 0.75$) and the mean CAI was 7.5% in males vs 7.0% in females ($p = 0.84$). In the CLP group, mean RAI was 2.6% in males vs 3.4% in females ($p = 0.50$), and mean CAI was 8.3% in males vs 10.1% in females ($p = 0.58$). Although female CLP patients showed a slight tendency toward greater asymmetry than males (35% of females vs 26% of males had ramus asymmetry >3%, and ~83% of females vs 81.5% of males had condylar asymmetry >3%), these differences were not significant (chi-square $p > 0.4$). Our findings of no sex-based disparities in mandibular asymmetry are consistent with recent studies on asymmetry in orthodontic patients.

Table 1: Demographic characteristics of the Class I malocclusion and cleft lip and palate (CLP) groups. Data are given as mean ± SD for age, and number (%) for sex.

Characteristic	**Class I (n = 75)**	**CLP (n = 75)**	**Total (N = 150)**	**p-value**
Age (years) (mean ± SD)	(12–18) 15.8 ± 1.8	(12–18) 14.9 ± 1.9	(12–18) 15.3 ± 1.9	0.010*
Sex				0.073**
Male	27 (36.0%)	38 (50.7%)	65 (43.3%)	
Female	48 (64.0%)	37 (49.3%)	85 (56.7%)	

[*]: p-value by independent t-test for age difference between Class I and CLP groups.
[**]: p-value by chi-square test for sex distribution between groups (comparison of proportion male vs female).

Table 2: Descriptive statistics for right and left mandibular ramus and condylar heights (in millimeters) in Class I and CLP groups. P values refer to comparisons between right and left sides within the same group (paired analysis).

Group	Ramus height (R)	Ramus height (L)	p-value	Condylar height (R)	Condylar height (L)	p-value
Class I (n = 75)	38.5 ± 5.3 mm	39.0 ± 5.4 mm	0.68*	5.7 ± 1.2 mm	5.9 ± 1.3 mm	0.21*
Median (IQR)	38.8 (34.5–42.7)	39.2 (34.8–42.9)		5.6 (5.0–6.4)	5.9 (5.0–6.8)	
Min, Max	28.0, 48.5	28.1, 49.0		3.5, 8.7	3.5, 8.5	
CLP (n = 75)	40.6 ± 6.0 mm	42.0 ± 6.1 mm	0.33*	5.9 ± 1.3 mm	5.5 ± 1.3 mm	0.17*
Median (IQR)	40.7 (35.8–45.1)	42.5 (36.0–47.0)		5.7 (5.0–6.8)	5.5 (4.7–6.3)	
Min, Max	22.0, 55.0	21.5, 54.5		3.4, 9.5	2.3, 9.2	

[*]: Paired t-test (within-group) comparing right vs left side measurements.

Table 3: Comparison of mandibular asymmetry indices (ramus and condyle) between Class I and CLP groups. Values are given as mean ± SD and median. The asymmetry index is the absolute percentage difference between right- and left-side measurements.

Asymmetry Index (%)	Class I (n = 75)	CLP (n = 75)	p-value
Ramus asymmetry	2.9 ± 2.4% (Median 2.0)	3.5 ± 3.8% (Median 2.0)	0.538*
Condylar asymmetry	7.2 ± 6.5% (Median 6.5)	9.5 ± 7.5% (Median 9.0)	0.067*

[*]: p-value by Mann–Whitney U test (comparison of asymmetry indices between Class I and CLP groups).

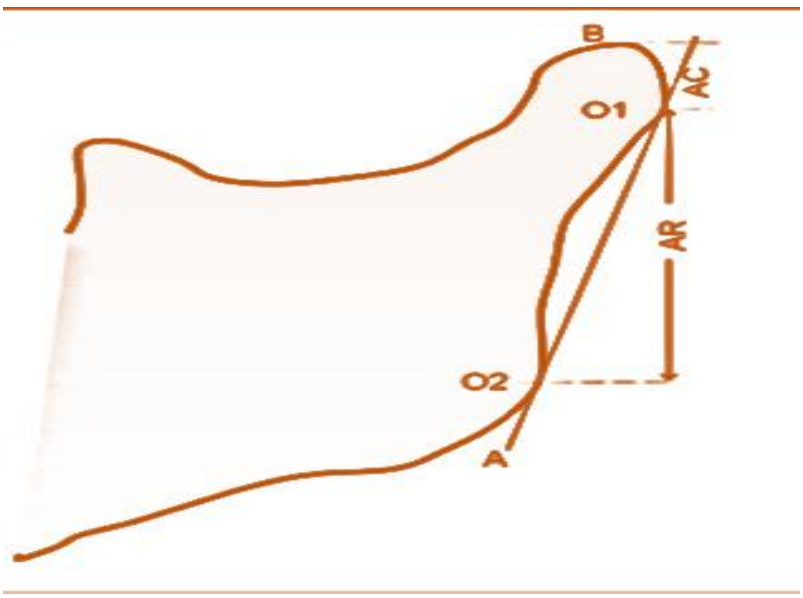

Figure 1: Schematic illustration of the Habets method showing reference points (O1, O2) and linear measurements used to determine condylar height (AC) and ramus height (AR). These measurements are taken along a tangent to the posterior ramal border to calculate the mandibular asymmetry index.

Figure 2: Digital panoramic radiograph (orthopantomogram) obtained with a Vatech PaX-i3D showing the Habets measurement technique for assessing mandibular vertical asymmetry. Red reference lines indicate ramus and condylar height measurements used to calculate the asymmetry index $(R - L)/(R + L) \times 100$.

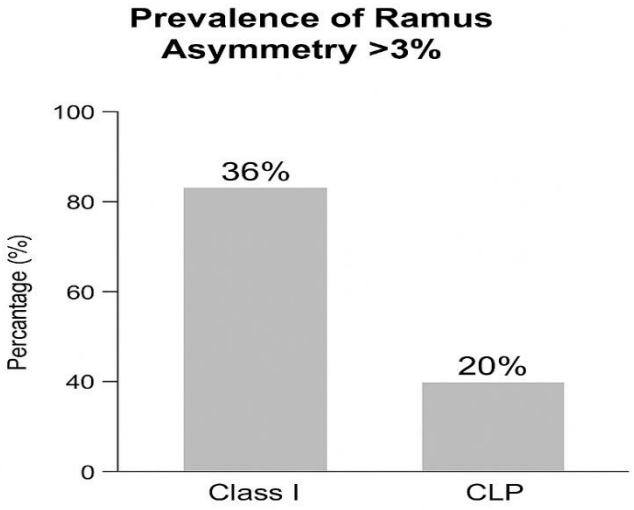

Figure 3: Prevalence of ramus asymmetry greater than 3% in Class I and CLP groups.

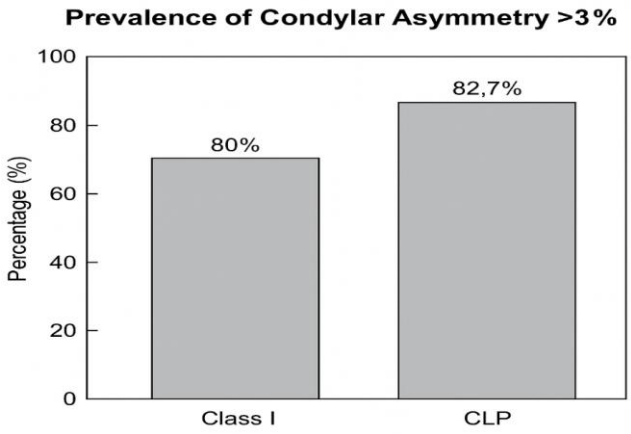

Figure 4: Prevalence of condylar asymmetry greater than 3% in Class I and CLP groups.

Discussion

This study evaluated mandibular vertical asymmetry in patients with cleft lip and palate compared to Class I malocclusion controls, using panoramic radiographic measurements. To our knowledge, it is one of the largest cross-sectional comparisons of mandibular asymmetry between CLP and non-CLP orthodontic populations in the Middle East. The key finding was that the non-syndromic CLP group did not exhibit significantly greater mandibular asymmetry than the Class I control group. Both groups demonstrated mild asymmetry in condylar and ramal heights (mean asymmetry indices above 3%), consistent with the notion that slight asymmetry is a normal finding in the general population. In fact, the prevalence of vertical condylar asymmetry (>3% difference) was around 80% in both groups, underscoring how common subtle mandibular asymmetry is, even among Class I individuals. Our results are consistent with prior observations that clinically acceptable asymmetry is frequently present and may not indicate pathology. In practical terms, a 5-10% asymmetry in condylar or ramus height (often translating to only 1-3 mm absolute difference) might be considered within normal variation and may not manifest as noticeable facial asymmetry or malocclusion.

Importantly, we found no statistically significant differences between the CLP and control groups in either ramus or condylar asymmetry indices. This suggests that having a repaired cleft lip and palate did not predispose patients in our sample to greater vertical mandibular asymmetry. This finding supports the work of [12], who also reported that unilateral CLP patients had mandibular asymmetry measurements comparable to those of non-cleft controls, while[13] noted no significant correlation between mandibular asymmetry and overall lower facial asymmetry in CLP individuals, proposing that the cleft-related facial asymmetry observed is likely due to other factors (such as cranial base or maxillary discrepancies) rather than the mandible itself. Our study reinforces this perspective: despite the maxillary deformity inherent in CLP, the mandible can often adapt or grow in ways that do not produce large unilateral deficiencies or excesses in vertical height.

Previous studies have found differences in mandibular symmetry between cleft and non-cleft groups, particularly with more advanced 3D imaging. For example, a study[14] observed greater mandibular asymmetry in unilateral CLP subjects with severe maxillary hypoplasia, while the mandible's growth direction may become asymmetric as a compensatory mechanism[15]. It has been reported that unilateral CLP patients with Class III relationships had significantly lower facial asymmetry[16]. In our CLP sample (which included both unilateral and bilateral clefts, mostly with Class I skeletal relations after treatment of the maxilla), any inherent asymmetry might have been mitigated by orthopedic and orthodontic interventions or simply not large enough to differentiate from the baseline asymmetry seen in controls.

In Class I malocclusion (with essentially symmetric craniofacial structure), any random differences in growth velocity between sides could lead to small asymmetries by the end of growth. The fact that we did not see a similar significant age trend in the CLP group might be due to the cleft patients receiving early interventions (such as maxillary expansions, alveolar bone grafts, etc.)[17]. Another interesting pattern was the slight reduction in condylar asymmetry in the oldest Class I patients; though not significant, this could imply that some condylar remodeling or normalization occurs in late adolescence, or it could be a chance finding. Overall, the age-related increase in ramus asymmetry for Class I aligns with general growth phenomena and has been reported in other contexts[18]. Regarding sex differences, our results showed no significant difference in asymmetry between males and females. This is held true for both ramus and condylar asymmetry indices and in both cleft and non-cleft groups. These findings concur with several reports in the literature that failed to find sex as a determinant of mandibular asymmetry severity. For instance, a study[19] found no consistent gender differences in ramus or total mandibular asymmetry in a sample of children with various malocclusions[20].

Both cleft and non-cleft patients can have asymmetry indices of 5–10% without visible facial asymmetry. However, indices well above 6% are beyond the typical magnification error range.

Future research could complement these findings by assessing transverse asymmetry using PA cephalograms or 3D imaging to obtain a more complete picture of mandibular asymmetry in CLP[15].

Conclusion

- In this Mosul sample, adolescents with repaired cleft lip and palate (CLP) did not exhibit greater vertical mandibular asymmetry than those with Class I malocclusion.
- There were no significant differences between CLP and non-cleft groups in right–left ramus height or condylar height asymmetry indices.
- Mild mandibular asymmetry was a common finding in both groups. The majority of patients in each group

showed a condylar asymmetry index above 3%, indicating slight vertical condyle height discrepancies within normal variation.

- Within the Class I malocclusion group, older patients tended to have slightly greater ramus asymmetry.
- No significant sex differences in mandibular asymmetry were observed. Both males and females in CLP and Class I groups had comparable asymmetry indices.
- Panoramic screening does not replace 3D evaluation when clinical asymmetry is suspected, but it is a simple method for diagnosis.

References

1. Dong Y, Wang Xm, Wang Mq, Widmalm Se. Asymmetric muscle function in patients with developmental mandibular asymmetry. J Oral Rehabilitation. 2008;35(1):27-36.
2. Thiesen G, Gribel BF, Freitas MPM, Oliver DR, Kim KB. Mandibular asymmetries and associated factors in orthodontic and orthognathic surgery patients. Angle Orthod. 2018;88(5):545-51.
3. Meran ZD. A Modified Naso-Alveolar Molding Device for Unilateral Cleft Lip and Palate. Sulaimani Dent J. 2023;10(1):20-6.
4. Naqvi ZA, Shivalinga B, Ravi S, Munawwar SS. Effect of cleft lip palate repair on craniofacial growth. J Orthod Sci. 2015;4(3):59-64.
5. Shetye PR, Evans CA. Midfacial morphology in adult unoperated complete unilateral cleft lip and palate patients. Angle Orthod. 2006;76(5):810-6.
6. Ras F, Habets LLMH, Ginkel FCV, Prahl-Andersen B. Three-Dimensional Evaluation of Facial Asymmetry in Cleft Lip and Palate. Cleft Palate-Craniofacial J. 1993;31(2):116-21.
7. Kurt G, Bayram M, Uysal T, Ozer M. Mandibular asymmetry in cleft lip and palate patients. Eur J Orthod. 2010;32(1):19-23.
8. Cakan DG, Yilmaz RBN, Bulut FN, Aksoy A. Dental anomalies in different types of cleft lip and palate. J Craniofacial Surg. 2018;29(5):1316-21.
9. Abdulqader A, Faiq T, Abdulaziz J. A comparative evaluation of sagittal condylar guidance between dentate and edentulous patients using CBCT: an in vivo study. Sulaimani Dent J. 2025;12(1):27-34.
10. Samatha K, Byahatti SM, Ammanagi RA, Tantradi P, Sarang CK, Shivpuje P. Sex determination by mandibular ramus: A digital orthopantomographic study. J Forensic Dent Sci. 2016;8(2):95-8.
11. Habets Llmh, Bezuur Jn, Naeiji M, Hansson Tl. The Orthopantomogram®, an aid in diagnosis of temporomandibular joint problems. J Oral Rehabilitation. 1988;15(5):465-71.
12. Bell A, Lo TWR, Brown D, Bowman AW, Siebert JP, Simmons DR, et al. Three-dimensional assessment of facial appearance following surgical repair of unilateral cleft lip and palate. Cleft Palate-Craniofacial J. 2012;51(4):462-71.
13. Stauber I, Vairaktaris E, Holst A, Schuster M, Hirschfelder U, Neukam FW, et al. Three-dimensional Analysis of Facial Symmetry in Cleft Lip and Palate Patients Using Optical Surface Data. J Orofac Orthop Fortschritte Kieferorthopädie. 2008;69(4):268-82.
14. Jena AK, Singh SP, Utreja AK. Effects of sagittal maxillary growth hypoplasia severity on mandibular asymmetry in unilateral cleft lip and palate subjects. Angle Orthod. 2011;81(5):872-7.
15. Paknahad M, Shahidi S, Bahrampour E, Beladi AS, Khojastepour L. Cone beam computed tomographic evaluation of mandibular asymmetry in patients with cleft lip and palate. Cleft Palate-Craniofacial J. 2016;55(7):919-24.
16. Meyer-Marcotty P, Stellzig-Eisenhauer A. dentofacial self-perception and social perception of adults with unilateral cleft lip and palate. J Orofac Orthop Fortschritte Kieferorthopädie. 2009;70(3):224-36.
17. Ren Y, Steegman R, Dieters A, Jansma J, Stamatakis H. Bone-anchored maxillary protraction in patients with unilateral complete cleft lip and palate and Class III malocclusion. Clin Oral Investig. 2019;23(5):2429-41.
18. Mendoza LV, Bellot-Arcís C, Montiel-Company JM, García-Sanz V, Almerich-Silla JM, Paredes-Gallardo V. Linear and volumetric mandibular asymmetries in adult patients with different skeletal classes and vertical patterns: A cone-beam computed tomography study. Sci Rep. 2018;8(1):12319.
19. Hlatcu AR, Galan E, Milicescu Ștefan, Teodorescu E, Ionescu E. An evaluation of the ramus mandibular asymmetry on the panoramic radiography. Appl Sci. 2023;13(13):7645.
20. Sezgin OS, Celenk P, Arici S. Mandibular asymmetry in different occlusion patterns. Angle Orthod. 2007;77(5):803-7.

College of
Dentistry